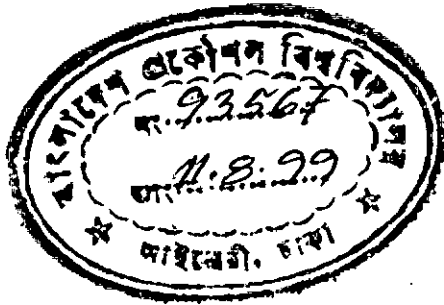# AN IMPROVED DESIGN RATIONALE FOR

MAT FOUNDATION BASED ON

FINITE ELEMENT ANALYSIS

A THESIS BY

ALOK SUTRADHAR

Submitted in partial fulfilment of the requirements for the degree of

MASTER OF SCIENCE IN CIVIL ENGINEERING

DEPARTMENT OF CIVIL ENGINEERING

BANGLADESH UNIVERSITY OF ENGINEERING AND TECHNOLOGY

DHAKA

JULY, 1999

#93567#

Dedicated to

my mother

AN IMPROVED DESIGN RATIONALE FOR MAT FOUNDATION BASED ON FINITE ELEMENT ANALYSIS
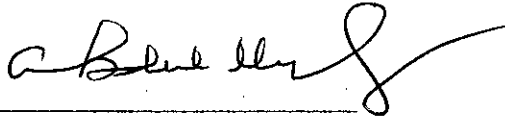
A THESIS BY
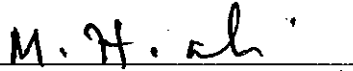
ALOK SUTRADHAR

Approved as to the style and content by

Dr. Sohrabuddin Ahmad   Chairman
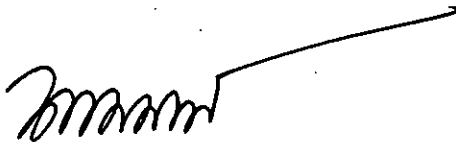Professor   (Supervisor)
Department of Civil Engineering
BUET, Dhaka.

Dr. Abdul Muqtadir   Member
Professor   (Co-supervisor)
Department of Civil Engineering
BUET, Dhaka.

Dr. M. Hossain Ali   Member
Professor and Head
Department of Civil Engineering
BUET, Dhaka.

Dr. M. Shamim Z. Bosunia   Member
Professor
Department of Civil Engineering
BUET, Dhaka.

A. S. M. Abdul Hamid   Member
Director   (External)
Khalid and Partners Ltd.
8/9 Lalmatia, Block C, Dhaka.

DECLARATION

Declared that, except where specified references are made to other investigators, the work embodied in this thesis is the result of investigation carried out by the author under the supervision of Professor Sohrabuddin Ahmad and Professor Abdul Muqtadir of Civil Engineering Deapartment, BUET.

Neither the thesis nor any part thereof has been submitted or is being concurrently submitted in candidature for any degree at any other institution.

_____

Author

ACKNOWLEDGEMENT

The author wishes to express his indebtedness to Dr. Sohrabuddin Ahmad, Professor of Civil Engineering, BUET for his continuous guidance, invaluable suggestions and affectionate encouragement at every stage of this study.

The author expresses his profound gratitude to Dr. Abdul Muqtadir, Professor of Civil Engineering, BUET for his constant guidance, suggestions and encouragement at all phases of this work.

The author is grateful to Dr. Shamim Z. Bosunia, Professor of Civil Engineering, BUET for his constructive and valuable suggestions at various stages of this study.

The author treasures a sacred belief in his parents for having bestowed upon him the gift of life and for keeping the unflinching faith in him over the years. This achievement is, but their grace. The author is grateful to his family members, colleagues specially Anwar, Ashfaque, Badre, Shakil, friends specially Jaya and well-wishers for their cooperation and companionship extended to him.

CONTENTS

ABSTRACT

With the growing demand of high-rise buildings mat foundation is now frequently used. To study in-depth the analysis and design of mat foundation, first the foundation model depicting soil is examined. Performance of Winkler model is being checked with two parameter models. It has been found that in spite of failure to represent any continuity among springs, Winkler foundation gives very good idealisation of soil proving it to be a recommended model for design of foundations. Critical review has been done on the performances of Conventional method, ACI method and finite element method. Finite element method being the best one in terms of all aspects has exposed the short comings of other methods. From the present study the extent of the use of other methods has been unveiled. It reveals that in ACI method the thickness governed by flexural shear will be high with respect to FE method. Also in Conventional method the steel required by negative moment will be more compared to FE method. So FE method results in substantial economy than both ACI and Conventional method. It also implies that this economy will increase with high column loads. Sensitivity analysis on material and geometric parameters of mat foundation has been done. This in fact paved the way to explore reshaping of mat foundation for a better economy.

Mat foundation is a relatively heavy and costly structure. Economy in mat has been an engineers dream for many years. However, this was not possible for lack of appropriate design method and guideline. With the availability of the most powerful tool Finite Element Analysis method it is now possible to attain economy by changing the configuration of mat geometry. In this study a well verified guideline for design of non-uniform mat foundation has been presented. Sensitivity analysis of all relevant parameters have been performed. By using this guideline it has been revealed that thickness away from column can be reduced up to 35%. And economy achievable in terms of volume of concrete and reinforcement is about 20 to 30 % with respect to uniform thickness mats. To facilitate the design of the non-uniform mat foundation, a full pledged windows based software MATFEA has been developed.

LIST OF SYMBOLS

R	Resultant of all column loads
X's	x coordinates of the columns the corner of the mat
Y's	y coordinates of the columns with respect to the corner of the mat
P's	Column loads
n	Total number of columns
L_{x_m}	x dimension of mat
B_{y_m}	y dimension of mat
e_x	x eccentricity of R with respect to the center of the mat
e_y	y eccentricity of R with respect to the center of the mat
q	Soil pressure at any point under the mat
A	Plan area of mat
I_x & I_y	Moment of inertia of mat area w.r.t. x and y axes
x, y	Coordinates of locations where soil pressures are desired with respect to the center of the mat
q_a	Average soil pressure under the strip
q_i	Soil pressure at the corners of the strip
Q_a	Average load on the strip
B	Width of the strip
L	Length of the strip
n_s	No of columns in the strip
P_i^s	Strip column loads
e_r	Eccentricity of the resultant of the strip column loads w.r.t. the Left end of the strip
r's	Distance of the strip column loads from the left end of the strip
q_1 and q_2	Soil pressure intensity at the left and the right end of the strip respectively
E	Modulus of elasticity of materials used in structure
E_s	Modulus of elasticity of soil

I_F	Moment of inertia of footing
E	Modulus of elasticity
f_c	Ultimate concrete strength in psi
t	Thickness of mat in inch
ν	Poisson's ratio of concrete
k	Modulus of subgrade reaction
r	Radial distance of the point under investigation from P
M_r and M_t	Radial and tangential moments for a unit width of mat
Q	Shear force per unit width of mat
w	Mat displacement
Ψ, R's and Z's	functions first introduced by Schleicher (1926)
M_x & M_y	Bending moment about y and x axes respectively,
φ	Angle of the radial line passing through the point under consideration w.r.t. the positive x axis in a clockwise direction
M_c, V_c & w_c	End correction to moment, shear and displacement respectively
M_e & V_e	End moment and shear respectively
p	Total soil reaction pressure
n	Soil pressure distribution parameter of Baker's method
J	Torsional factor
Ω	Adjustment factor
α	Angle of orientation of the grid element
H_d	Number of X directional divisions
V_d	Number of Y directional divisions
$[\sigma']$	Local stress matrix
$[\sigma]$	global stress matrix
$[\theta_c]$	Direction cosine matrix of the local axes w.r.t. the global axes
σ's and σ''s	Global and local normal stresses respectively
τ's and τ''s	Global and local shear stresses respectively
σ_b & σ_t	Bottom and top normal stresses respectively
τ_b & τ_t	Bottom and top shear stresses respectively
t	Thickness of the mat at the location of the stresses

C_c	Distance of the reinforcement centroid from the nearest mat surface
LL	Live load
DL	Dead load
WL	Wind load
d	Effective depth of mat
ρ	Steel ratio
ρ_{max}	Maximum steel ratio
ρ_{min}	Minimum steel ratio
M_u	Ultimate moment capacity
A_s	Steel area
b	Width of the mat strip to be designed
v_{pu}	Ultimate punching shear strength
v_{fu}	Ultimate flexural shear strength
ν	Poison's ratio
f_y	Yield strength of steel
M	Acting bending moment
V_p	Acting punching shear
A_s^{avg}	Weighted average steel area per unit width
t_{avg},	Weighted average thickness of mat
d_s	Slope width
d_g	Width of greater thickness
t_g	Greater thickness
t_s	Smaller thickness
Δt	Change in thickness
$t_{tentative}$	Tentative thickness for the first trial of mat with non-uniform thickness
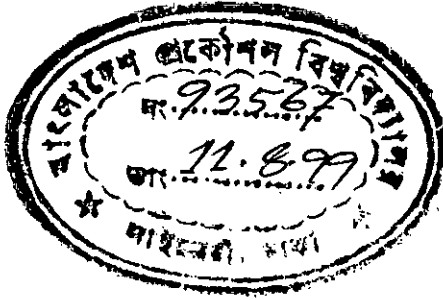
CHAPTER 1

INTRODUCTION

1.1 GENERAL

Mat foundations are commonly used under structures wherever the column loads or soil conditions result in conventional footings or piles occupying most of the site. For many multi-storied buildings a single mat foundation is more economical than constructing a multitude of isolated foundation elements. Mat foundations due to their continuous nature provide resistance to independent differential column movements, thus enhancing the structure's performance. Mats can bridge across weak pockets in the non-uniform substratums, thus equalizing foundation movements. Mat foundations are predominantly used in regions where the underlying stratum consists of clayey materials with low bearing capacity. This is also used as a load distributing element placed on piles or directly on high bearing capacity soil or rock. The various advantages of mat foundations are :

(a)   use of the raft as a basement floor,

(b)   use of the flexural stiffness to reduce differential settlements due to swelling and shrinking of active soils,

(c)   use of the flexural stiffness to reduce contact pressures in regions of higher soil compressibility, and

(d)   use of the raft in combination with piles to reduce total settlement.

Mat foundations are also popular for deep basements both to spread the column loads to a more uniform pressure distribution and to provide the floor slab for the basement. A particular advantage for basements at or below the ground water table is to provide a water barrier. For all these advantages, mat foundations are becoming increasingly popular.

There are several categories of mat foundation problems which by their nature require sophisticated computer analysis, since long hand methods would not be directly applicable. These are :

i) mats of unusual or complex shapes

ii) mats where it is deemed necessary that a varying subgrade modulus must be used.

iii) mats with non-uniform thickness

iv) mats where large moments or axial forces are transmitted to the mat from laterally loaded shear walls, trusses, or frames; and

v) mats where rigidity of superstructure significantly affects mat behavior and stress distribution.

There are several types of mat foundation i.e.,

i) flat plate,

ii) plate thickened under column,

iii) waffle slab,

iv) plate with pedestal, and

v) plates with stiffeners as basement walls.

Fig. 1.1 illustrates several mat foundation configurations as might be used for buildings. The most common mat foundation configuration is the flat plate type. This type of foundation tends to be heavily overdesigned due to additional cost of and uncertainty in analysis.

1.2   BACKGROUND OF THE STUDY

There are several methods for the analysis of mat, but none is accurate and convenient enough. There are some approximate methods which are considerably crude and are in use for a long time. Recently, there are some computer based methods available. However, these computer based methods idealize mat unrealistically. The modeling of soil also has got its own limitations.
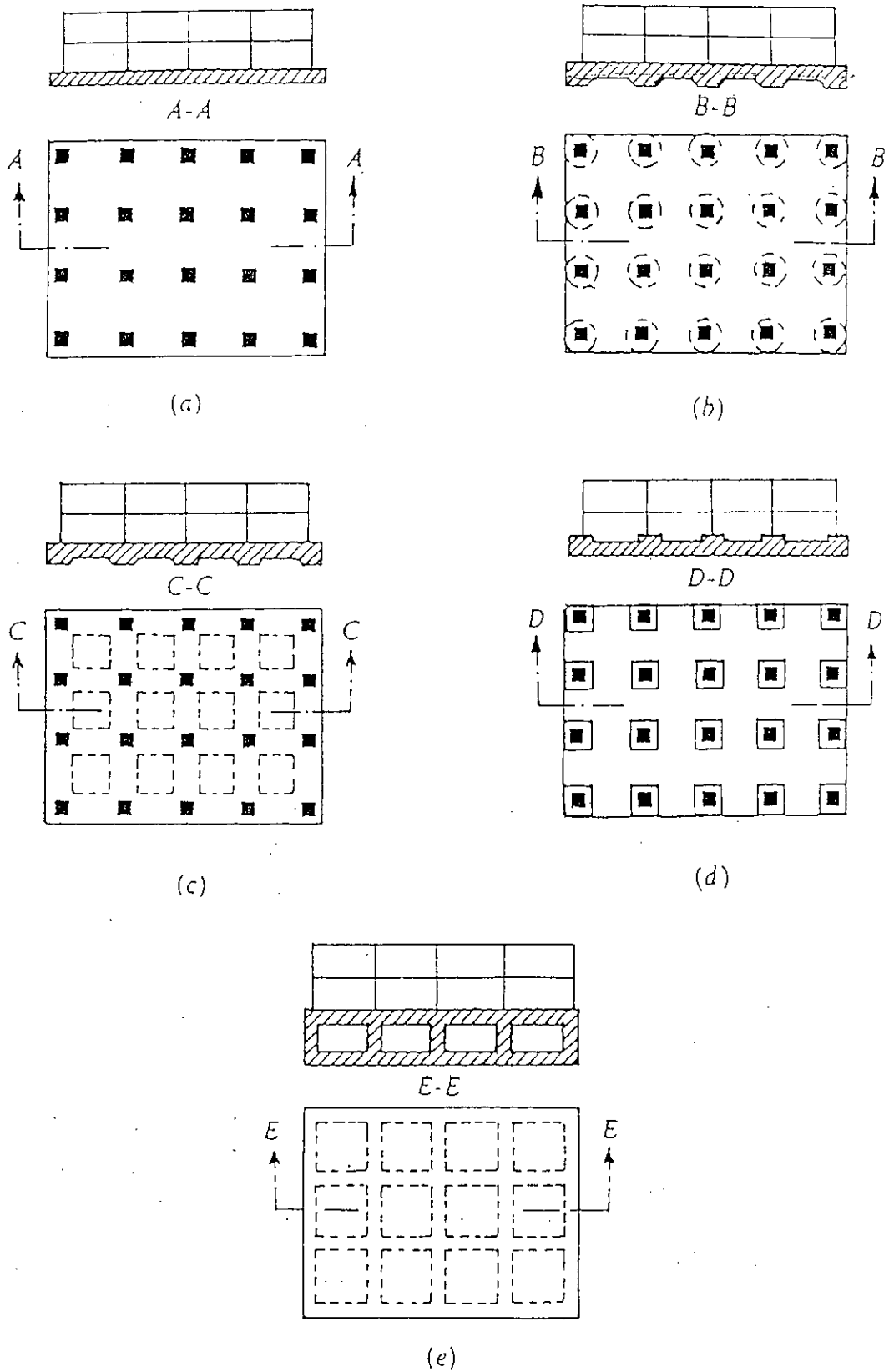
Fig. 1.1.　Common types of mat foundation : (a) flat plate ;　(b) plate thickened under columns ;　(c) waffle slab ;　(d) plate with pedestals and (e) basement wall as part of mat.

In the most common and simplified method, known as Conventional method, column loads are distributed under the mat; then the mat is divided into strips midway between the column lines and the force system acting on each strip is adjusted to establish equilibrium. Finally each strip is designed as a combined footing. This is repeated for the other direction. This method is recommended by ACI when adjacent spans and column loads do not vary by more than 20%. However, in this method mat is considered to be fully rigid in determining the soil pressure and also the divided strips lose their plate characteristics i.e. two way bending.

One of the most popular methods of mat analysis is the ACI Approximate Flexible method (Committee 336) which is essentially based on the analysis of Schleicher (1926). In this method, as the name implies, the mat is considered to be a flexible plate acted upon by concentrated column loads and resting on a Winkler medium. Effect of each load is calculated as if the plate were infinite. Forces for each individual column are summed up. To have the edges free from forces, the mat is divided into strips and the forces obtained by this approach on the edges are applied in opposite direction on the respective edges considering each strip to be supported on semi-infinite elastic foundation [Hetenyi (1946)]. Finally this new set of forces are added to the previous ones. Shukla (1984) presented design aids for using this method. Later, this method was further modified by Mician (1985). However, this complicated and lengthy approximate method fails to take into account the boundary conditions and moments from columns.

Baker (1948) proposed a method of mat foundation analysis where the mat is divided into column strips resting on Winkler medium and each strip is analyzed separately. A particular soil pressure distribution of unknown magnitude is assumed and applied on both the column strip and the supporting soil. The magnitude of soil pressure is determined by taking the maximum differential displacements of the column strip and the supporting soil as the matching criteria. However, the detailed deflected shapes of the column strip and the supporting soil do not match in this

3

method. Also, this method can not take into account column base moments and fails to represent the plate characteristics of mat.

Bowles (1974) has proposed Finite Grid method in which the mat is reduced into a grid system consisting of beam-column elements resting on Winkler medium. Solution to the problem is obtained following the stiffness matrix approach. According to Bowles, there is a little computational improvement if the soil is modeled using its modulus of elasticity and Poison's ratio instead of its modulus of subgrade reaction. However, the plate characteristics of mat is lost in this method. Also, the program requires extensive data in generating the grid geometry, sectional and material properties.

There is also Finite Difference method [Bowles (1974), Deryck and Severn (1960, 1961)] where the mat is modeled as large flat plate on elastic medium. The fourth order differential equation as given by plate theory is then numerically solved using finite difference technique. Handling column moments is beyond the scope of this method. Also, interpretation of the boundary points is cumbersome in this method.

At BUET, Hossain (1993) conducted a comparative study of the available analysis methods of mat foundation and felt the need for a rigorous finite element study of the problem. Later, Molla (1995) tested the performance of Mindlin plate element in finite element analysis of mat foundation and also compared the results with those from other available methods. The study of Molla opened a wide horizon for a rigorous finite element study of the problem with more appropriate and versatile element in search of a more economic design of mat. Sutradhar (1995) compared the analysis of mat foundation by Finite Element method using Ahmad's thick shell element with those by Finite Grid method and Finite Difference method.

Lefas, Georgiannou and Sheppard (1996) presented an iterative procedure for analysis and design of mat foundation based on a soil-structure interaction procedure developed using well-marketed programs *VDISP* by *OASYS, STAAD-III/ISDS* by

4

Research Engineers and *Supercalc* by Computer Associates. VDISP is a geotechnical program for calculating vertical displacements at specified points due to any pattern of loading on an elastic half-space representing the ground. From VDISP the spring constant K_s is entered into the STAAD-III grillage and the raft is analysed.

Liou and Lai (1996) presented a simplified structural analysis model for mat foundation with grid floor beams as stiffeners. The model becomes grid floor beams on an elastic foundation with loadings applied at the intersections of floor beams. The yield line theory (Johansen 1962) for bottom slabs is employed to lump the subgrade reaction springs to the location under grid floor beams.

Morshed (1997) conducted comparative analysis between finite element method using Ahmad thick shell element with ACI method and Conventional method. He also suggested a non-uniform mat foundation. His findings paved the way for developing a design rationale for mat foundation.

1.3   OBJECTIVE OF THE PRESENT RESEARCH

The present research has been aimed at the following objectives :

(i)   To analyse mat foundation with a two parameter foundation model and compare with Winkler foundation model.

(ii)   To establish an economic design guideline for rectangular mat foundation.

(iii)   To conduct significant parametric study of both uniform and non-uniform thickness mat foundations

(iv)   To epitomize the basis of suitability of various methods of mat foundation.

(v)   To develop a Windows 95/98 based software for analysis and design of mat foundation using finite element method of analysis, which will also

give graphs for deflection, shear and moment diagram of any prescribed line in the mat.

1.4   METHODOLOGY

For analyzing mat foundation by finite element technique soil has been modeled as Winkler medium and Ahmad's general thick shell finite element (1969,1970) has been used.

In an attempt to make a two parameter foundation model a thorough survey of the related literatures has been made. Limitations and assumptions of such models has been thoroughly studied to choose the closest reasonable model. Comparative assessments has been carried out between two parameter and Winkler foundation model.

Efforts have been made to substantiate the findings from the sensitivity study of the parameters which are critical in mat foundation design.

A simple design method for non-uniform mat foundation has been proposed and critical aspects of the guide lines of this method has been verified. A number of cases has been tested.

A Windows 95/98 based complete software has been developed which can analyse both uniform and non-uniform mat foundations. Finally, a suggestion for future study has been offered.

CHAPTER   2

LITERATURE REVIEW

2.1 GENERAL

Analysis of mat foundation requires study of two aspects, the soil- structure interaction and the various methods of analyzing the mat.

The mechanical response of naturally occurring soils can be influenced by a variety of factors. These include shape, size and mechanical properties of the individual soil particles, the configuration of the soil structure, the intergranular stress history and the presence of soil moisture, the degree of saturation and the soil permeability. These factors generally contribute to stress-strain phenomena which display markedly non-linear, irreversible and time dependent characteristics. Thus an attempt to solve a soil-foundation interaction problem taking into account of all such material aspects is clearly an onerous task. In order to obtain meaningful and reliable information for practical problems it becomes necessary to idealize the behavior of soil by depicting soil models.

There are several methods to analyse mat foundation. These are a) Conventional method, b) ACI approximate flexible method, c) Baker's method, d) Finite difference method and e) Finite grid method.

Conventional method is the crudest one. Here mat is treated as a rigid slab. All the other methods are based on Winkler spring model. ACI method is based on Schleicher's solution of infinite flexible slab on continuous spring support and Baker's method is designed to emulate that solution. Finite grid and Finite difference methods are numerical analysis methods and require extensive computer support though they do not offer any substantial improvement in results over Schleicher's solution. The first two

methods are generally used.

2.2 FOUNDATION MODEL

Generally the analysis of bending of beams on an elastic foundation is developed on the assumption that the reaction forces of the foundation are proportional at every point to the deflection of the beam at that point. This assumption was first introduced by Winkler (1867) and formed the basis of Zimmermann's classical work (1930) on the analysis of railroad track. It has been shown by Föppl's classical experiment (1922) and Hetenyi's analytical work (1946) that Winkler's assumption in spite of its simplicity leads to satisfactory results in stress analysis of beams on an elastic foundation.

On the other hand, by means of the hypothesis of isotropic, linearly elastic semi-infinite space, the physical properties of a natural foundation can be correctly described. To bridge the gap between theses two extreme cases, interactions between Winkler's springs were considered by several authors. Hetenyi (1950) treated the problems of beams or plates on an elastic foundation by assuming a continuous beam or plate embedded in the material of foundation, which is itself without any continuity. Pasternak (1954) assumed that the shear interactions exist between the springs. Vlasov and Leont'ev (1966) also considered the shear interactions in the foundation and formulated their problems by using a variational method. They solved a large number of problems involving beams, plates and shells on two parameter model elastic foundation.

2.2.1 WINKLER MODEL

The idealised model of soil media proposed by Winkler (1867) assumes that deflection w, of the soil medium at any point on the surface is directly proportional to the stress, q applied at that point and independent of stresses applied at other locations, i.e.

$$q(x,y) = kw(x,y) \qquad\qquad (2.1)$$

where k is termed the modulus of subgrade reaction with units of stress per unit length. There are indications that this assumption is already to be found in the works of Euler, Fuss, Bubnov and Zimmermann (Korenov, 1960; Hetenyi, 1966). The equation is usually the response function or the kernel function of Winkler model. Physically Winkler's idealisation of the soil medium consists of a system of mutually independent spring elements with spring constant k (Fig. 2.1). One important feature of this soil model is that the displacement occurs immediately under the loaded area and outside this region the displacements are zero. Also for this model the displacements of a loaded region will be constant whether subjected to an infinitely rigid load or a uniform flexible load.

2.3 TWO PARAMETER ELASTIC MODELS

The inherent deficiency of the Winkler model in depicting the continuous behaviour of real soil masses and the mathematical complexities of the elastic continuum has led to the development of many other simple soil response models. These models possess some of the characteristic features of continuous elastics solids (Kerr, 1964; Hetenyi, 1966).

The term 'two parameter' signifies the fact that the model is defined by two independent elastic constants. The development of these two-parameter soil models has been approached along two distinct lines. The first type proceeds from the discontinuous Winkler model and eliminates its discontinuous behaviour by providing mechanical interaction between the individual spring elements. Such physical models of soil behaviour has been proposed by Filonenko-Borodich (1940, 1945), Hetenyi (1946), Pasternak (1954) and Kerr (1964) where interaction between the spring elements is provided by either elastic membranes, elastic beams or elastic layers capable of purely shearing deformation. The second approach starts from the elastic continuum model and
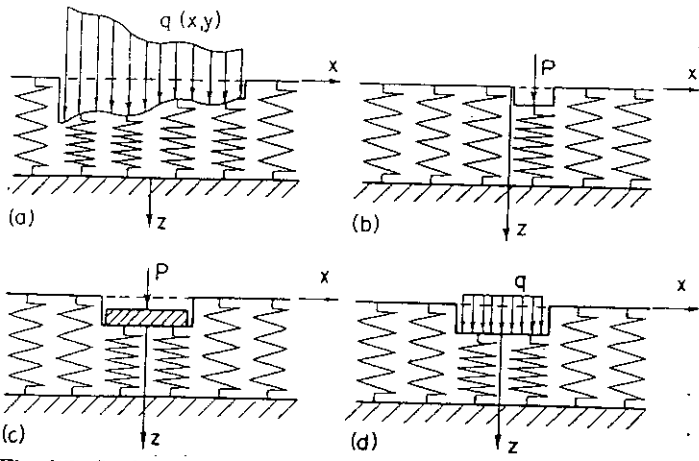
9

Fig. 2.1. Surface displacements of the Winkler model due to (a) a non-uniform load, (b) a concentrated load, (c) a rigid load, (d) a uniform flexible load.
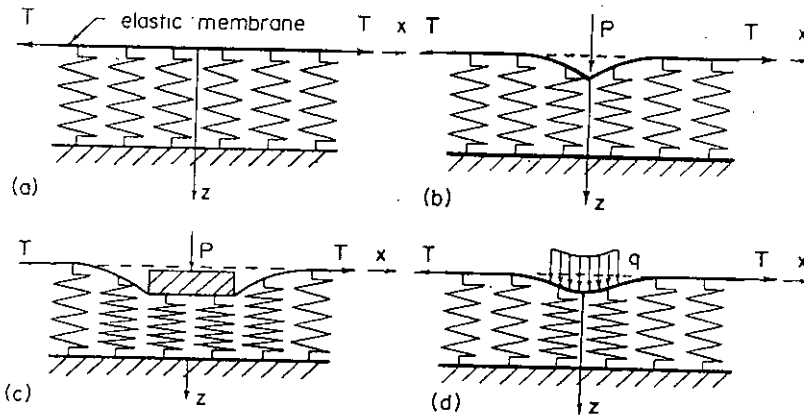

Fig. 2.2 Surface displacements of the Filonenko-Borodich model. (a) Basic model, (b) concentrated load, (c) rigid load, (d) uniform flexible load.

introduces constraints or simplifying assumptions with respect to the distribution of displacements and stresses. The soil models proposed by Reissner (1958) and Vlazov and Leontiev (1966) take into consideration such simplifications.

2.3.1 FILONENKO- BORODICH MODEL

The model proposed by Filonenko-Borodich model (1940,1945) acquires continuity between the individual spring elements in the Winkler model by connecting them to a thin elastic membrane under a constant tension T (Fig.2.2). By considering the equilibrium of the membrane-spring system, it can be shown that for three-dimensional problems (e.g. rectangular or circular foundations) the surface deflection of the soil medium due to a pressure q is given by

$$q(x,y) = k\omega(x,y) - T\nabla^2\omega(x,y) \qquad (2.2)$$

where

$$\nabla^2 = \frac{\partial^2}{\partial x^2} + \frac{\partial^2}{\partial y^2}$$

is Laplace's differential operator in rectangular cartesian coordinates. In the case of two-dimensional problems this equation reduces to

$$q(x) = kw(x) - T\frac{d^2w(x)}{dx^2} \qquad (2.3)$$

The two elastic constants necessary to characterise the soil model are K and T. Typical examples of surface deflection profiles of this particular model due to concentrated, flexible and rigid external loads are shown in Fig.2.2

2.3.2   HETENYI MODEL

In the model proposed by Hetenyi (1946), interaction between the independent spring elements is accomplished by incorporating an elastic plate in three-dimensional problems, or an elastic beam in two-dimensional problems. The response function for this model is given by

$$q(x,y) = k\omega(x,y) - D\nabla^4\omega(x,y) \qquad (2.4)$$

where D ($= E_p h^3/12(1-v_p^2)$) is flexural rigidity of the plate. Here again, for two-dimensional problems.

Eqn.2.4 reduces to

$$q(x) = kw(x) - D\frac{d^4 w(x)}{dx^4} \qquad (2.5)$$

2.3.3   PASTERNAK MODEL

The model for soil behaviour proposed by Pasternak (1954) assumes the existence of shear interaction between the spring elements. This can be accomplished by connecting the spring elements to a layer of incompressible vertical elements which deform in traverse shear only (Fig.2.3). The deformations and forces maintaining equilibrium in the shear layer are shown in Fig.2.3. By assuming that the shear layer is isotropic in the x, y plane with shear modulii $G_x = G_y = G_p$, we have

$$\tau_{xz} = G_p\gamma_{xz} = G_p\frac{\partial w}{\partial x}, \qquad \tau_{yz} = G_p\gamma_{yz} = G_p\frac{\partial w}{\partial y}, \qquad (2.6)$$

The total shear forces per unit length of the shear layer are
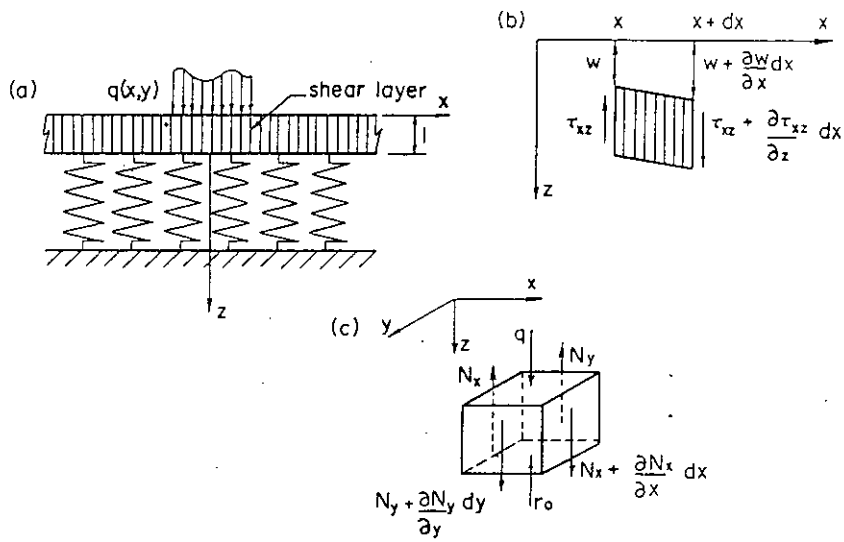
Fig. 2.3 The Pasternak model. (a) The basic model, (b) stresses in the shear layer, (c) forces acting on the shear layer.
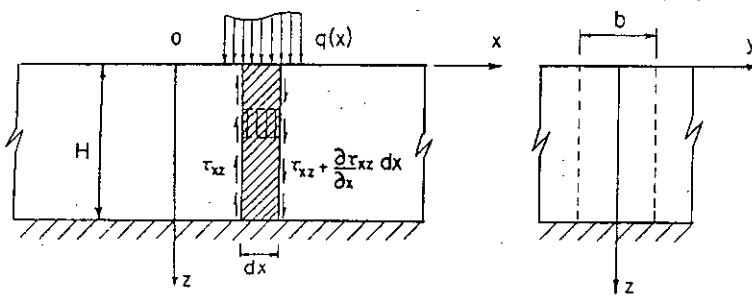

Fig.2.4 . The Vlazov model. Stresses in a single elastic layer.

$$N_x = \int_0^1 \tau_{xz}dz = G_p\frac{\partial w}{\partial x} \; ; \qquad N_y = \int_0^1 \tau_{yz}dz = G_p\frac{\partial w}{\partial y} \; ; \qquad (2.7)$$

For the force equilibrium in the z-direction

$$\frac{\partial N_x}{\partial x} + \frac{\partial N_y}{\partial y} + q - r_o = 0 \qquad (2.8)$$

Using the condition $r_o = kw$ and Eqn.(2.6) in (2.8) we get

$$q(x,y) = k\omega(x,y) - G_p\nabla^2\omega(x,y) \qquad (2.9)$$

2.3.4 REISSNER MODEL

The model proposed by Reissner (1958) is also derived by introducing displacement and stress constraints that simplify the basic equations for a linear elastic isotropic continuum. By assuming that the in-plane stresses (in the x, y plane) throughout a soil layer of thickness H are negligibly small ($\sigma_{xx} = \sigma_{yy} = \tau_{xy} = 0$) and that the displacement components u, v and w in the rectangular cartesian coordinate directions x, y, z respectively, satisfy conditions

$$u = v = w = 0 \text{ on } z = H; \qquad u = v = w = 0 \text{ on } z = 0 \qquad (2.10)$$

it can be shown that response function for the soil model is given by

$$c_1 w - c_2\nabla^2 w = q - \frac{c_2}{4c_1}\nabla^2 q \qquad (2.11)$$

where w is the vertical displacement of the surface of the elastic layer, $z = 0$, and q is the external load. The constants c_1 and c_2 characterising the soil response eqn. are related to E_s and v_s by $c_1 = E_s/H$, and $c_2 = HG_s/3$, where E_s and G_s are the elastic modulus and shear modulus, respectively, of the soil layer. Also it is noted that for a constant or linearly varying stress after redefining $c_1 = k$ and $c_2 = G_p$. Eqn.(2.11) is identical to eqn.(2.2) or (2.9).

Here again as a consequence of assuming that in-plane stresses σ_{xx} , σ_{yy} and τ_{xy} are zero, the shear stresses τ_{xz} and τ_{yz} are independent of z. These stresses are constant throughout the depth of the elastic layer for a given location x, y. Such an assumption would prove to be particularly unrealistic for a thick soil layer.

2.3.5 VLAZOV MODEL

The model of soil response proposed by Vlazov (1949) presents an example of the second type of two-parameter elastic model which is derived by introducing displacement constraints that simplify the basic equations for a linear elastic isotropic continuum. Vlazov's approach to the formulation of the soil model is based on the application of a variational method. By imposing certain restrictions upon the possible distribution of displacements in an elastic layer, he was able to obtain a soil response function similar in character to eqn.(2.3) and (2.9).

The state of plane strain in the elastic layer (Fig.2.4) in x-z plane is considered first. The state of strain in the foundation layer is assumed to be such that the displacement components are

$$u(x, z) = 0 \ , w(x, z) = w(x)h(z) \qquad (2.12)$$

The function h(z) describes the variation of displacements w(x,z) in the z direction. Several such variations have been proposed by Vlazov and Leontiev (1966) including the linear and exponential variations

$$h(z) = (1-\eta) \; ; \; h(z) = \frac{\sinh[\gamma(H-z)/L]}{\sinh[\gamma H/L]} \tag{2.13}$$

where $\eta = z/H$ and γ and L are constants.

Using the stress strain relations for plain strain conditions (Timoshenko and Goodier, 1970) we obtain

$$[\;\sigma_{xx}\;;\;\sigma_{zz}\;] = \frac{E_0}{(1-v_0^2)}w(x)\frac{dh(z)}{dz}[v_0;1]$$

$$\tau_{xz} = \frac{E_0}{2(1+v_0)}\frac{dw(x)}{dx}h(z) \tag{2.14}$$

where $E_0 = E_s/(1-v_s^2)$ and $v_0 = v_s(1-v_s)$ and E_s, v_s respectively the elastic modulus and Poisson's ratio for the elastic material. The equation of equilibrium in the z- direction is obtained by Lagrange's principle of virtual work; i.e. by equating to zero the total work of all internal and external forces on an element over any arbitrary virtual displacement. The virtual work contribution from the external forces

$$U_e = bq(x)h(0)dx + b\int_0^H \frac{\partial \tau_{xz}}{\partial x}h(z)dzdx \tag{2.15}$$

And the virtual work contribution from internal forces is

$$U_i = -b\int_0^H \sigma_{zz}\frac{dh(z)}{dz}dzdx \tag{2.16}$$

14

Using the conditions $U_e + U_i = 0$ and the eqn.(2.14)-(2.16), we obtain the response function as

$$q(x) = kw(x) - 2t\frac{d^2w(x)}{dx^2}$$

(2.17)

where

$$k = \frac{E_0}{(1-v_0^2)}\int_0^H\left(\frac{dh}{dz}\right)^2 dz, \qquad t = \frac{E_0}{4(1+v_0)}\int_0^H(h)^2 dz$$

(2.18)

2.3.6   COMMENTS ON VARIOUS MODELS

It can be seen that eqn.2.9 is identical with eqn. 2.2 if T is replaced by G_p, Thus the surface deflection profiles for Pasterak model are very similar to those obtained for the Filonenko-Borodich model. With the two-parameter models considered so far, the Winkler case can be recovered as a limiting case, as T, D and G_p tend to zero.

By comparing (2.17) with (2.3) and (2.9) it is apparent that the shear modulus G_p, the membrane tension T and the spring constant k are directly related to the elastic constant E_s and v_s of the soil layer. Here therefore is a physical interpretation of the modulus of subgrade reaction, k.

2.3.7 DETERMINATION OF ELASTIC CONSTANTS FOR TWO PARAMETER MODEL

The effectiveness of these soil models is dependent on the following factors :

i) the ease and accuracy with which material parameters encountered in the idealized soil models could be determined from either laboratory or field tests.

ii) the reliability and accuracy of the theoretical predictions, as verified by experimental or field studies of foundation behaviour.

(a) Poisson's ratio

Poisson's ratio for a soil may be evaluated from the ratio of the radial strain to axial strain during a tri-axial compression test. It is found that in general the test procedure influences the value of Poisson's ratio. For example although relatively constant values of Poisson's ratio are obtained from zero radial strain tests, the Poisson's ratio as determined by tri-axial compression tests vary with magnitude and range of the deviatoric stress m(Jacob, 1957; Barkan, 1962; Bishop and Henkel, 1962; Wade, 1963) Some typical values for the Poisson's ration v_s are shown in table 2.1 and table 2.2. In general values of 0.30 - 0.35 for sands and 0.40 - 0.50 for clays have been observed.

Terzaghi (1943) calculated a value of 0.30 for sand and values 0.40-0.43 for clays based on elastic considerations. That is, by considering the at rest value of earth pressure and the linear elastic stress- strain relations, it can be shown that

$$v_s = K_a/(1+K_a)$$

where $K_a = \tan^2(45 - \phi/2)$, and ϕ is the angle of internal friction.

Barkan (1962) indicates a range of 0.3-0.35 for sands. Tsytovich(1963) recommends Poisson's ratio values of 0.15-0.25 for sands and 0.35-0.40 for clays.

Table 2.1 Typical ranges for Poisson's ratio after Bowles (1977)

Type of Soil	v_s
Clay, saturated	0.4-0.5
Clay, unsaturated	0.1-0.3
Sandy clay	0.2-0.3
Silt	0.3-0.35
Sand (dense)	0.2-0.4
Coarse (void ratio = 0.4-0.7)	0.15
Fine grained (void ratio = 0.4 - 0.7)	0.25
Rock	0.1-0.4 (depends somewhat on type of rocks)

Table 2.2 Typical ranges for Poisson's ratio after Zeevaert (1972)

Type of soil	Compressibility	v_s
Lacustrine clays and silts	Very high	0.43-0.35
Clays and silts; lacustrine sandy silts; residual soils; loose volcanic dust	High	0.35-0.30
Compact clays and silts; fine aeolian sediments; residual soils and volcanic semi compact sediments; fine alluvium	Medium	0.30-0.25
Sans, compact gravels, alluvial soils; compact and well-graded sediments	Low	0.25
Sands, gravelly soils; compact, cemented and well-graded alluvial sediments	Very low	< 0.25

17

(b)   Modulus Of Elasticity

The modulus of elasticity is often determined from unconfined, triaxial, or oedometer compression tests. Plate loading tests and pressometer tests may also be used to determine the in situ modulus of elasticity of the soil. Some typical values of the modulus of elasticity are shown in table 2.3.

The modulus of elasticity is found to vary with the void ratio and also depends on the moisture content (Barkan, 1962) . The variation of E_s with the moisture content, m, may be expressed as

$$E_s = E_{s0} [1 - m^2/m_0^2]$$

where E_{so} is the modulus of elasticity at m=0 and m_0 is the moisture content at $E_s = 0$. Limiting value for m are approximately from 15 to 29% depending upon the type of soil constituent.

Barkan (1962) and Konovalov and Rudnitskii(1964) have observed that the modulus of elasticity for granular soils can also be affected by its porosity which in turn is influenced by the size and shape of the soil particles.

Bjerrum (1964) suggested the following relationship based on experiences with normally consolidated clays

$E_s = [250 \text{ to } 500] c_u$

in which c_u represents the undrained shear strength obtained from unconfined compressive tests or from field vane tests.

18

Table 2.3   Range of values of E_s for selected soils (after Bowles 1977)

Type of soil	E_s (kN/m^2)
Very soft clay	300-3000
Soft clay	2000-4000
Medium clay	4500-9000
Hard clay	7000-20000
Sandy clay	30000-42500
Glacial till	10000-16000
Loess	15000-16000
Silt	2000-20000
Silty sand	5000-20000
Loose sand	10000-25000
Dense sand	50000-100000
Dense sand and gravel	80000-200000
Loose sand and gravel	50000-140000
Shale	140000-1400000

Table 2.4   Some typical values for v_s and δ (after Litvinov, 1951)

Type and consistency of soil	v_s	δ
Dense sand	0.25	0.84
Loose sand	0.30	0.74
Clayey sand and silt	0.30	0.74
Firm and stiff sand-clays or silt-clays	0.35	0.63
Firm and stiff clays	0.40	0.47
Very stiff clays	0.20	0.90

here $\delta = (1+v_s)(1-2v_s)/(1-v_s)$

2.4   ANALYSIS METHODS

2.4.1 CONVENTIONAL METHOD OF ANALYSIS

In this method mat is treated as infinitely rigid giving planer soil pressure distribution. The mat is divided in both directions into strips centered on the column lines and having widths equal to half the spacing of column lines on each side of the column lines. Each strip is loaded by column loads and supported by soil pressure. This method can be used where the mat is very thick and column spacing and loading are fairly uniform. Though quite suitable for hand calculation, this method simply fails to represent the reality with mat foundation such as shear concentration near the loads.

The procedure for the conventional analysis consists of the following steps:

(1) The resultant of all loads acting on the mat and its location is determined from :

$$R = \sum_{i=1}^{n} P_i \tag{2.19}$$

$$e_x = \frac{\sum_{i=1}^{n} P_i X_i}{\sum_{i=1}^{n} P_i} - L_{x_m} \tag{2.20}$$

$$e_y = \frac{\sum_{i=1}^{n} P_i Y_i}{\sum_{i=1}^{n} P_i} - B_{y_m} \tag{2.21}$$

where

    R   = resultant of all column loads,

    X's   = x coordinates of the columns w.r.t. the corner of the mat,

    Y's   = y coordinates of the columns w.r.t. the corner of the mat,

P's = column loads,

n = total number of columns,

L_{x_m} = x dimension of mat,

B_{y_m} = y dimension of mat,

e_x = x eccentricity of R w.r.t. the center of the mat,

e_y = y eccentricity of R w.r.t. the center of the mat.

(2) The slab is divided into strips in x and y directions, one direction at a time, half way in-between the column lines. Each strip is assumed to act as an independent beam supported by soil pressure and acted upon by column loads. Steps 3 to 6 will be applicable to each of these strips.

(3) The soil pressure distribution is calculated using the equation:

$$ q = R(\frac{1}{A} + \frac{e_x x}{I_y} + \frac{e_y y}{I_x}) \qquad (2.22) $$

where

q = soil pressure at any point under the mat,

A = plan area of mat,

I_x, I_y = moment of inertia of A w.r.t. x and y axes,

x, y = co-ordinates of locations where soil pressures are desired w.r.t. the center of the mat.

Soil pressure is calculated at the four corners of the strip and their average is obtained from

$$ q_a = \sum_{i=1}^{4} q_i \qquad (2.23) $$

where

q_a = average soil pressure under the strip,

q_i = soil pressure at the corners of the strip.

This time a check is made that the maximum soil pressure is less than the allowable bearing capacity.

(4) q_a and the strip column loads are modified to enforce static force equilibrium. First, the average load on the strip is calculated by

$$Q_a = \frac{1}{2} \left(|BLq_a| + \left| \sum_{i=1}^{n_s} P_i^s \right| \right)$$ (2.24)

where

Q_a	= average load on the strip,
B	= width of the strip,
L	= length of the strip,
n_s	= no of columns in the strip,
P_i^s	= strip column loads.

The modified average soil pressure is calculated by

$$\overline{q}_a = \frac{Q_a}{LB}$$ (2.25)

The modified column loads F_i are determined from

$$F_i = \frac{Q_a}{\sum_{i=1}^{n_s} P_i^s} P_i^s$$ (2.26)

(5) To ensure moment equilibrium $\overline{q}_a$ is then shaped as a trapezoid so that the resultants of soil pressure and column loads meet at the same point. The end magnitudes of the soil pressure trapezoid is calculated as follows :

$$e_r = \frac{\sum_{i=1}^{n_s} F_i r_i}{\sum_{i=1}^{n_s} F_i} \qquad (2.27)$$

$$q_1 = 2\overline{q}_a(2 - \frac{3e_r}{L}) \qquad (2.28)$$

$$q_2 = 2\overline{q}_a(\frac{3e_r}{L} - 1) \qquad (2.29)$$

where

e_r = eccentricity of the resultant of the strip column loads w.r.t. the left end of the strip,

r's = distance of the strip column loads from the left end of the strip,

q_1 and q_2 = soil pressure intensity at the left and the right end of the strip respectively.

(6) The shear force and bending moment are calculated at the various points of the strip for the modified column loads and soil pressure.

Arora (1992) proposes that as the analysis is approximate, the actual reinforcement provided should be twice the computed values.

Applicability And Limitations

According to the ACI Committee 336 (1966), the design of mats may be accomplished using the conventional method if :

i) The average of the two adjacent spans in a continuous strip is less than 1.75/λ *(λ is defined later)* and adjacent column loads and column spacing do not vary by more than 20 percent of the greater value.

ii) The relative stiffness factor K_r is found to be greater than 0.5, where

$$K_r = \frac{EI_B}{E_s B^3}$$
(2.30)

where

E	= modulus of elasticity of materials used in structure,
I_B	= moment of inertia of structure per unit length,
E_s	= Modulus of elasticity of soil and
B	= Width of footing.

An approximate value of EI_B per unit length of building can be found by summing flexural rigidity of footing (EI_F), the flexural rigidity of each framed member (EI_b) and the flexural rigidity of any shear walls ($Eah^3/12$) where *a* and *h* are the thickness and height of the walls respectively; EI_B is given by:

$$EI_B = EI_F + \Sigma\, EI_b + \Sigma\, \frac{Eah^3}{12}$$
(2.31)

where

I_F	= Moment of inertia of footing.

2.4.2   ACI APPROXIMATE FLEXIBLE METHOD

ACI Committee 336 (1966) suggested this method for the general case of a flexible mat supporting columns at random locations with varying intensities of load. This procedure

is essentially based on Schleicher's solution of circular plate on Winkler medium. Shukla (1984) provided charts for easy calculation of moments and shear following this method.

The effect of a concentrated load on a flexible infinite slab resting on continuous spring support has been found to damp out quickly away from the load. It is, therefore, possible to consider mat as a plate of infinite dimension and determine the effect of a column load in a specific region, called the zone of influence, surrounding the load. This zone of influence is generally not large and beyond this zone moments and shears in mat is insignificant. The total effect of all the column loads at any point can thus be determined by superimposing the effect of all the column loads within whose zones of influence the point lies. If moments and shears are found along the edges then these are later applied in opposite direction at the same location and with a semi-infinite beam analysis their effects inside the mat is calculated and superimposed on the previous solution to have the final moments and shears. The later part of the analysis is called end correction and is a way of getting rid of the errors acquired by treating the mat infinite. Mat deflections, though unrealistic, can be calculated in the same manner.

This method can not take care of column base moments, does not model boundary conditions realistically and gives unsatisfactory result near the edges.

A problem can be systematically solved through the following steps.

(1) The flexural rigidity of the mat, D is calculated.

$$D = \frac{Et^3}{12(1 - v^2)}$$
(2.32)

where

    E   = modulus of elasticity,

            = 57000$\sqrt{f_c}$ psi for concrete (ACI 318-83, Section 8.5.1),

f_c = ultimate concrete strength in psi,

t   = thickness of mat in inch,

v   = Poisson's ratio of concrete (0.15 to 0.25).

(2) The radius of effective stiffness L is then calculated as follows:

$$L = \sqrt[4]{\frac{D}{k}} \qquad (2.33)$$

where

k   = modulus of subgrade reaction.

Radius of influence for any column load is 4L and calculation of deflections, bending moments, and shear forces due any column load will be limited within this zone around that column.

(3) Since the effect of each load is transmitted through the mat in a radial direction, polar co-ordinate system was used in the original solution. The radial and tangential moments, the shear and deflection at a point are calculated using the following formulae:

$$M_r = -\frac{P}{4}[Z_4\left(\frac{r}{L}\right) - (1-v)\frac{Z_3'\left(\frac{r}{L}\right)}{\frac{r}{L}}] \qquad (2.34)$$

$$M_t = -\frac{P}{4}[vZ_4\left(\frac{r}{L}\right) + (1-v)\frac{Z_3'\left(\frac{r}{L}\right)}{\frac{r}{L}}] \qquad (2.35)$$

$$Q = -\frac{P}{4L}Z_4'\left(\frac{r}{L}\right) \qquad (2.36)$$

$$w = \frac{PL^2}{4D}Z_3\left(\frac{r}{L}\right) \qquad (2.37)$$

26

$$Z_3\left(\frac{r}{L}\right) = \frac{1}{2}Z_1\left(\frac{r}{L}\right) - \frac{7}{11}\left[R_1\left(\frac{r}{L}\right) + Z_2\left(\frac{r}{L}\right)\log_e\{1.781\frac{r}{L}\}\right] \tag{2.38}$$

$$Z_4\left(\frac{r}{L}\right) = \frac{1}{2}Z_2\left(\frac{r}{L}\right) + \frac{7}{11}\left[R_2\left(\frac{r}{L}\right) + Z_1\left(\frac{r}{L}\right)\log_e\{1.781\frac{r}{L}\}\right] \tag{2.39}$$

$$Z_1\left(\frac{r}{L}\right) = \sum_{i=1}^{\infty} \frac{(-1)^{i+1}\left(\frac{r}{L}\right)^{4(i-1)}}{2^{4(i-1)}[\{2(i-1)\}!]^2} \tag{2.40}$$

$$Z_2\left(\frac{r}{L}\right) = \sum_{i=1}^{\infty} \frac{(-1)^{i}\left(\frac{r}{L}\right)^{4(i-1)+2}}{2^{4(i-1)+2}[\{2(i-1)+1\}!]^2} \tag{2.41}$$

$$R_1\left(\frac{r}{L}\right) = \sum_{i=1}^{\infty} \frac{(-1)^{i+1}\psi\{2(i-1)+1\}\left(\frac{r}{L}\right)^{4(i-1)+2}}{2^{4(i-1)+2}[\{2(i-1)+1\}!]^2} \tag{2.42}$$

$$R_2\left(\frac{r}{L}\right) = \sum_{i=1}^{\infty} \frac{(-1)^{i+1}\psi(2i)\left(\frac{r}{L}\right)^{4i}}{2^{4i}[\{2i\}!]^2} \tag{2.43}$$

$$\psi(n) = \sum_{i=1}^{n} \frac{1}{i} \tag{2.44}$$

where

P	= concentrated load,
r	= radial distance of the point under investigation from P,
M_r & M_t	= radial and tangential moments for a unit width of mat,
Q	= shear force per unit width of mat,
w	= mat displacement,
Ψ, R's and Z's	= functions first introduced by Schleicher(1926).

The Z and R functions have the characteristic features of exponential waves and it is accurate enough to calculate only 4 or 5 terms of those.

4) The radial and tangential moments are then converted into bending moments in cartesian co-ordinate system (Fig. 2.5) using the following formulae, whereas shear and displacements in the cartesian coordinate system remains the same.

$$M_x = M_r \cos^2 \phi + M_t \sin^2 \phi \qquad (2.45)$$

$$M_y = M_r \sin^2 \phi + M_t \cos^2 \phi \qquad (2.46)$$

where

M_x , M_y = bending moment about y and x axes respectively,

ϕ = angle of the radial line passing through the point under consideration w.r.t. the positive x axis in a counter clockwise direction.

(5) For the resultant effect of all the column loads, radii of influence of whose overlap at points of interest, the moments, shears and displacements due to individual columns are superimposed.

(6) If the edge of the mat is within the influence zone of some of the columns, at the end of the afore mentioned procedure there will be bending moments and shear forces along the edges. Since in a real life problem the edges should be free of forces, a correction should be applied. This is done as follows:

The mat is divided into strips of unit width in both directions. Assuming the strips as semi-infinite beams; shears and moments equal and opposite to those obtained in the previous analysis is applied and their effects at various points are superimposed on the respective values obtained earlier.

For moment, shear and deflection in a semi infinite beam, the following relationships are used :

$$M_c = M_e A_{\lambda r} - s \times \frac{V_e}{\lambda} B_{\lambda r} \qquad (2.47)$$

$$Q_c = -s \times 2 M_e \lambda B_{\lambda r} - V_e C_{\lambda r} \qquad (2.48)$$

$$w_c = -\frac{2 M_e \lambda^2}{k} C_{\lambda r} + s \times \frac{2 V_e \lambda}{k} D_{\lambda r} \qquad (2.49)$$

$$\lambda = \sqrt[4]{\frac{kB}{4 E I_b}} \qquad (2.50)$$

$$A_{\lambda r} = e^{-\lambda r}(cos\lambda r + \sin \lambda r) \qquad (2.51)$$

$$B_{\lambda r} = e^{-\lambda r} \sin \lambda r \qquad (2.52)$$

$$C_{\lambda r} = e^{-\lambda r}(cos\lambda r - \sin \lambda r) \qquad (2.53)$$

$$D_{\lambda r} = e^{-\lambda r} cos \lambda r \qquad (2.54)$$

where

M_c, V_c & w_c = end correction to moment, shear and displacement respectively,

M_e, V_e = end moment and shear respectively,

B = width of mat strip = 1,

I_b = moment of inertia of mat strip,

s = 1 for left side end forces,

  = -1 for right side end forces,

r = distance of the point under consideration from the end conditioning force M_e or V_e .

Variation of $A_{\lambda r}$, $B_{\lambda r}$, $C_{\lambda r}$ and $D_{\lambda r}$ with r and variation of C_{mr} and C_{mt} with x is shown in Fig.2.5 and Fig 2.6 respectively.
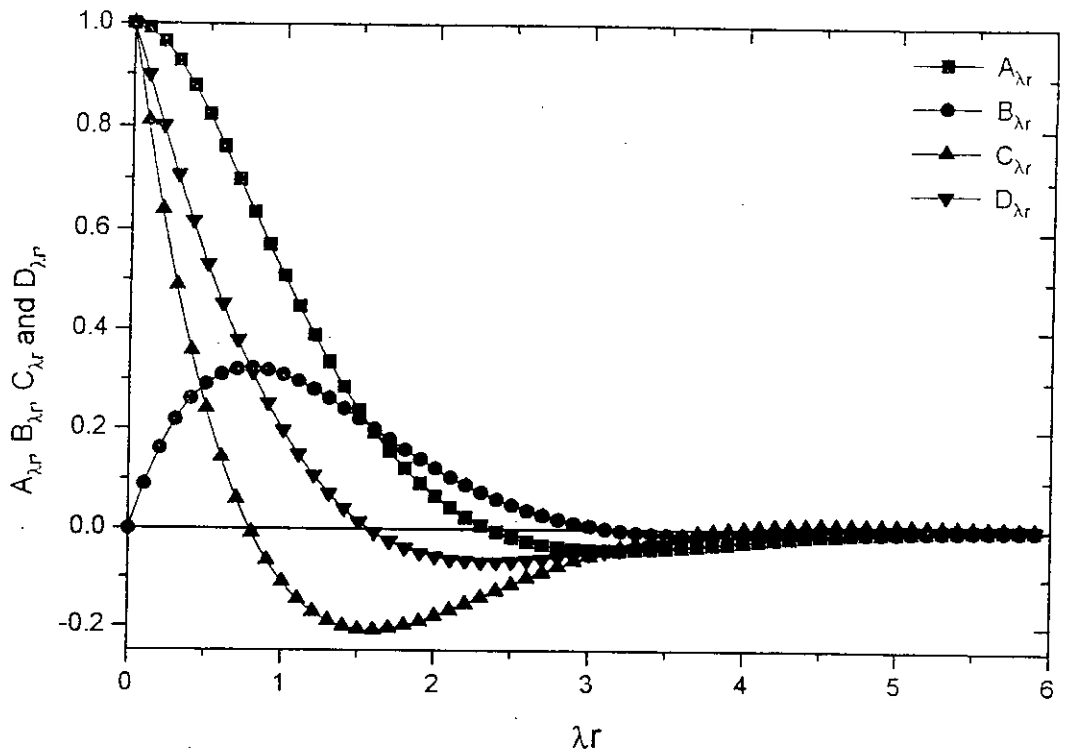
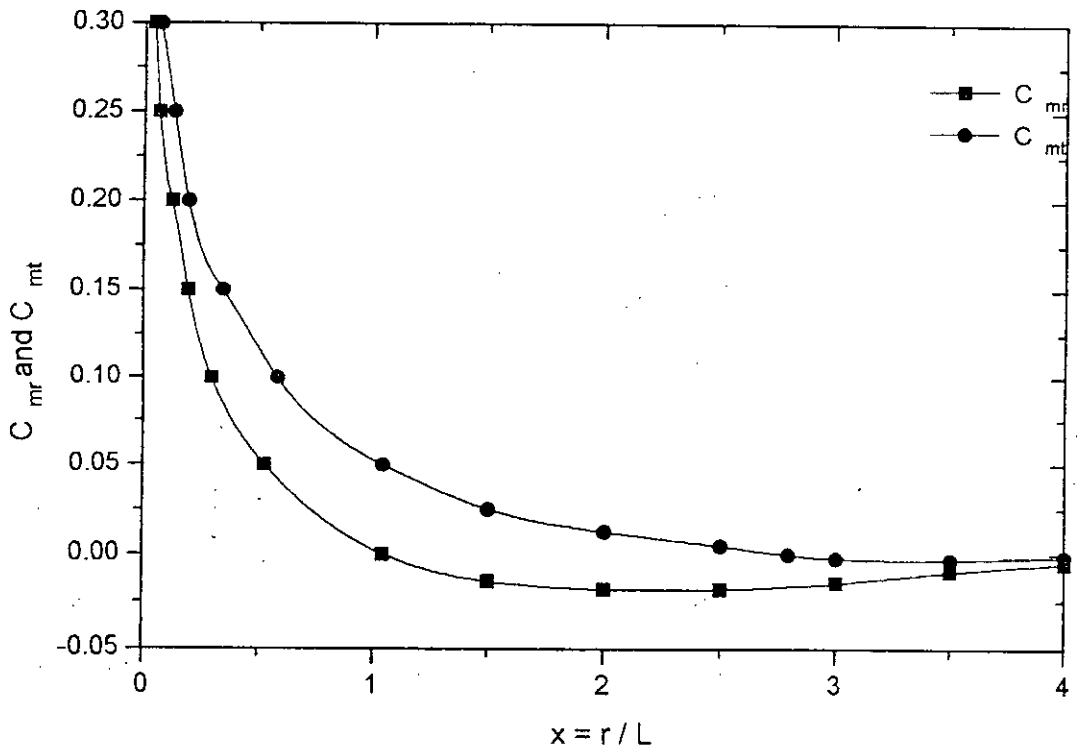Fig. 2.5 Variation of $A_{\lambda r}$, $B_{\lambda r}$, $C_{\lambda r}$ and $D_{\lambda r}$ with λr.

Fig. 2.6 Variation of C_{mr} and C_{mt} with $x = r / L$ [After Shukla (1984)].

CHAPTER 3

FINITE ELEMENT ANALYSIS OF MAT FOUNDATION

3.1 GENERAL

Finite element technique is the most powerful and versatile of all the available numerical analysis techniques. In this method, the structure to be analyzed is modeled as an assemblage of a finite number of discrete interconnected elements and the displacements of the connecting points, called the nodal points, of these elements are taken as the basic unknowns. The applied loads are transformed into equivalent nodal loads and for each element, the relationship between the nodal loads and nodal displacements is established. Then with a suitable assembling of the element load-displacement relationship, sufficient number of load-displacement relations for the whole structure can be found which, upon solution, give the nodal displacements. Once known, these displacements are used to calculate stresses at the nodes or at points within the elements.

3.2 IDEALIZATION OF MAT FOUNDATION ON WINKLER MODEL

3.2.1 Selection of Element

Mat foundation is a three dimensional thick plate structure. In case of mat, transverse flexural shears and bending moments are the most important internal forces produced in response to the loads it usually encounters e.g. axial column forces and column base moments. Thick shell element [Ref. 3] is one of the most suitable elements which matches all of these above mentioned criteria. It can represent the thickness of the mat by its very own geometry. Also, in thick shell elements the nodal variables are taken to be the displacements of nodal normals which, though approximately normal to the undeformed middle surfaces of the elements, are not necessarily

normal to the deformed middle surface, leaving scope for transverse shear stress and shear strain calculation.

The program that is used is as the core computer program was written by Ahmad (1969) who also devised the element. There are two types of Ahmad's element, namely 8 noded element and 12 noded element. For the present study the first one is used since it gives results accurate enough.

3.2.2 Element Mesh Configuration

The simplest element division scheme is adopted for mat. It makes both data generation and result interpretation straight forward. The mesh used here is a rectangular grid with the option of finer elements near column loads. The mesh is characterized by the number of X and Y directional divisions of the grid and at present, each of these can be increased upto fifty. Details of the mesh are shown in Fig 3.1.

3.2.3 Element and Node Numbering and Determination of the Front Width

The program uses frontal solution technique to evaluate nodal displacements. So in order to minimize computer memory requirement, the front must be as narrow as possible. This is accomplished by efficient numbering of elements. Front can be narrowed by numbering the elements serially from one corner of the mat to the other. As the Gauss point stresses are calculated element wise, so the numbering of Gauss points is done elementwise. Since two point Gauss integration is used (though three point integration is possible within the scope of the program), each element contains four Gauss points. The node numbering scheme is such that it makes nodal coordinate generation simple. Nodes are numbered serially from one corner of the mat to the other corner. Details of the node and element numbering scheme are given in Fig. 3.2 and Fig. 3.3.
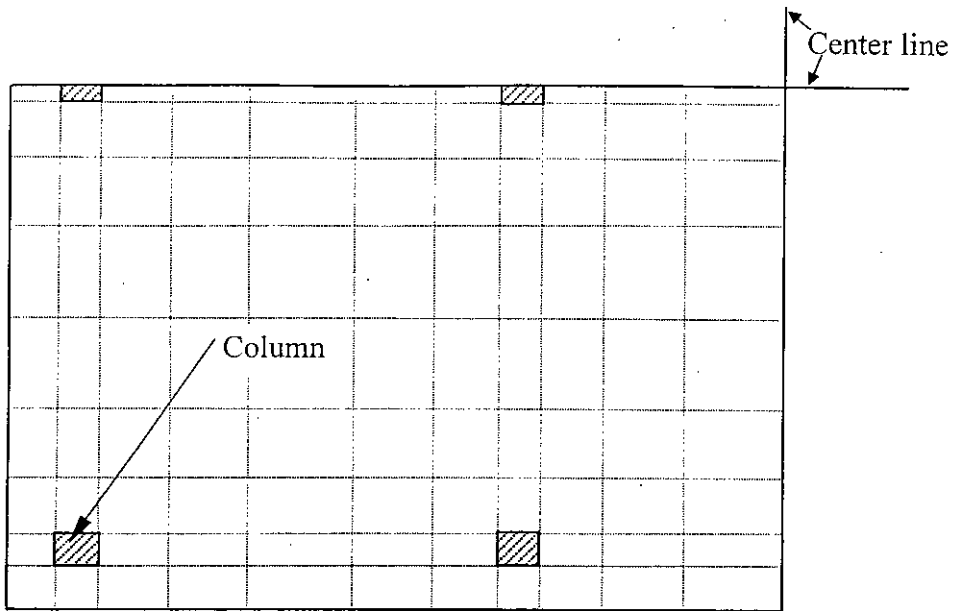
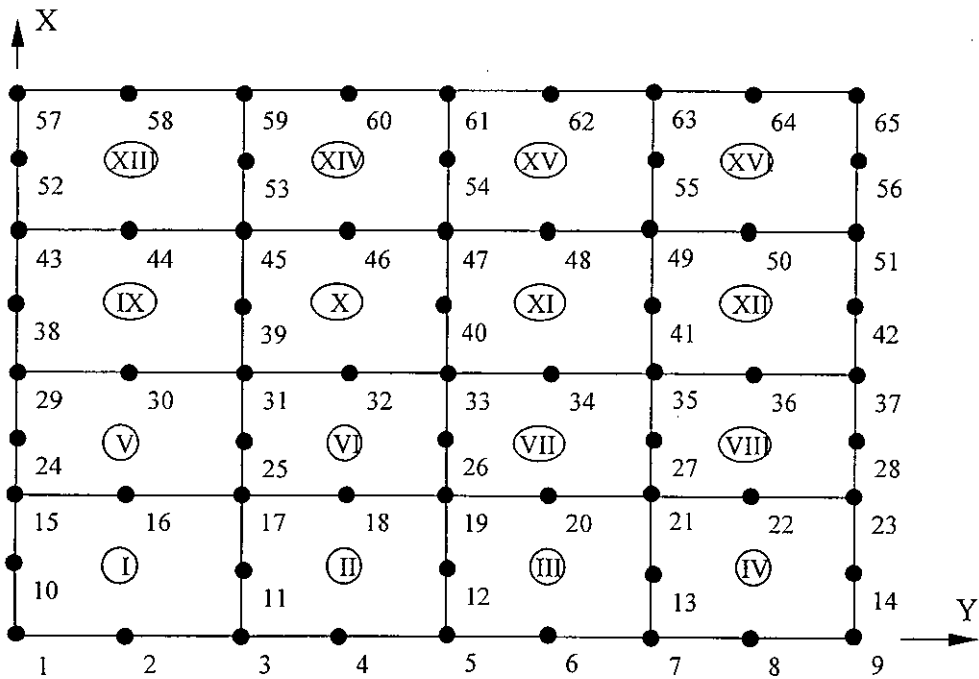Fig. 3.1. Typical finite element mesh for mat foundation.

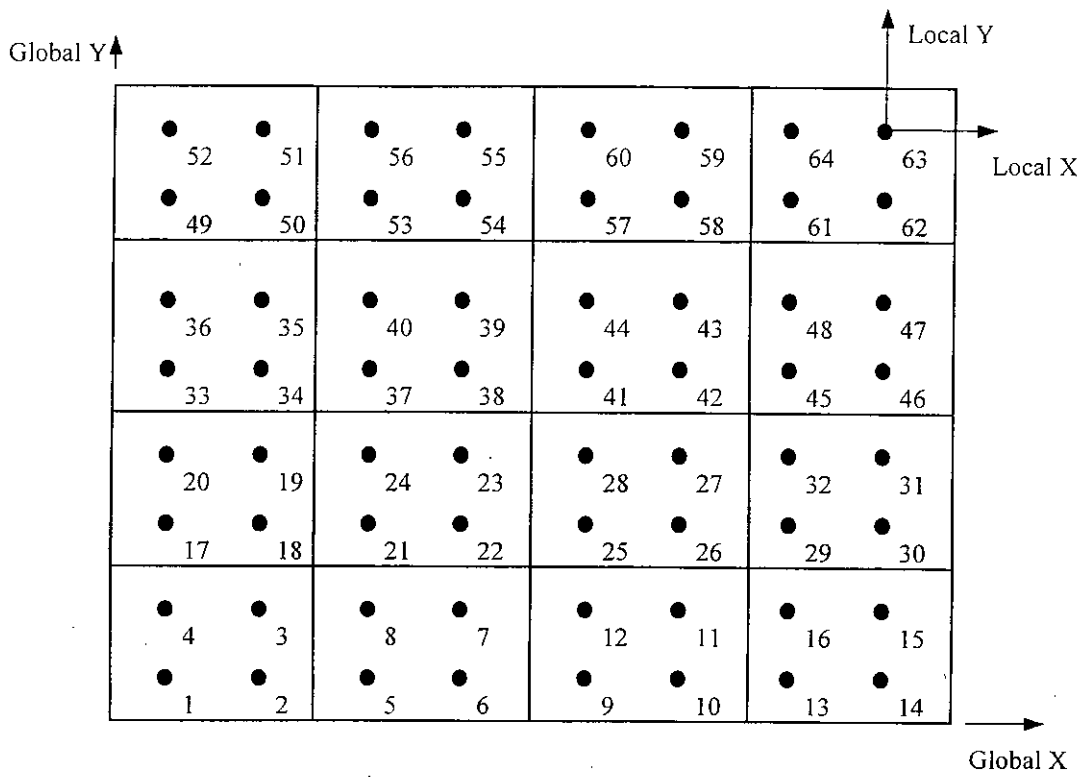Fig. 3.2. A typical finite element mesh for mat with element and node numbering.

Fig. 3.3. A typical finite element mesh for mat with Gauss point numbering and global and local axes (Z axes are perpendicular to the XY plane at the intersection of X and Y axes of the corresponding system).
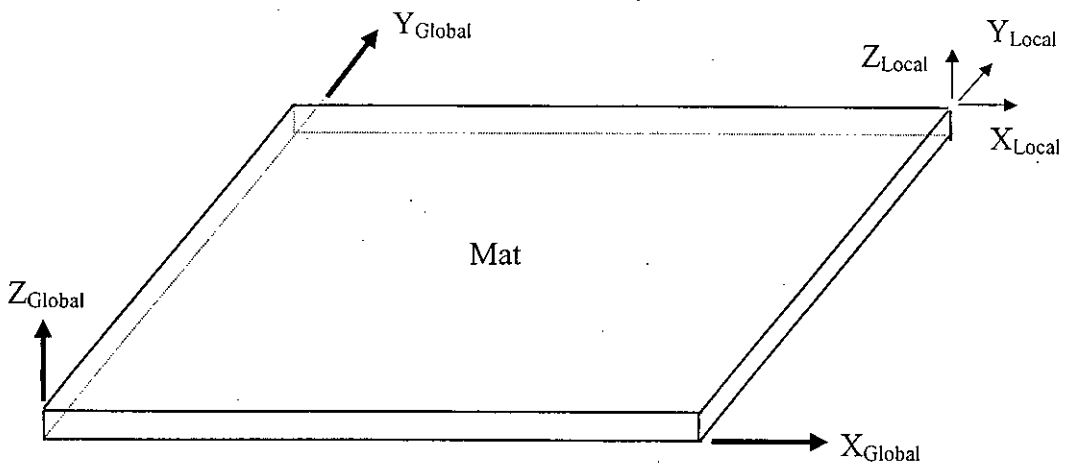

Fig. 3.4. Global and local coordinate systems for mat foundation.

Under the scheme adopted, total number of elements N_e, total number of nodes N_n, total number of Gauss points N_g and the front width F_w can be calculated as follows:

$$N_e = H_d \times H_v \tag{3.1}$$

$$N_n = H_v \times (3 \times H_d + 2) + 2 \times H_d + 1 \tag{3.2}$$

$$N_g = 4 \times N_e \tag{3.3}$$

$$F_w = 40 + 16 \times (H_d - 1) \tag{3.4}$$

where

$\quad H_d \quad$ = number of X directional divisions,

$\quad V_d \quad$ = number of Y directional divisions.

3.2.4   Selection of the Global and the Local Axes

As the mat is a flat block type structure, selection of the global and local axes is very straight forward. The global axis system is so selected that the bottom face of the mat away from the columns is the XY plane (i.e. in case of greater thickness of mat under the columns, the extra thickness goes below the XY plane), the leftmost face of the mat is the YZ plane and the front face is the ZX plane. Details are shown in Fig. 3.4.

The program takes data and gives output with respect to the global axes but to calculate shears and moments, stresses in local coordinate system are needed. The advantage of the simple shape of mats under consideration is taken by choosing a local axis system parallel to the global one having its origin at the node of interest.

3.2.5   Modeling of Soil and Boundary Conditions

Supporting soil is modeled as Winkler medium . Soil springs may be uniform or may be zoned to incorporate the coupling effect of soil springs.

Uniformly distributed soil springs are first concentrated at the nodes. This is done element wise and by lumping the total spring stiffness under an element at its nodes. There are two approaches to accomplish this purpose. These are :

(a) Equivalence between the nodal spring stiffnesses and the distributed spring stiffness under the concerned element is made by adopting a model which assumes that middle nodes takes twice as much stiffness as the corner nodes.

(b) Middle nodes takes thrice as much stiffness as the corner nodes according to the contributing area concept as shown in Fig. 3.5.

3.2.6 Application of Column Loads

Both column axial loads and column base moments can be applied. Column axial load may be applied as concentrated load or it may be distributed over an area equal to the cross-section of the column by taking an element, designated as *column element*, there and applying the load as a uniform surface pressure (Fig. 3.6). Similarly, column base moments may be concentrated or distributed. The later is accomplished by resolving column base moment into nodal loads acting at the nodes of the column element along the sides parallel to the axis of the moment (Fig. 3.6).In this case, middle nodes take four times load than corner nodes as justified by the shape functions.

To simulate the higher rigidity of column elements with respect to other portions of the mat, modulus of elasticity of column elements is increased.

3.2.7 Transformation of Stresses and Calculation of Shear Forces and Bending Moments

For calculating bending moments and shear forces, global stresses are transformed into local stresses first. This is done as follows :
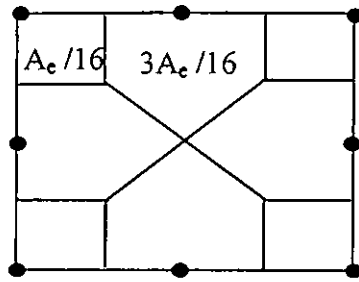
Fig. 3.5. Distribution of nodal springs by contributing area (A_e = area of the element).

(a)

(b)

$p_c = P / C_X C_Y$

(c)

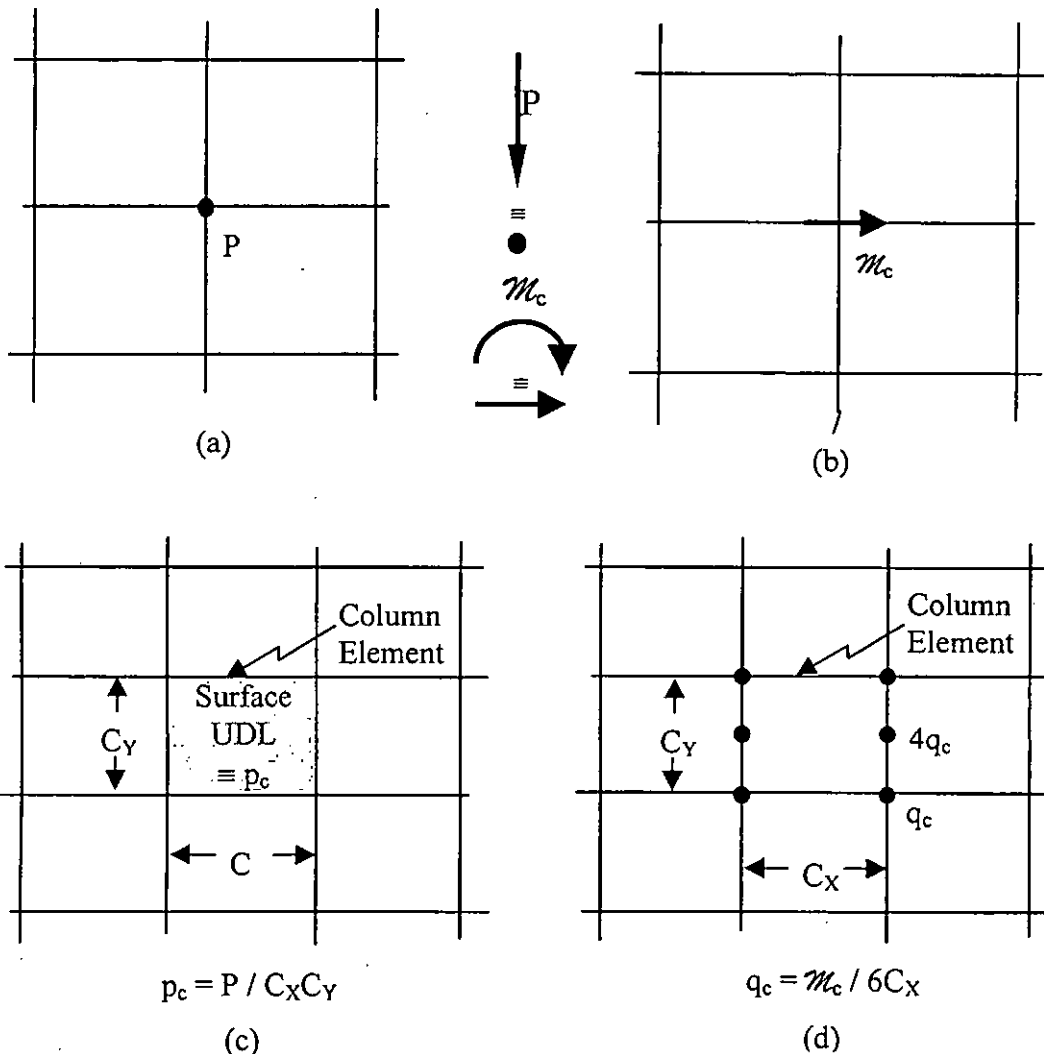$q_c = \mathscr{M}_c / 6C_X$

(d)

Fig. 3.6. Different modes of application of load : (a) Concentrated axial column load; (b) Concentrated column base moment; (c) Distributed axial column load and (d) Distributed column base moment ($\mathscr{M}_c$ = column base moment and P = column axial load).

36

$$[\sigma'] = [\theta_c][\sigma][\theta_c]^T \tag{3.5}$$

where

$[\sigma']$ = local stress matrix,

$[\sigma]$ = global stress matrix,

$[\theta_c]$ = direction cosine matrix of the local axes w.r.t. the global axes.

Here

$$[\sigma'] = \begin{bmatrix} \sigma'_{xx} & \tau'_{xy} & \tau'_{zx} \\ \tau'_{xy} & \sigma'_{yy} & \tau'_{yz} \\ \tau'_{zx} & \tau'_{yz} & \sigma'_{zz} \end{bmatrix} \tag{3.6}$$

$$[\sigma] = \begin{bmatrix} \sigma_{xx} & \tau_{xy} & \tau_{zx} \\ \tau_{xy} & \sigma_{yy} & \tau_{yz} \\ \tau_{zx} & \tau_{yz} & \sigma_{zz} \end{bmatrix} \tag{3.7}$$

$$[\theta_c] = \begin{bmatrix} \cos\theta_{x'x} & \cos\theta_{x'y} & \cos\theta_{x'z} \\ \cos\theta_{y'x} & \cos\theta_{y'y} & \cos\theta_{y'z} \\ \cos\theta_{z'x} & \cos\theta_{z'x} & \cos\theta_{z'x} \end{bmatrix} \tag{3.8}$$

where

σ's and σ'''s   = global and local normal stresses respectively,

τ's and τ'''s   = global and local shear stresses respectively,

θ's   = angles between the global and local axes.

In Equation 3.6 and Equation 3.7, the first subscript of any stress term denotes the normal to the surface on which the stress acts and the second one stands for its own direction. In Equation 3.8, the first subscript of any angle term represents the local axis and the second one denotes the global axis.

Now, as the selected local and global axis systems are parallel, $[\theta_c]$ is a unit matrix. So local stresses are the same as the global stresses. Sign of any stress is obtained by multiplying the sign of the normal of the plane on which it acts by that of the direction of the stress itself.
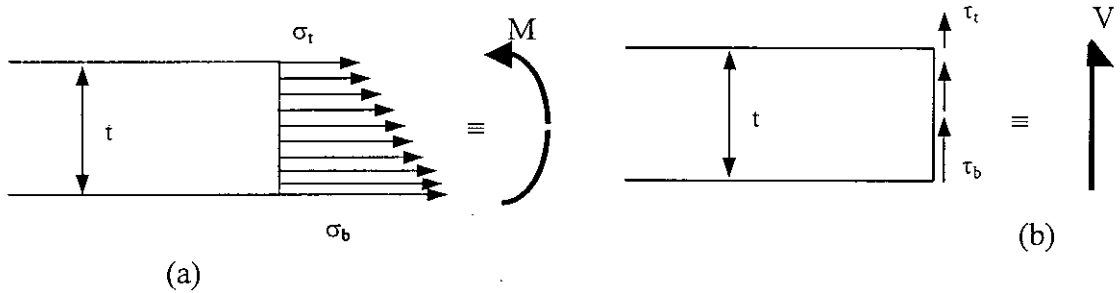
Fig. 3.7. Calculation of (a) bending moment and (b) shear force from normal and shear stresses respectively.

Having found the local stresses, bending moments and shear forces per unit width can be calculated at the Gauss or nodal points, using Gauss point or nodal stresses respectively, according to the following formulae for any desired direction (Fig. 3.7)

$$M = (\sigma_b - \sigma_t) \times t^2 \div 12 \qquad (3.9)$$

$$V = (\tau_b + \tau_t) \times t \div 2 \qquad (3.10)$$

where

σ_b, σ_t = bottom and top normal stresses respectively,

τ_b, τ_t = bottom and top shear stresses respectively,

M = bending moment per unit width,

V = shear force per unit width,

t = thickness of the mat at the location of the stresses.

Bending moments are positive if they cause compression at the top fibers. Shear forces are positive if they act downward on the right faces of z directional sections through the mat at the corresponding locations.

38
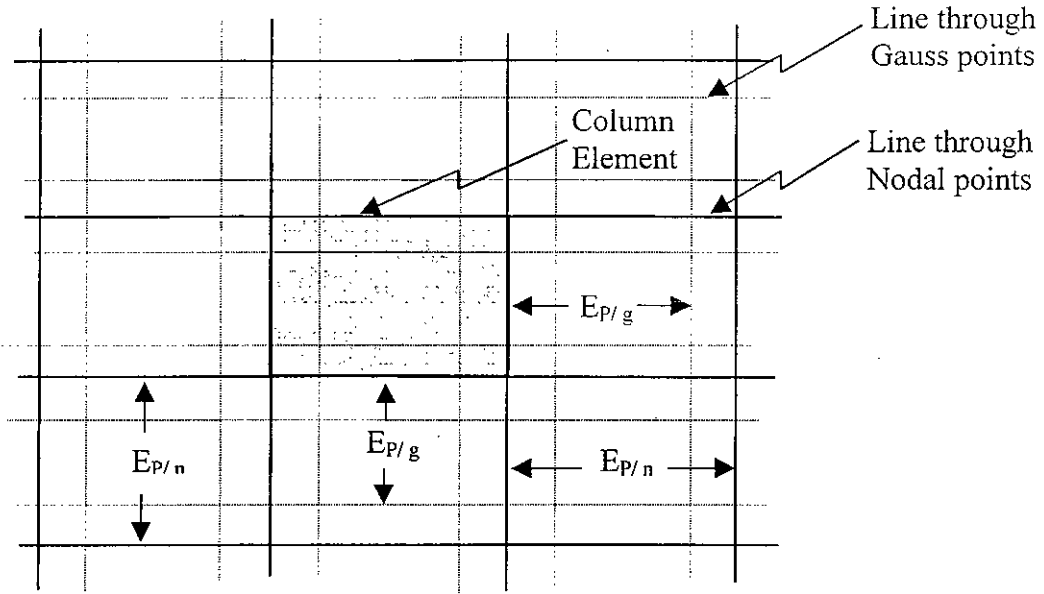
$E_{P/n} = d/2$ & $E_{P/g} = 0.394d$ for nodal stress analysis

$E_{p/g} = d/2$ & $E_{P/n} = 0.634d$ for Gauss stress analysis

Fig. 3.8.   Adjustment of element dimensions around columns for punching shear calculation.

3.2.8   Calculation of Punching Shear

Punching shear around a column is calculated by taking elements of width $E_{p/n}$ around the column and integrating the flexural shear forces per unit width at the nodes or Gauss points along or near the outer periphery of these elements (Fig. 3.8). Here

$$E_{P/n} = d/2 \text{ for nodal stress analysis,}$$

$$\qquad\qquad 0.634d \text{ for Gauss point stress analysis,} \qquad (3.11)$$

$$d = t - C_c . \qquad\qquad (3.12)$$

where

C_c = distance of the reinforcement centroid from the nearest mat surface.

To perform the numerical integration of the nodal or Gauss point shear forces in order to obtain punching shear, Gauss integration scheme is used in case of Gauss point stress analysis. For nodal stress Simpson's method is followed on Gauss stress.

39

3.3   SOME CRITICAL ASPECTS OF FINITE ELEMENT ANALYSIS OF MAT FOUNDATION

3.3.1   Selection of Finite Element Mesh

Since FE is a numerical approach, accuracy of solution increases with the number of elements to which the mat is divided. However, solution is by its very nature converging and a point comes when further refinement of finite element mesh adds nothing significant to the accuracy. Taking the maximum deflection as the deciding criterion, a plot of maximum deflection versus the number of elements in the finite element mesh of the example mat (Fig.3.9) shows that number of elements in excess of 300 takes more computational time. So a final mesh of 361 elements (19 rows and 19 columns of elements) is selected which appears to be more than sufficient for the present study. (Fig. 3.10)

3.3.2   Effect of Column Rigidity

Columns are monolithically built with mat and they act integrally with it. Height of columns highly increases the rigidity of mat at these locations. This effect is realized by increasing the value of modulus of elasticity of the portions of mat under the columns. To quantify this effect, column deflections, column face moments and shears are plotted against the ratio of the modulus of elasticity of the under-column portions and that of the rest of the mat in Fig.3.11 through Fig.3.12. It appears that effect of column rigidity dies out with the increase of this modulus of elasticity ratio. Examining these, a modulus of elasticity ratio of 8 is found to be justified.
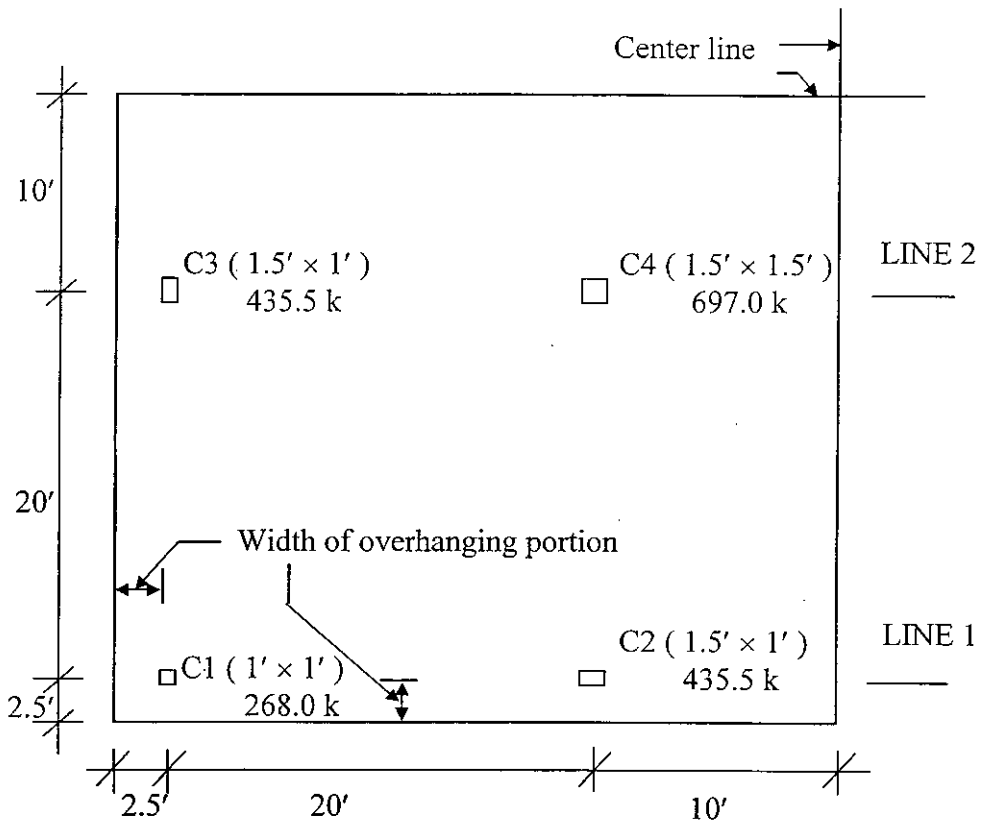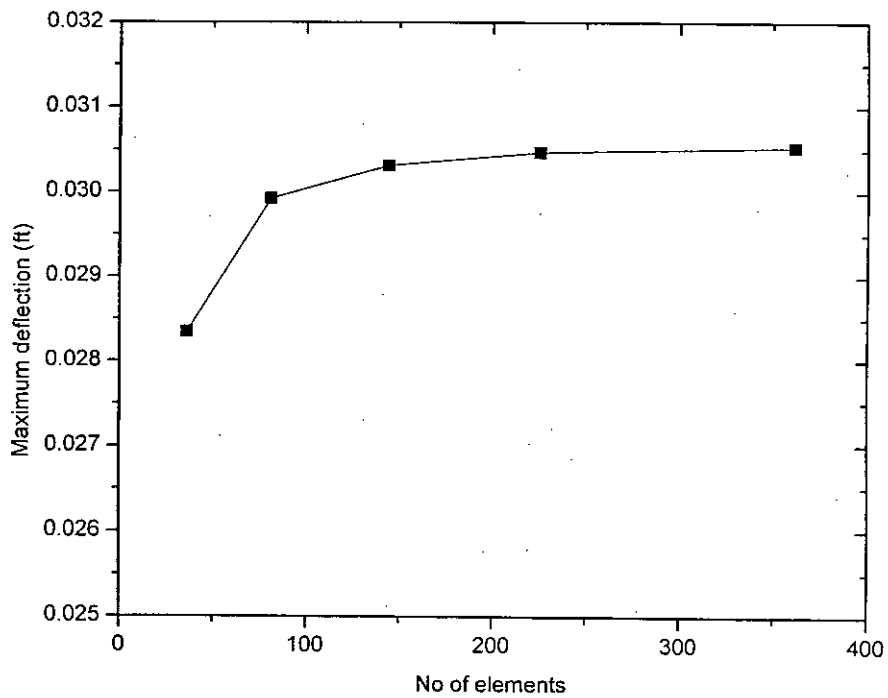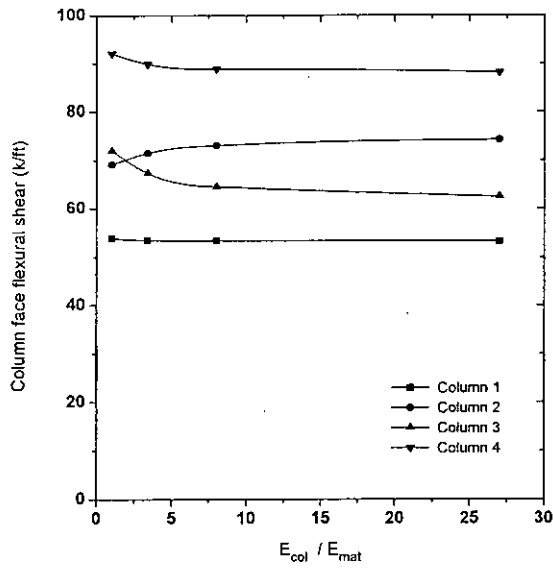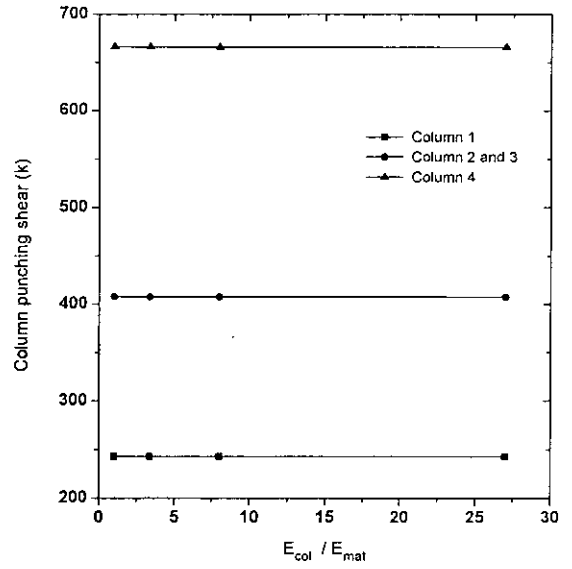
Fig. 3.9 Plan of the example mat
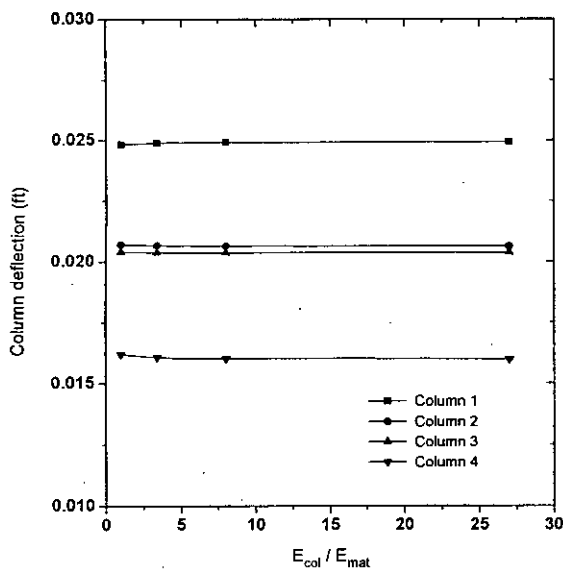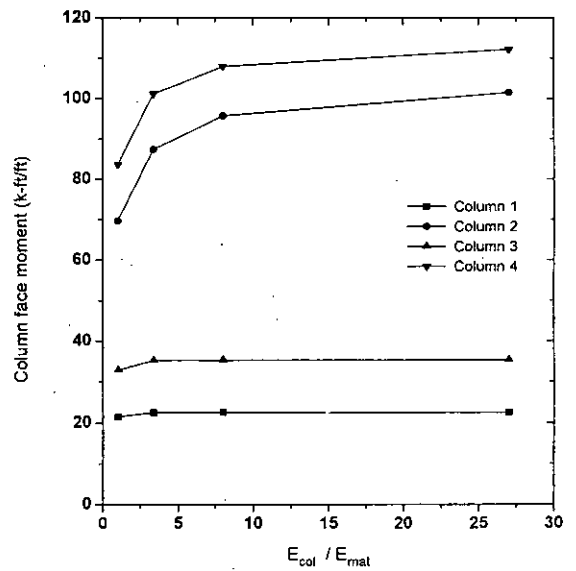

Fig. 3.10   : Effect of mesh refinement on deflection

41

Fig. 3.11 : Effect of column rigidity on (a) flexural and (b) punching
shear (mat thickness 3 ft)

Fig. 3.12 : Effect of column rigidity on (a) column deflection
and (b) column face bending moment

3.4 FINITE ELEMENT ANALYSIS ON TWO PARAMETER FOUNDATION MODEL

3.4.1 Two Parameter Foundation Model

A single layer elastic foundation of finite thickness H is considered. The subject matter will be restricted to the problems where the horizontal displacement is negligible. With this assumption, the distribution of displacements and the normal stresses in the vertical z direction over the height H is determined by a function $\Psi(z)$. In addition, it is assumed that the shear stress at the interface between the compressible layer and the rigid base equals to zero. The vertical displacement could therefore be expressed as

$$W(x, y, z) = W(x, y) \, \Psi(z) \tag{3.13}$$

in which $W(x, y)$ = the vertical deflection of the foundation surface and $\Psi(z)$ = the function of transverse distribution of the displacements, chosen in accordance with the nature of the foundation.

For a relatively thin compressible layer of foundation, the variation of the normal stresses with depth may be small and therefore could be considered as constant with depth. Under these conditions, the form of the $\Psi(z)$ function could be

$$\psi(z) = \frac{H - z}{H} \tag{3.14}$$

In a thick layer of foundation, the normal stresses vary considerably with depth and therefore the form of $\Psi(z)$ function must take a different form. In order to account for the decrease of the displacements and the normal stresses with depth, the $\Psi(z)$ function could be selected as

$$\psi(z) = \frac{\sinh \gamma (H - z) / m}{\sinh \gamma H / m} \tag{3.15}$$
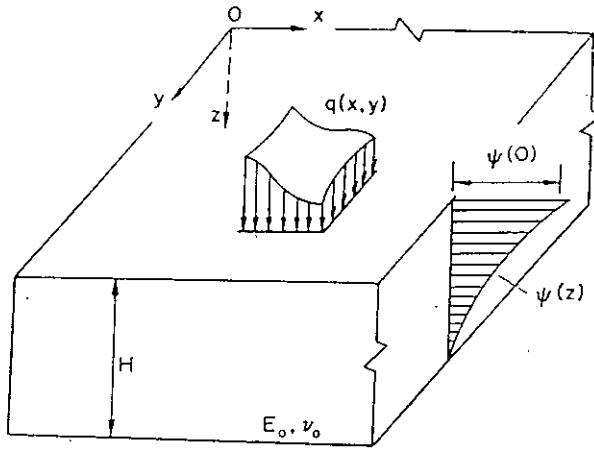
Fig 3. 14   Single-layer two-parameter foundation model.

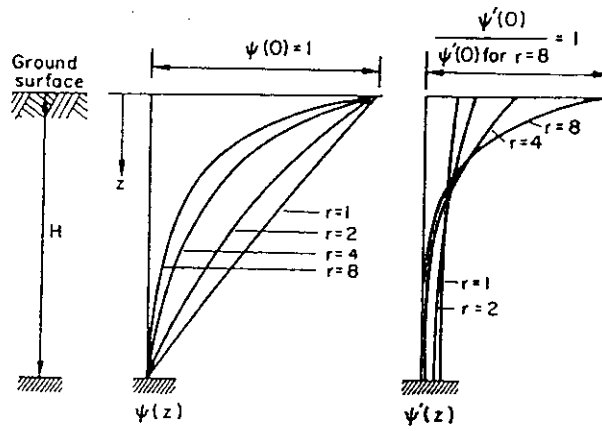Fig. 3.15   Rate of decrease of functions $\psi(z)$ and $\psi'(z)$ with depth.
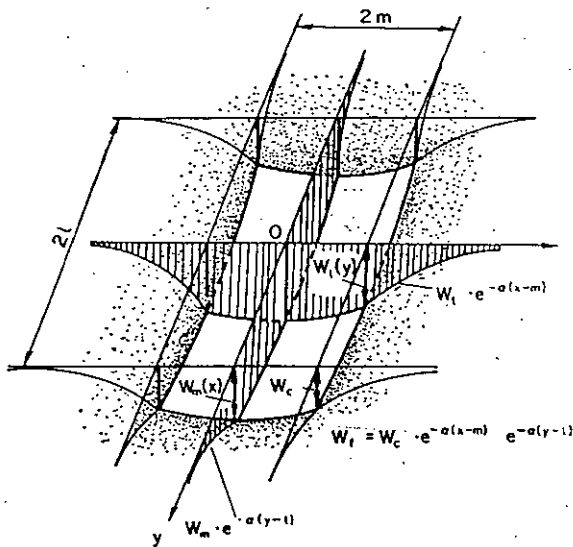

Fig 3.16 Displacements of foundation surface beyond plate edges.

where m is one of the dimensions of the subsequently considered plate (Fig.3.14) and γ is a constant determining the rate of decrease of the displacements with depth (Fig.3.15). With this form of $\Psi(z)$, it is seen that the normal stresses vary with depth as the hyperbolic cosine. This form of $\Psi(z)$ can also be used for the semi-infinite layer where H becomes infinity.

Depending on the nature of the particular problem many analytical expressions in addition to equation (3.14) and (3.15) can be selected. In fact, the expression could be based on experimental data of normal stress distribution.

Based on the conventional stress-strain and strain-displacement relationships, together with the displacement of all points expressed by equation (3.13), the condition of equilibrium of the foundation model to an externally distributed load q(x, y) on the surface (Fig.3.14) is given by the differential equation

$$-2t\nabla^2 w(x, y) + kw(x, y) = q(x, y)\,\Psi(0) \qquad (3.16)$$

in which

$$\nabla^2 = \frac{\partial^2}{\partial x^2} + \frac{\partial^2}{\partial y^2}$$

is the Laplace operator, and

$$k = \frac{E_0}{1-v_0^2}\int_0^H \psi(z)^2\,dz\;; \qquad t = \frac{E_0}{4(1+v_0)}\int_0^H \psi(z)^2\,dz \qquad (3.17)$$

are the two elastic parameters of the single-layer foundation; in which

$$E_0 = \frac{E_s}{1-v_s^2} \quad \text{and} \quad v_0 = \frac{v_s}{1-v_s}\;.$$

43

where E_s and v_s are respectively the modulus of elasticity and Poisson's ratio of the foundation.

For the transverse displacement function as described by equation (3.14), the two parameters k and t become

$$k = \frac{E_0}{H(1-v_0^2)}; \qquad t = \frac{E_0 H}{12(1+v_0)} \qquad (3.18)$$

For the transverse displacement function as described by equation (3.15), the two parameters k and t become

$$k = \frac{E_0 \gamma}{2m(1-v_0^2)} \cdot \frac{\sinh(\gamma H/m)\cosh(\gamma H/m) + \gamma H/m}{\sinh^2 \gamma H/m}$$

$$t = \frac{E_0 m}{8\gamma(1+v_0)} \cdot \frac{\sinh(\gamma H/m)\cosh(\gamma H/m) - \gamma H/m}{\sinh^2(\gamma H/m)} \qquad (3.19)$$

3.4.2 Plates On An Elastic Single-Layer Foundation Model With Two Parameters

Consider a plate on an elastic single-layer foundation whose properties are as described previously. Friction and adhesion between the plate and the surface of the foundation will be neglected.

$$\nabla^2 \nabla^2 w(x,y) = \frac{p*(x,y)}{D} \qquad (3.20)$$

in which, p*(x, y) is the distributed load on the plate and

$$D = \frac{Eh^3}{12(1-\mu^2)}$$

is the flexural rigidity of the plate.

Since the plate lies on an elastic foundation, the distributed load consists of the given surface loads p(x, y) and the foundation bearing pressure q(x, y),

$$p*(x,y) = p(x,y) - q(x,y) \qquad (3.21)$$

Substitution of equation (3.17) and (3.21) into equation (3.20), with the assumption that
$\Psi(0) = 1$, yields :

$$D \nabla^2 \nabla^2 w(x, y) - 2t \nabla^2 w(x, y) + kw(x, y) = p(x, y) \qquad (3.22)$$

An examination of equation (3.22) shows that the first term depends on the internal bending stresses in the plate, while the second and third terms depend on the reactions of the elastic foundation, distributed over the surface supporting the plate and caused by the compressive and shearing strains in the elastic foundation.

In addition to these forces and the distributed load p(x, y), the fictitious reactions Q which act along the plate edges must be considered. These fictitious reactions are introduced to make allowance for the three dimensional deformation of the elastic foundation beyond plate edges. For the case of rectangular or polygonal plates, fictitious concentrated reactions R arise at the plate corners.

3.4.3   Determining the Edge and Corner Reactions

In order to determine the fictitious edge reactions Q and corner reactions R, one must know the distribution of vertical displacements of the elastic foundation surface beyond the plate edges.

Depending on the nature of the particular foundation property, many complex analytical or experimental expressions can be selected for the three dimensional displacements of the elastic foundation beyond the plate edges. In the present analysis, the vertical displacements w_f are assumed to obey the following approximate exponential law (Fig.3.16)

In the positive direction of the x axis

$$w_f(x, y) = w_l(y)e^{-\alpha(x - m)} \qquad (3.23)$$

in the positive direction of the y axis

$$w_f(x, y) = w_m(x)e^{-\alpha(y - l)} \qquad (3.24)$$

where $\alpha = \sqrt{(k/2t)}$; $w_l(y)$ and $w_m(x)$ are respectively the vertical pressure along the long plate and short plate edges. The following law is also assumed for the vertical displacements of the foundation in the region $|x| > m$, $|y| > l$

$$w_f(x, y) = w_c e^{-\alpha(x - m)} e^{-\alpha(y - l)} \qquad (3.25)$$

where w_c is the vertical displacement of the plate corner.

Employing the deflection functions of equations (3.23-3.25) the generalized equilibrium conditions of a differential plate element can be set through the principle of virtual work and the fictitious edge and corner reactions can be obtained

$$Q_l = 2t\left[\alpha w_l + \left(\frac{\partial w}{\partial x}\right)_l - \frac{1}{2\alpha}\left(\frac{\partial^2 w}{\partial y^2}\right)_l\right], \qquad (3.26)$$

where the derivation of $w(x, y)$ are taken at $x = \pm m$,

46

$$Q_m = 2t \left[\alpha w_m + \left(\frac{\partial w}{\partial y} \right)_m - \frac{1}{2\alpha} \left(\frac{\partial^2 w}{\partial x^2} \right)_m \right],$$

where the derivation of w(x, y) are taken at y = ± 1, and

$$R = 1.5 t w_c \tag{3.27}$$

Where w_c is the corner deflection.

3.4.4 Finite Element Stiffness Formulation

The formulations described above are valid for an arbitrary plate finite element, i.e. arbitrary shape and displacement patterns.

The equilibrium equation of a plate lying on an elastic foundation has been shown in previous section [equation (3.22)]. This equation may also be written in a stiffness matrix form for any appropriate developed plate finite element,

$$[k_1]\{\delta\} - 2t[k_2]\{\delta\} + k[k_3]\{\delta\} = \{p\} \tag{3.28}$$

or

$$[k^*]\{\delta\} = \{p\} \tag{3.29}$$

in which,

{p} = vector of nodal loads on the plate element;

{δ} = vector of element flexural nodal displacements;

$[k_1]$ = conventional element stiffness matrix for plate flexure, corresponding to term $D\nabla^4 w$ in equation (3.22);

$2t[k_2]$ = friction stiffness matrix of foundation beneath the plate element corresponding to term $2t\nabla^2 w$ of equation (3.22); and

$k[k_3]$ = compressive stiffness matrix of foundation beneath the plate element corresponding to term kw in equation (3.22).

47

It is of interest to point out that equation (3.28) can be visualized as an equilibrium equation of motion of a freely vibrating plate with a harmonic frequency equal to unity and the plate mass density equal to k, while the plate is subjected to a pair of orthogonal in-plane compressive stresses equal to 2t (no in-plane shear). With this analogy in mind, it is clear that 'friction stiffness' matrix $2t[k_2]$ of the foundation beneath the plate element is similar to the 'initial stress' matrix for the buckling and large deflection analysis of plate, in which the two orthogonal in-plane stresses equal to 2t and in-plane shearing stresses vanishes. It is also clear that the 'compressive stiffness' matrix $k[k_3]$ of the foundation beneath the plate element is identical to the 'consistent mass' matrix of a freely vibrating plate element where the mass density is replaced by compressive spring constant k and the natural frequency is set to unity.

After assemblage, the overall stiffness matrix for the total system is symbolized by capital-letters as below:

$$[K_1]\{\Delta\} - 2t[K_2]\{\Delta\} + k[K_3]\{\Delta\} = \{P\} \qquad (3.30)$$

$$[K^*]\{\Delta\} = \{P\} \qquad (3.31)$$

3.4.5 Analysis Of Plates With Free Edges

The determine of edge and corner fictitious reactions of a loaded plate on an elastic foundation requires the knowledge of the deflection shape of the plate while the deflection shape cannot be found until the fictitious reactions of the plate edges and corners are known. To analyze such a problem requires the solution of equation (3.26) to (3.31) simultaneously. An iterative approach seems desirable at this point and is proposed below:

(1)   neglect the fictitious edge and corner reactions as given by equations (3.26) to (3.27), then apply the boundary conditions and external loads to solve equation (3.30) for nodal deflections $\{\Delta\}$,

48

(2)   based on the nodal deflections, the fictitious edge and corner reactions can be obtained from equations (3.26) to (3.27) by the use of standard forward finite difference technique. For simplicity of computer programming, the same finite element gridwork may be used as the gridwork for finite difference,

(3)   apply the external load and the fictitious reactions obtained in previous step simultaneously to obtain solutions for a revised vector of nodal deflections $\{\Delta\}$ from equation (3.31), and

(4)   employ the revised nodal deflections $\{\Delta\}$ to seek revised fictitious reactions and repeat processes (2) and (3) until the desired convergence of iteration is achieved.

During the iterative process, the total stiffness matrix $[K^*]$ has to be inverted only once since it is always constant for a given problem. The repetitive calculations of plate deflections and fictitious reactions need relatively short computing time when comparing with the time needed for inverting system stiffness matrix $[K^*]$.

A general finite element computer program for analyzing plates on a two parameter elastic foundation model, coded in FORTRAN IV has been collected [Ref. 41] The program is capable of handling plates with complex loading and edge conditions, particularly when the edges are partly supported and partly free.

49

CHAPTER 4

COMPARATIVE STUDY AND SENSITIVITY ANALYSIS

4.1 GENERAL

A comparative study on the performance of Winkler soil model to two parameter soil model is performed. Efforts are made to epitomize the various findings from the comparative studies of analysing methods. This is done from both analysis and design aspect. Sensitivity analysis of important parameters related to mat foundation on various items are done.

4.2 COMPARISON BETWEEN WINKLER AND TWO PARAMETER MODEL

To make a comparative study two sample problems are selected based on two kinds of loading, ie. uniformly loaded plate and centrally loaded plate.

(1) *Uniformly loaded plate*

Consider a rectangular plate with free edges resting on an elastic foundation acted upon by a uniformly distributed load of intensity p. Vlazov model is taken as two parameter model because it is the most versatile.
It is assumed that

$$l = 2\text{m},$$

The parameter determining the rate of decrease of the displacement with the foundation depth $\gamma = 1.5$, which appears in eqn. 3.15

$$\text{Flexibility index of plate r} \ = \frac{\pi E_0 l^2 m}{D(1 - v_0^2)} = 1.0,$$

It is further assumed that the plate lies on an elastic foundation of infinite depth,

$H = \infty$. Because of the symmetrical nature of the problem only one quadrant of the plate will be considered. The quadrant is idealized by 16 finite elements as shown in Fig 4.1.
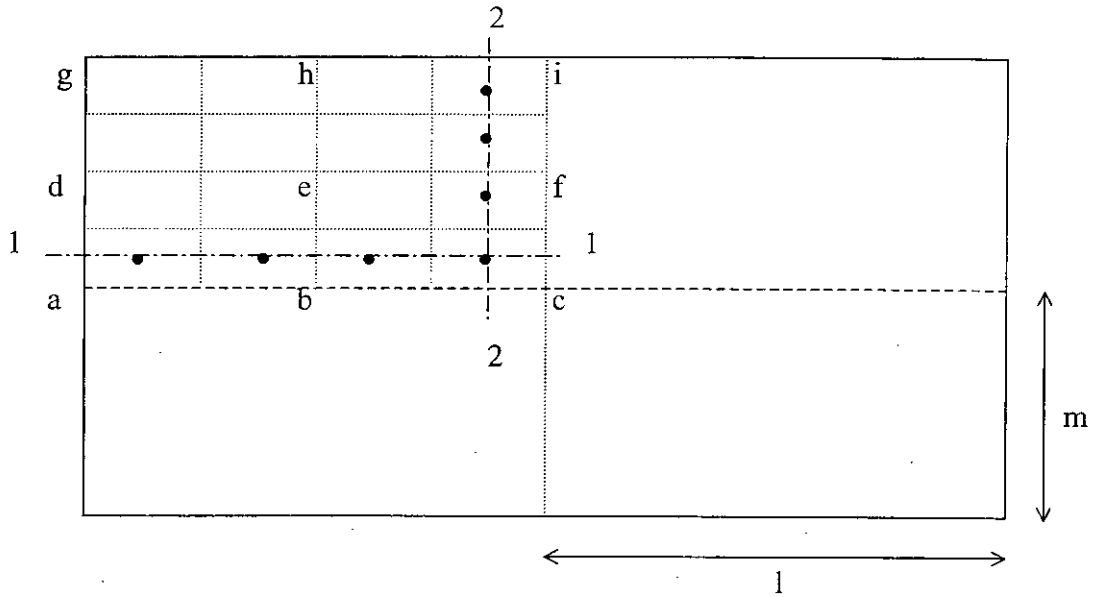

Fig. 4.1   Finite Element Gridwork of the rectangular plate

For comparison non-dimensional parameters are taken which are; nondimensionalized deflection wE_0/pm, bending moments M_x/pm^2 and M_y/pl^2.
The same problem is now done taking Winkler's model as representation of soil. The actual values of the two solutions are tabulated numerically in Table 4.1 and 4.2.

Table : 4.1 Comparison of Dimensionless deflection between models

	Location	Two parameter model	Winkler model	Difference w.r.t. Two parameter model
Dimensionless Deflection wE_0/pm	a	0.6898	0.7301	5.84 %
	b	0.7080	0.7498	5.91%
	c	0.7165	0.7592	6.04%
	d	0.6859	0.7290	6.28%
	e	0.7060	0.7484	6.01%
	f	0.7151	0.7578	5.97%
	g	0.6850	0.7364	7.50%
	h	0.7050	0.7471	5.97%
	i	0.7151	0.7568	5.83%

Table 4.2   Comparison of Dimensionless moment between models

	Location	Two parameter model	Winkler model	Difference w.r.t. Two parameter model
Dimensionless Moment M_y/pl^2	Line 1-1 From centre	0.06270	0.0702	11.96%
		0.05433	0.0619	13.93%
		0.03729	0.0425	13.97%
		0.01024	0.0114	11.33%
Dimensionless Moment M_x/pm^2	Line 2-2 From centre	0.11601	0.1346	16.01%
		0.09992	0.1131	13.181%
		0.06902	0.0773	12.05%
		0.02290	0.0250	9.17%

The variation of nondimensionalised deflection and moments are plotted against distance from the centre of plate in Fig. 4.2 to Fig. 4.4.

From this graph it is evident that using two parameter model reduces deflection and also bending moment. But the variation is not so significant in terms of design or analysis view point. A variation of 5-6% is seen in deflection while 9-15% in moment. So it reveals that Winkler model gives reasonably close results compared to two parameter model.

(2)   *Centrally loaded plate*

The same problem as the previous one is considered with the exception that the plate is acted upon by a central load P instead of uniform load. The same finite element grid is used. This time for comparison, non-dimensional parameter for deflection $10wE_0m/P$, moments M_x/P and M_y/P for sections 2-2 and 1-1 respectively are taken. The results are tabulated in Table 4.3 and 4.4.
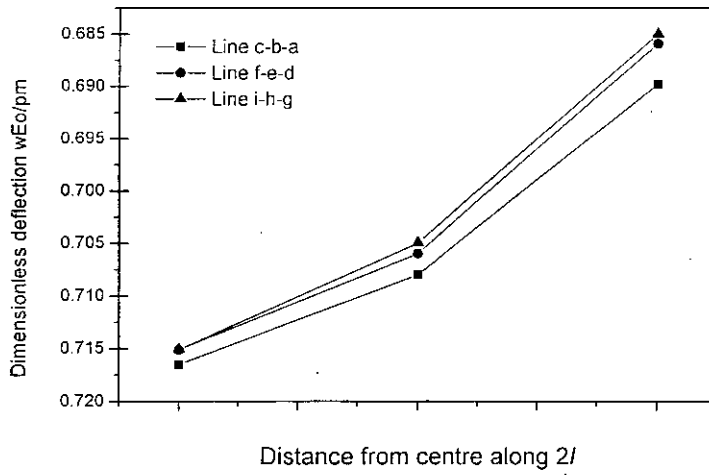
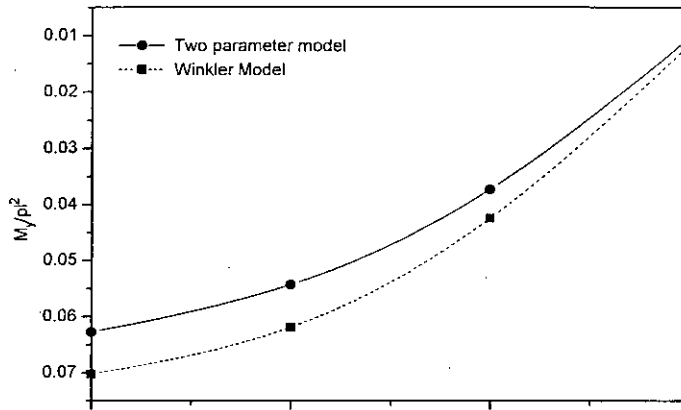Fig. 4.2 Comparison of deflection wE_0/pm of uniformly loaded plate

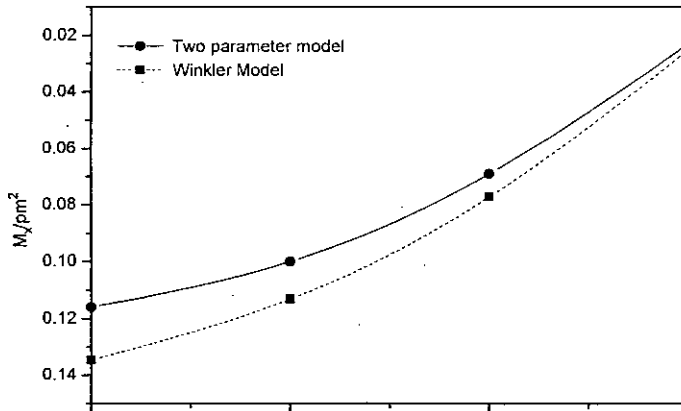Fig. 4.3 Comparison of bending moment M_y/pl^2 at section 1-1 of uniformly loaded plate

Fig. 4.4 Comparison of bending moment M_x/pm^2 at section 2-2 of uniformly loaded plate

Table : 4.3   Comparison of Dimensionless deflection between models

	Location	Two parameter model	Winkler model	Difference w.r.t. Two parameter model
Dimensionless Deflection $10wE_0m/P$	a	0.7882	0.8435	7.02%
	b	0.9195	0.9794	6.51%
	c	0.9919	1.0534	6.20%
	d	0.7865	0.8456	7.52%
	e	0.9162	0.9740	6.31%
	f	0.9825	1.0608	7.97%
	g	0.7795	0.8380	7.50%
	h	0.9062	0.9694	6.97%
	i	0.9662	1.0322	6.83%

Table 4.4   Comparison of Dimensionless moment between models

	Location	Two parameter model	Winkler model	Difference w.r.t. Two parameter model
Dimensionless Moment M_y/P	Line 1-1 From centre	0.1103	0.1202	8.98%
		0.04363	0.0482	10.05%
		0.01128	0.0124	9.5%
		-0.00045	0.0003	-
Dimensionless Moment M_x/P	Line 2-2 From centre	0.2345	0.2626	12.01%
		0.1137	0.1262	11.00%
		0.0484	0.0532	10.05%
		0.0099	0.0110	11.15%

The variation of nondimensionalised deflection and moments are plotted against distance from the centre of plate in Fig. 4.5 to Fig. 4.7
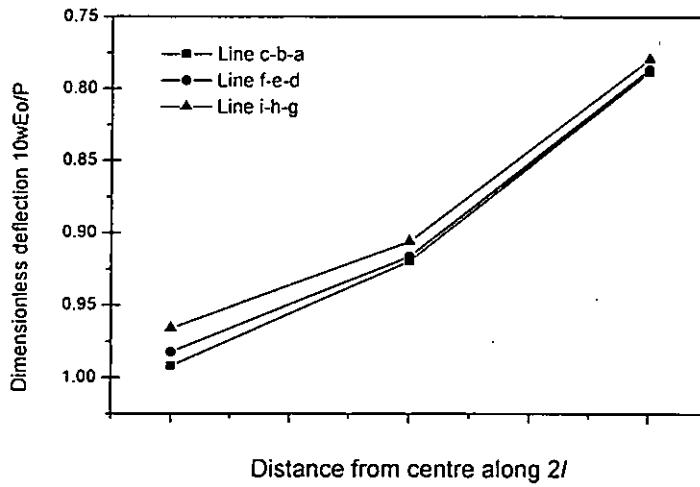
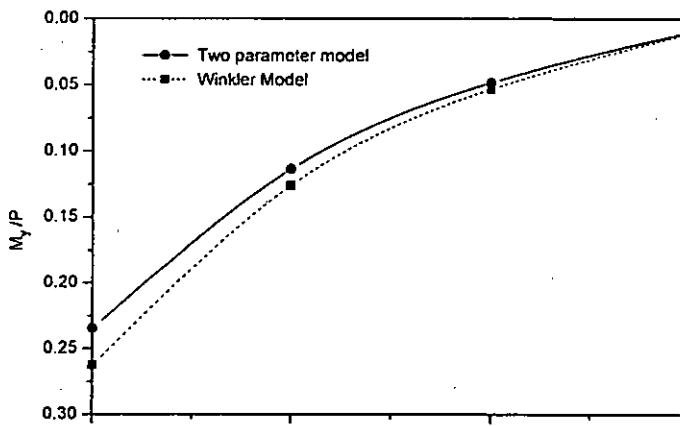Fig. 4.5 Comparison of deflection $10wE_0/P$ of centrally loaded plate

Fig. 4.6 Comparison of bending moment M_y/P at section 1-1 of centrally loaded plate
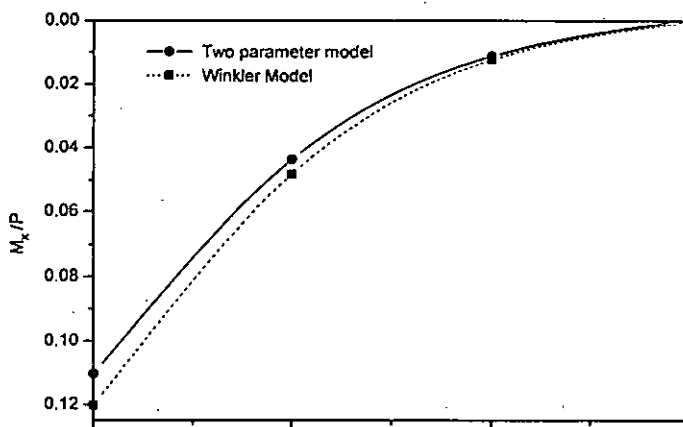

Fig. 4.7 Comparison of bending moment M_x/P at section 2-2 of centrally loaded plate
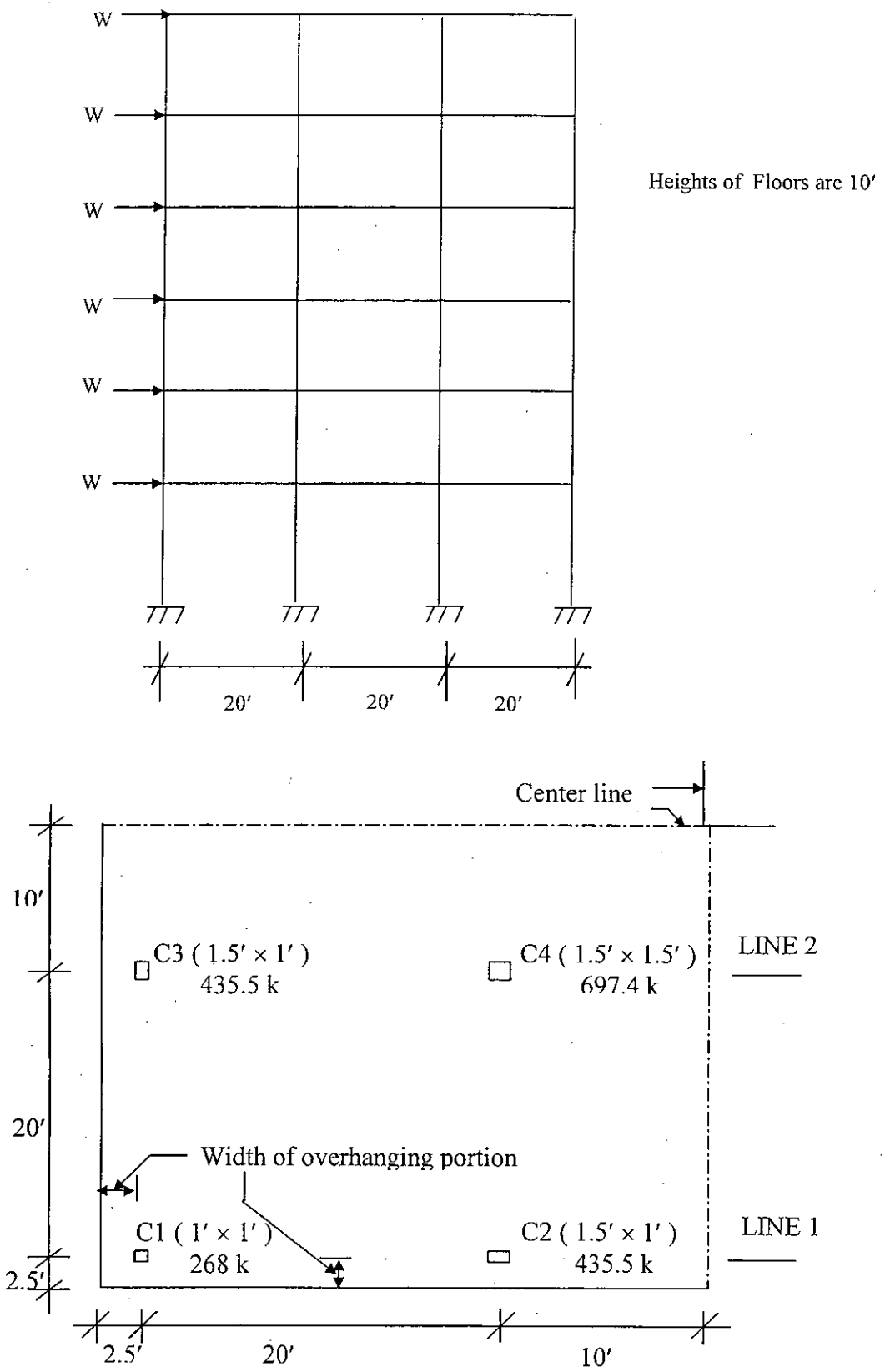
W →

W →

W →

W →

W →

W →

Heights of Floors are 10'

777   777   777   777

|— 20' —|— 20' —|— 20' —|

Center line →

10'

C3 (1.5' × 1')
435.5 k

C4 (1.5' × 1.5')
697.4 k

LINE 2

20'

Width of overhanging portion

C1 (1' × 1')
268 k

C2 (1.5' × 1')
435.5 k

LINE 1

2.5'

2.5'   20'   10'

Fig. 4.8   Building frame and plan of the mat

55

The results of deflection, bending moment, shear are shown in table 4.5 to 4.9,
In parenthesis (% w.r.t. FEM is shown). The relevant graph are plotted in Fig. (4.9-
4.12)

Table 4.5   Results of Column Deflections (in inches) by various methods:

Location	FEM	ACI	Conventional
C1	0.299 (100%)	0.593 (198%)	Cannot calculate
C2	0.248 (100%)	0.534 (216%)	Cannot calculate
C3	0.244 (100%)	0.527 (216%)	Cannot calculate
C4	0.192 (100%)	0.147 (76%)	Cannot calculate

Table 4.6   Results of Bending Moment (k-ft/ft) by various methods :

	Location	FEM	ACI	Conventional
Line 1	Column face +ve moment	95.76 (100%)	22.02 (23%)	Does not show
	In between Column −ve	-73.09 (100%)	-102.32 (140%)	-80.40 (110%)
Line 2	Column face +ve moment	107.97 (100%)	32.39 (30%)	Does not show
	In between Column −ve	-65.08 (100%)	-162.7 (250%)	-81.35 (125%)

For design purpose ACI code is followed. Readily solvable formulae are derived.

For $f_c' = 4$ ksi and $f_y = 60$ ksi, ρ_{max} = 0.0214, ρ_{min} = 0.0033

Thickness as required by various shears are tabulated in Table 4.10

Capacities :

Punching shear capacity per unit length of perimeter,

$V_{p/cap}$ $= v_{pu} \times d = 30.965 \times d$ kip , d in inches

Flexural shear capacity per unit width,

$V_{f/cap}$ = 15.483 × d kip, d in inches

d = t - 3.5 , all in inches

Moment Capacity, $M_{max/cap}$ = 0.93674 × d^2 k-ft/ft , d in inches

$M_{min/cap}$ = 0.17469 × d^2 k-ft/ft , d in inches

Steel $A_{s/max}$ = 3.08160 × d in^2/ ft , d in ft

$A_{s/min}$ = 0.48000 × d in^2/ ft , d in ft

Effective Depths :

Effective depth from punching shear requirement,

$$d_{punch} = \frac{1}{2}(-c + \sqrt{c^2 + 4.65 \times V_p})\ \text{in} ,\qquad V_p\ \text{in k/ft and}\ c\ \text{in inches}$$

V_p = Punching shear

c = Column dimension for a square column

Steel ratio ρ = $\dfrac{1}{17.7}(1 - \sqrt{1 - \dfrac{0.6556 \times M}{d^2}})$, M in k-ft and d in inches

M = Flexural moment

Effective Depth required for bending moment

$$d_{required/flexural\ moment} = \sqrt{\frac{M}{54\rho \times (1 - 8.85 \times \rho)}}\ ,\ \text{M in k-ft and d in inches}$$

$d_{\rho/min}$ = 2.3926 × $\sqrt{M}$, M in k-ft and d in inches

$d_{\rho/max}$ = 1.0332 × $\sqrt{M}$, M in k-ft and d in inches

Effective Depth required for flexural Shear

$d_{required/flexural\ shear}$ = 0.775 × V , V in k/ft and d in inches, V=Flexural shear

Table 4.7   Results of Punching Shears by various methods (kip/ft) :

Location	FEM	ACI	Conventional
C1	243.0 (100%)	203.0 (83.5%)	244.1 (100.5%)
C2 & C3	407.4 (100%)	380.7 (93.5%)	408.4 (100.3%)
C4	665.6 (100%)	682.0 (102.5%)	666.2 (100.1%)

Table 4.8 Results of Flexural shear in most highly stressed strip of unit width (kip/ft.) by various methods :

Location	FEM	ACI	Conventional
At column face C4	29.10 (100%)	37.30 (128.2%)	11.40 (39.18%)

Table 4.9   Results of Average Column Strip Flexural Shear (kip/ft.) by variuos methods:

Location	FEM	ACI	Conventional
Column Strip	14.50 (100%)	27.10 (187%)	13.10 (90.34%)

Table 4.10   Design Thickness inches by Different Shears :

| Kind of shear	FEM	ACI	Conventional
t required from Punching Shear	23.76(100%)	24.06(101.26%)	23.75 (100%)
t required from Flexural shear in most highly stressed strip of unit width	26.05(100%)	32.41(124.41%)	12.34(47.37%)
t required from Average column strip flexural shear	14.74(100%)	24.50(102.5%)	13.65(100.1%)
Design thickness t	24(100%)	24.50(102%)	24(100%)
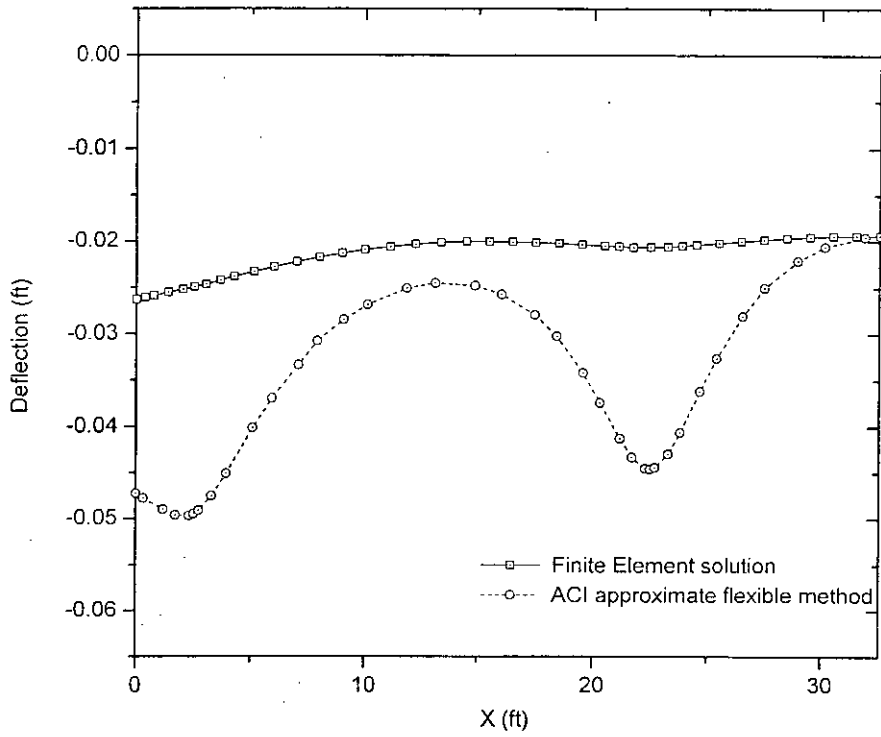
(a)
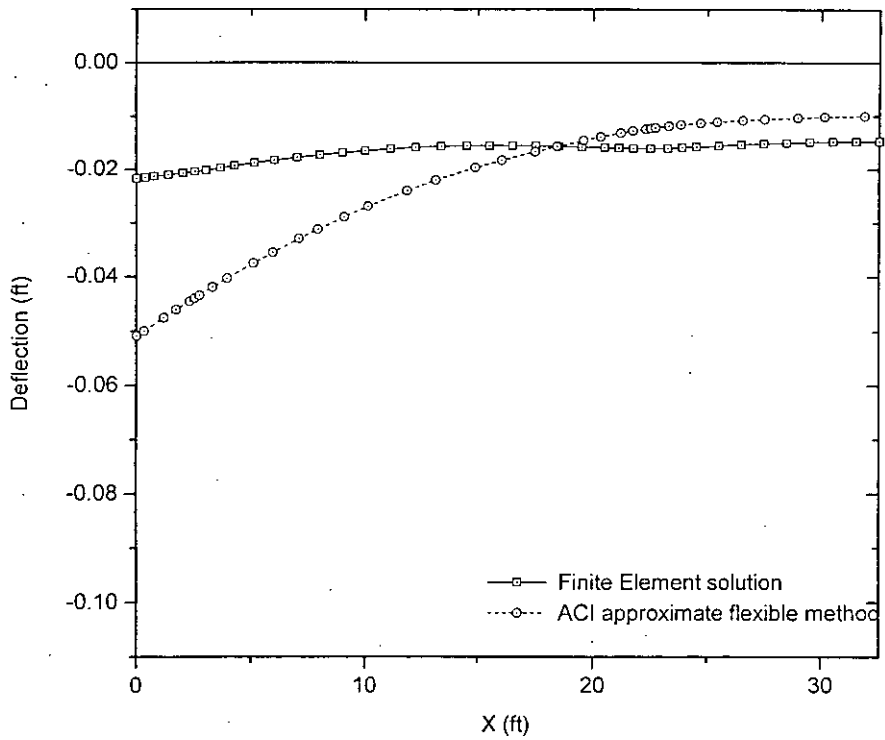
(b)

Fig. 4.9 : Comparison of deflection calculation by different methods of (a) LINE 1
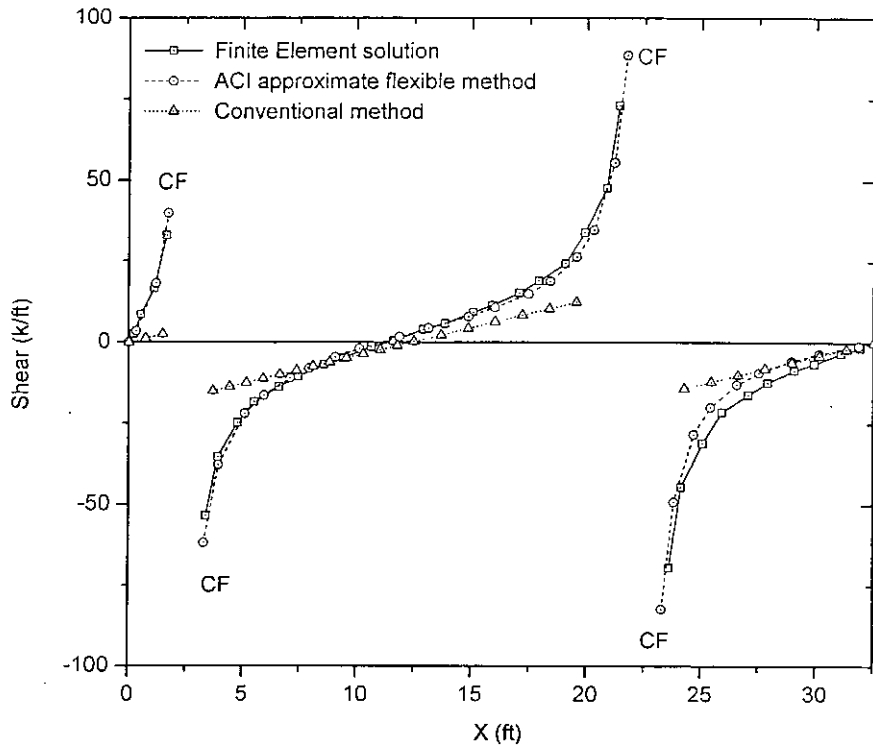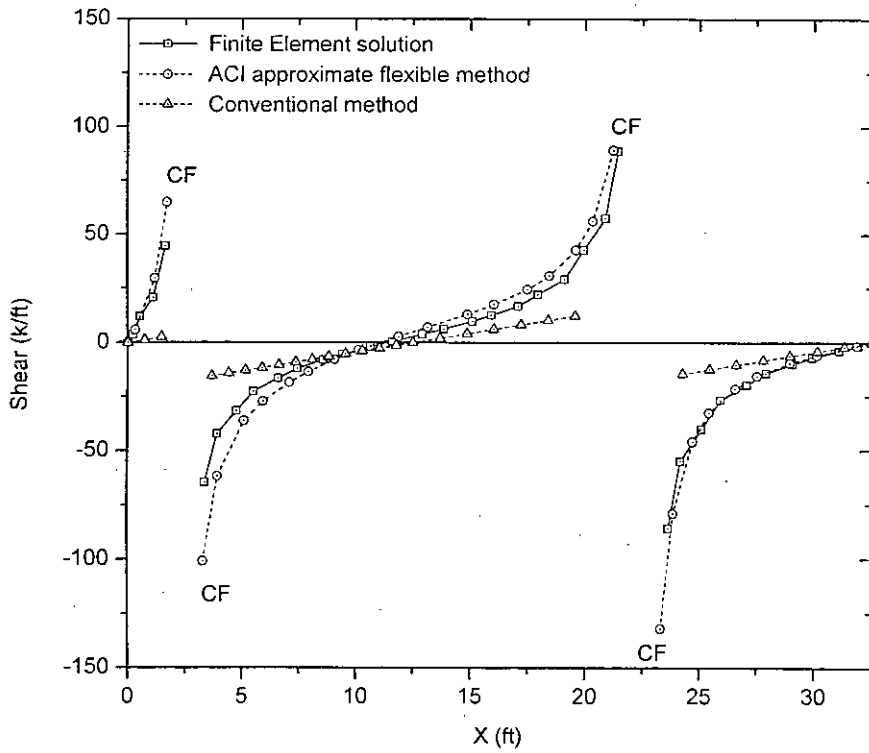and (2) LINE 2 (mat thickness 3 ft)
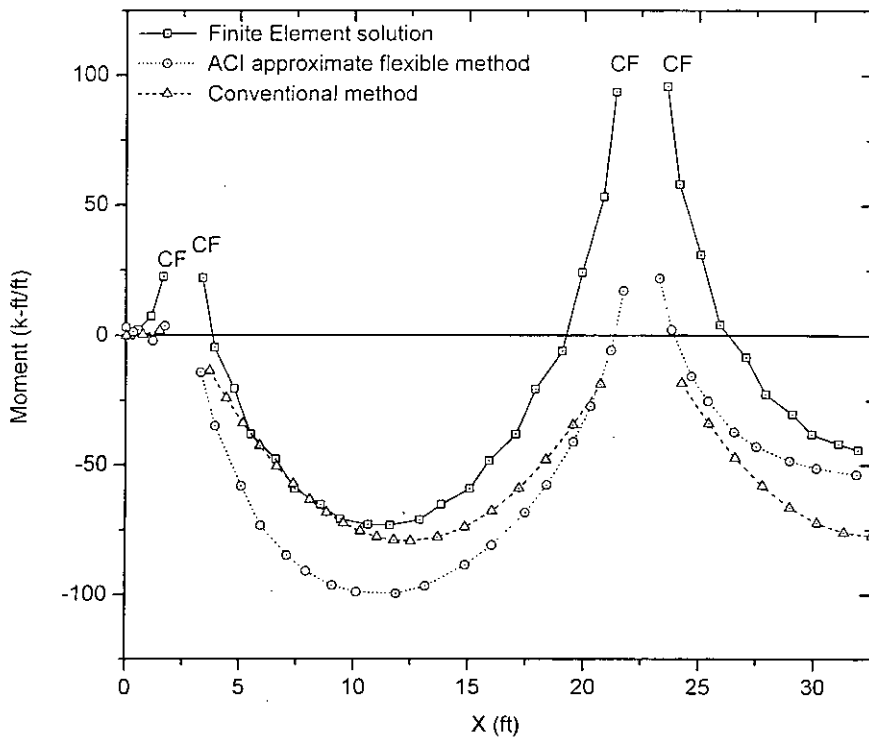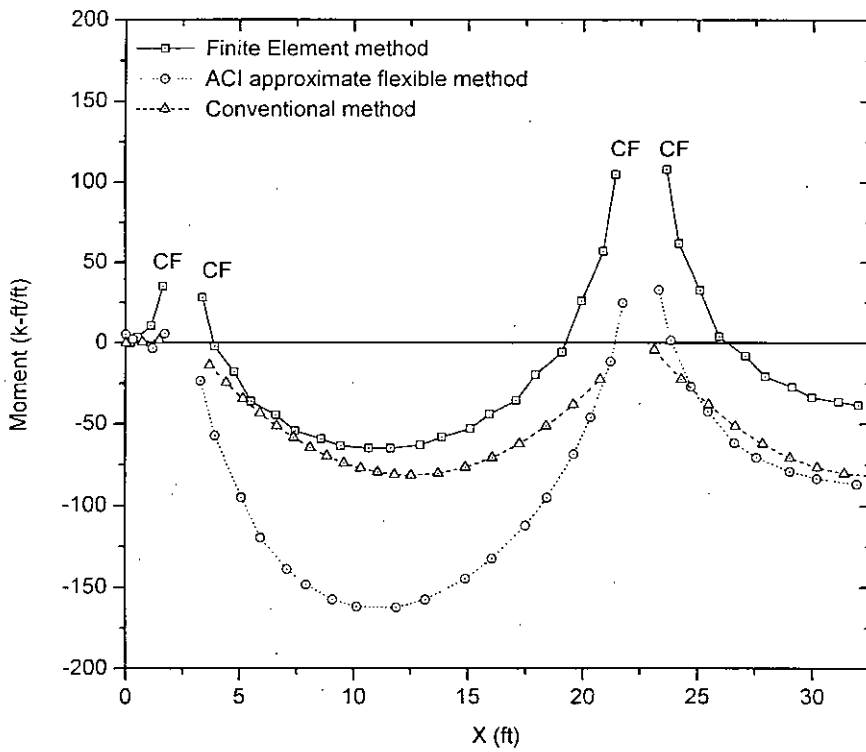
Fig. 4.10 : Comparison of bending moment calculation of (a) LINE 1
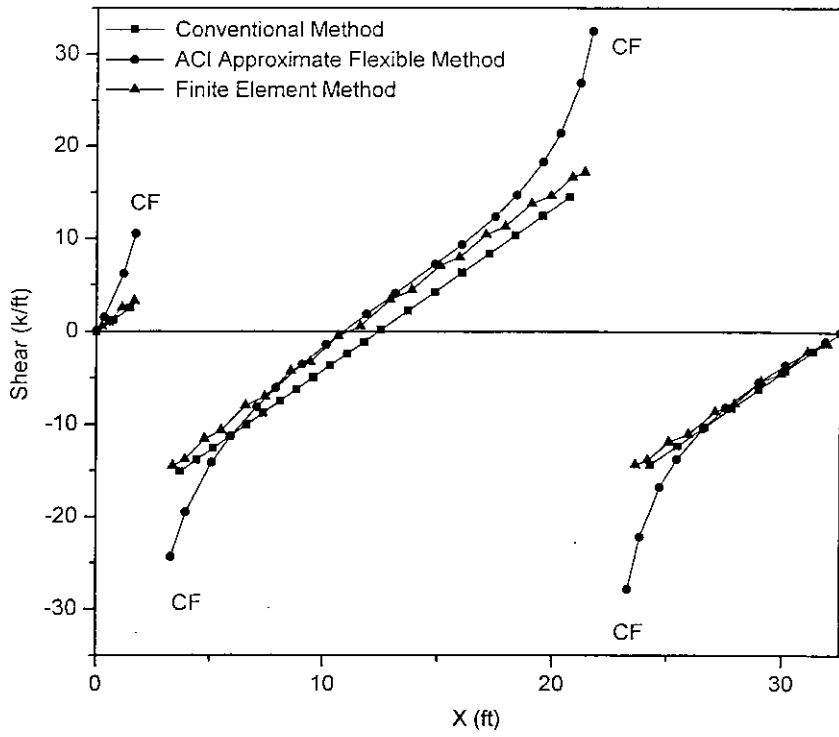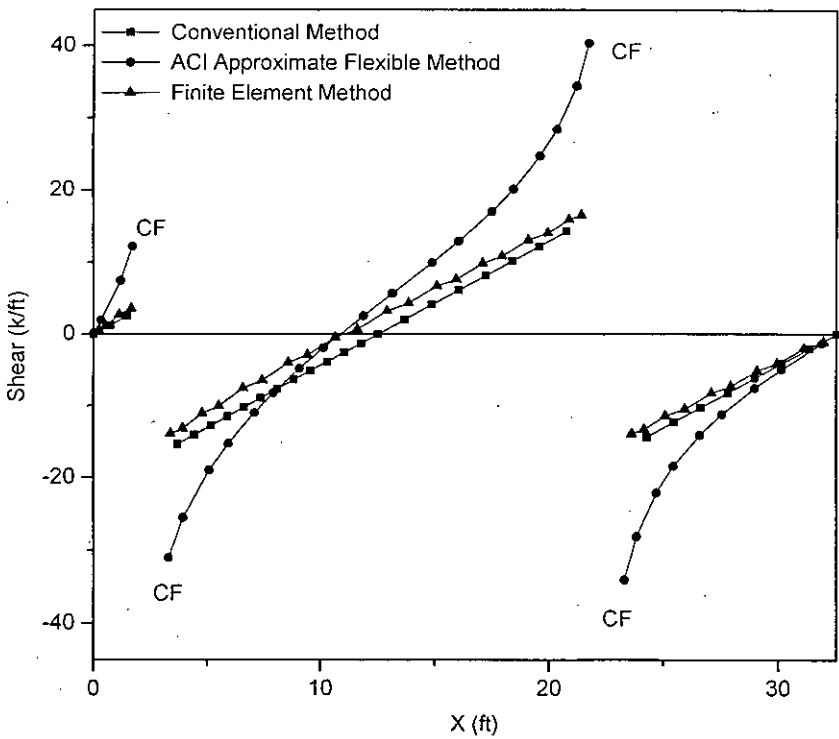and (b) LINE 2 by different methods (mat thickness 3 ft)

Fig. 4.11 : Comparison of shear force calculation of (a) LINE 1 and
(b) LINE 2 by different methods (mat thickness 3 ft)

(a)

(b)

Fig. 4.12 : Comparison of average strip shear calculation of (a) column strip 1 and (b) column strip 2 by different methods (mat thickness 3 ft)

It is unlikely that the most highly stressed strip of unit width will act individually to tackle the flexural shear. As a matter of fact, for the 3.00 ft thick mat (Fig. 4.8), a plot of lateral distribution of flexural shear along the column faces (Fig. 4.13) shows that distribution of shear is remarkably uneven for mat. High concentration of flexural shear occurs near the columns and the rate of decay of shear force magnitude away from the columns is very high. It is expected that a redistribution of shear will occur when material will be stressed beyond the elastic limit. Even within the elastic limit, a wide portion of any column strip will carry the total shear acting on it as a whole. While there is no experimental data available to quantify the width of this portion, case studies performed by [Morshed 1997]has made it clear that the shear force averaging width which gives design flexural shear equals to the flexural shear capacity of the thickness calculated from punching shear requirement. However, computer modeling, especially elastic analysis, is not sufficient to find which portion of a column strip actually acts integrally in resisting shear. But conventional practice of treating individual column strips as a whole has not been reported to result in any functional discrepancy so far. So, a reasonable solution seems to be that the entire column strip works together. As has been found by [Morshed 1997] even if 50% width of any column strip acts integrally, this approach of mat design will be on the safe side.

Average Bending Moment Across the Widths of Column Strips

If average column strip flexural shears are taken to be the design criteria, the same reasoning applies to bending moments. Magnitudes of moments decrease considerably due to the averaging (Fig. 4.14). When averaging is done across the widths of column strips, mat thickness is governed by punching shear in Conventional and FE method. For the ACI method, flexural shear still may control the design in this regard. However, in any method when mat thickness is reduced the bending moment capacity also reduces. For the present example (Fig. 4.8) 2 ft thickness seems adequate under the changed course of design (24.50 inches for ACI analysis) and calculations shows that average column strip moments still stay below
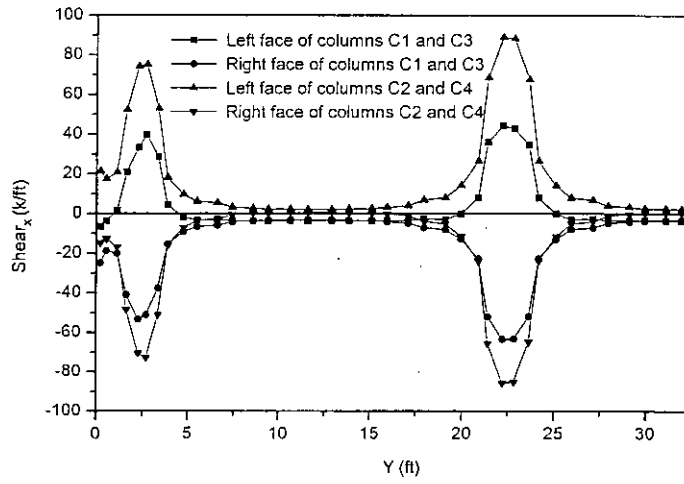
Fig. 4.13 : Lateral distribution of shear as calculated by FEM
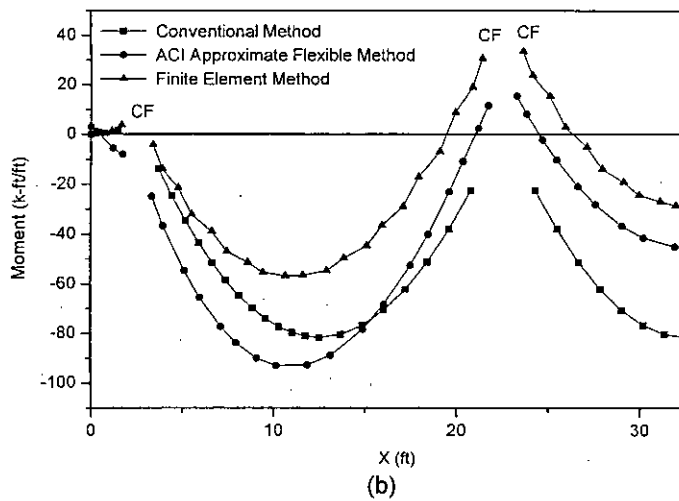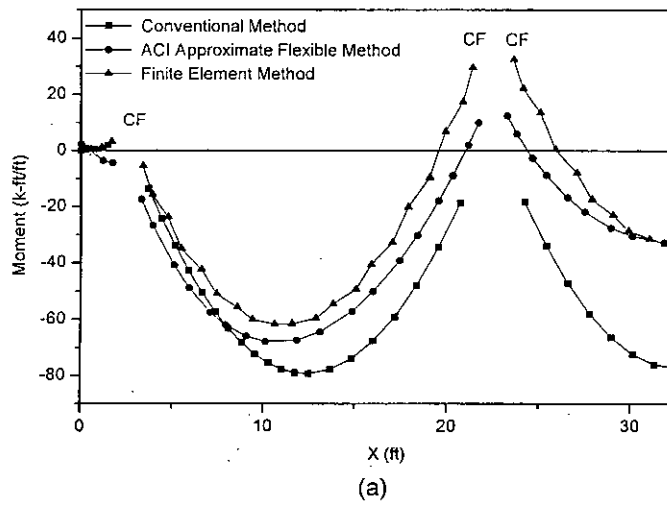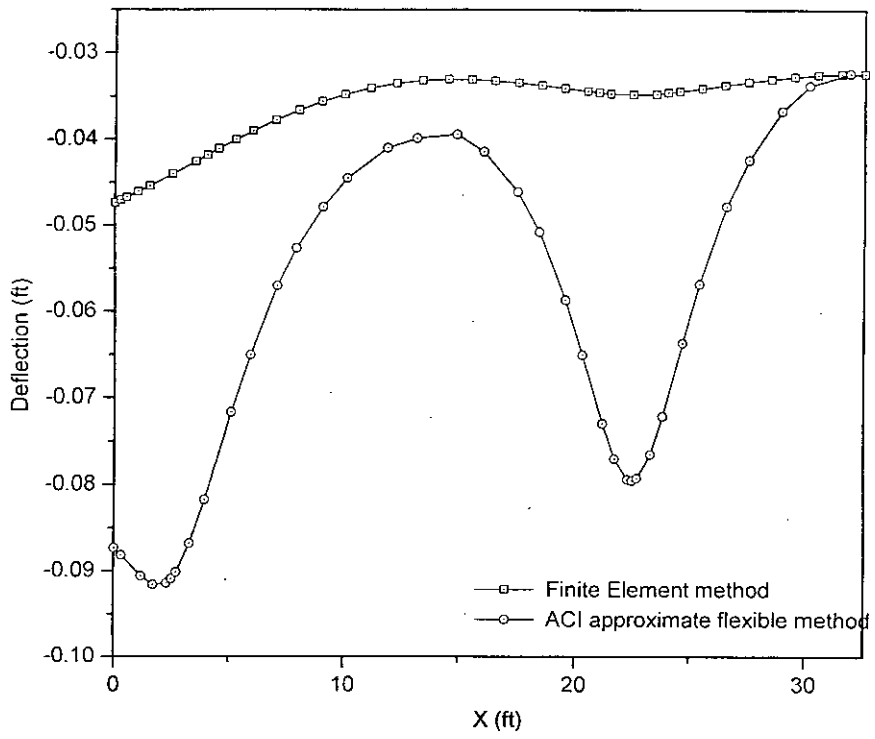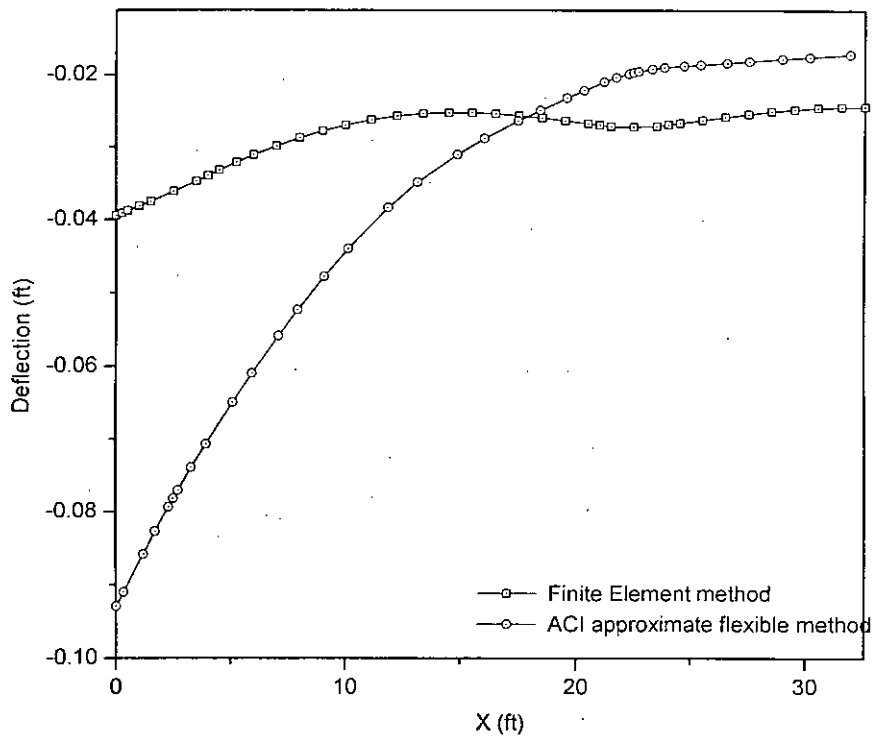(mat thickness 3 ft)

(a)

(b)

Fig. 4.14 : Comparison of average strip bending moment calculation of (a) column strip 1
and (b) column strip 2 by different methods (mat thickness 3 ft)

(a)

(b)

Fig. 4.15 : Comparison of deflection calculation of (a) LINE 1 and
(b) LINE 2 by different methods for a 12 story building
(mat thickness 2.5 ft)
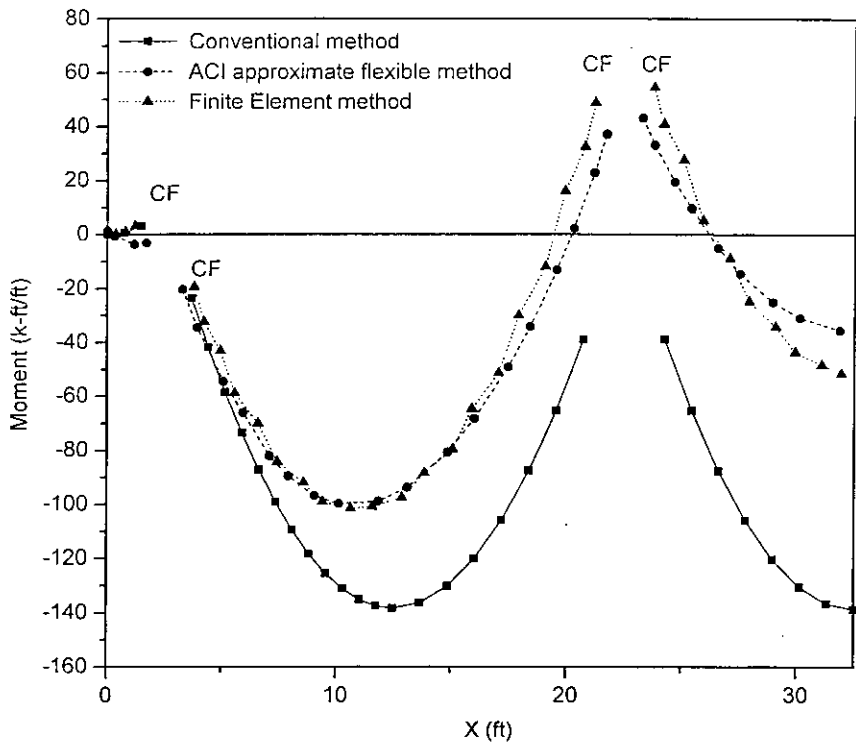
(a)
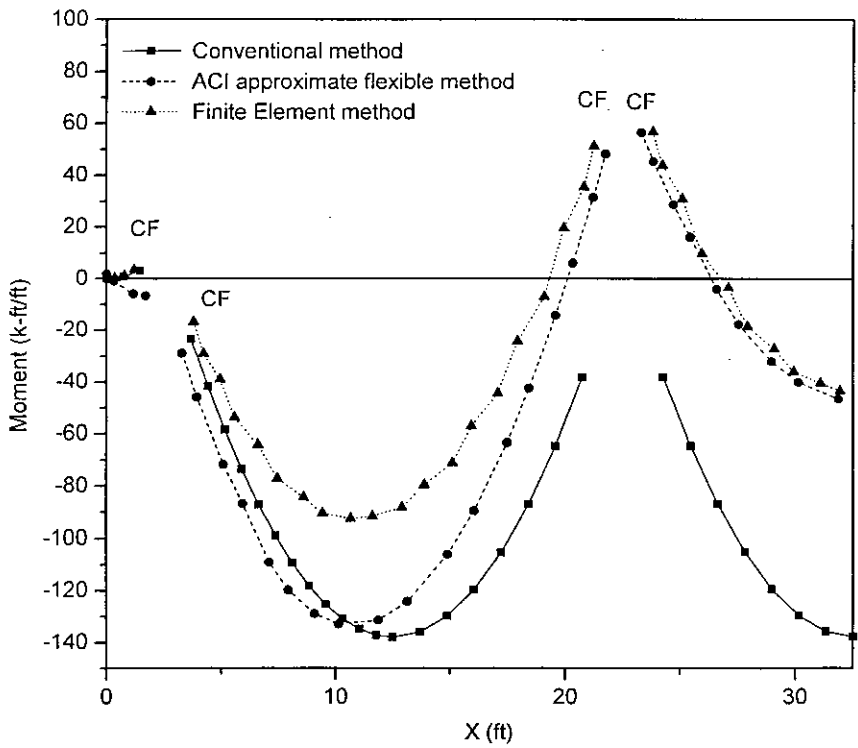
(b)

Fig. 4.16 : Comparison of moment calculation of (a) column strip 1
and (b) column strip 2 by different method for a 12 story
buliding (mat thickness 2.5 ft)

Fig. 4.17 : Comparison of shear force calculation of (a) column strip 1
and (b) column strip 2 by different methods for 12 story
building (mat thickness 2.5 ft)
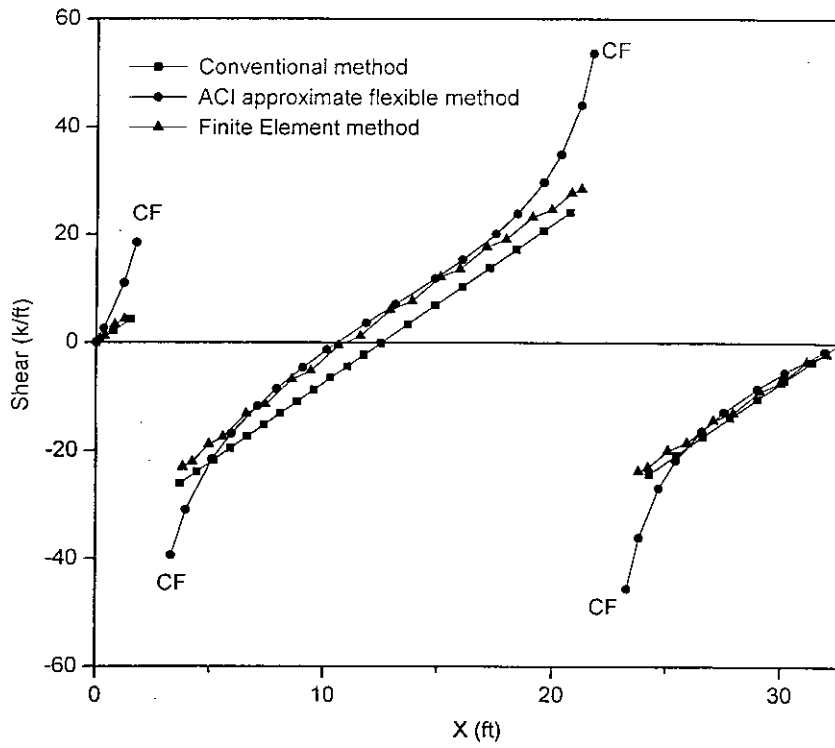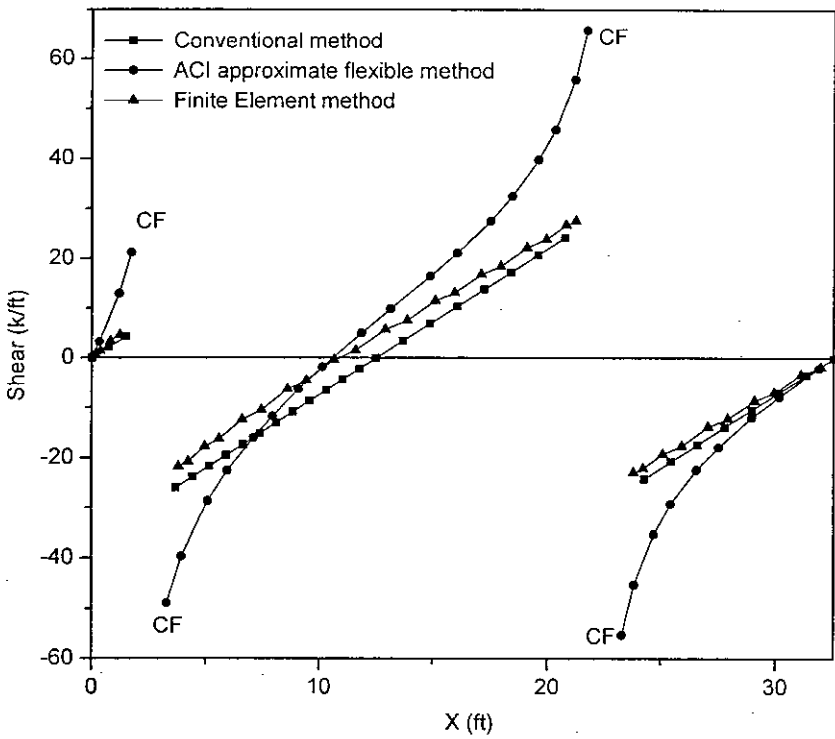
the minimum-steel moment capacity of the mat for FE and ACI methods. The situation is different for Conventional method.

Economic Evaluation

Economy of various methods are evaluated by parameter such as concrete volume and steel requirements. From the preceding study it can be revealed that in ACI methods the thickness governed by flexural shear will be high w.r.t. FE method. Also in Conventional method the steel required by negative moment will be more w.r.t. FE method. So FE method will result in substantial economy than both ACI and Conventional Method. It is also be implied that this economy will increase with high column loads.

This is done by selecting another mat for a 12 storied building. Displacement, bending moment and shear will be based on column strips. In calculating steel average steel volume per unit plan area of mat is used. The column dimensions $24''\times24''$, thickness 2.5 ft and C1, C2, C3 and C4 column (Fig. 4.8) loads 460 k, 735 k, 735 k and 1176 k respectively. The mat is analyzed and designed by the three methods. Displacement, bending moment and shear force diagrams of column strip 1 and 2 of this mat is shown in Fig. 4.15 through Fig. 4.17. In calculating total steel requirement *weighted average steel area per unit width* (A_s^{avg}), is used.

$$A_s^{avg} = \frac{\sum A_s \times A_A}{\sum A_A}$$

where

      A_s =   calculated steel area per unit width,

      A_A =   plan area of mat covered by A_s.

Design values and their comparison for different methods for the test mat.

Table 4.11

Method	t required from punching shear (in)	t required from flexural shear (in)	Selected t (in)	A_s^{avg} for +ve Moment (in²/ft)	A_s^{avg} for -ve Moment (in²/ft)	Relative Cost of concrete w.r.t. FE	Relative cost of steel w.r.t. FE
Conventional	29.6	21.4	30	1.06	1.20	100%	107%
ACI	30.0	39.0	40	1.44	1.44	133%	136%
FE	29.7	23.3	30	1.06	1.06	Not Applicable	

It is evident from table 4.11 that higher cost associated with Conventional method is due to the over estimation of negative moments and that of ACI method arises from the overestimation of flexural shears. ACI approximate flexible method, in spite of its rigorous nature of analysis, gives overdesign compared to FE method, particularly for heavily loaded mats. It appears that it is always better and more economic to use FE method.

The summary of the comparison between various are tabulated in Table 4.12

Table 4.12   Summary Of Comparison Between Various Methods

Parameter	Location	Conventional Method	ACI Method	FiniteElement Method
Deflection	At Col. Edge	Cannot Calculate	Overestimates	Basis
	In between. Column.	Cannot Calculate	Underestimate	Basis
Moment	Column Face +ve moment	Fails to predict any moment	Underestimate	Basis
	-ve moment between cols.	Moderately Overestimate	Overestimates * less at edges	Basis
Shear	Away from Column.	Compatible	Compatible	Basis
	Near Column.	Underestimates too much	Overestimates	Basis
Punching Shear	At d/2 from column face	Compatible	Underestimate * Compatible in central cols.	Basis
Flexural Shear	At d from column face	Underestimates	Overestimates	Basis
Thickness	Whole Mat	Compatible * Governed by Punching Shear	Moderately overestimates * Governed by Flexural Shear	Basis *Governed by Punching Shear
+ve Steel	+ve moment areas	Governed by minimum steel requirements	Governed by minimum steel requirements	Governed by minimum steel requirements
-ve steel	-ve moment areas	Moderately Overestimates	Largely Overestimates	Basis
Economic Evaluation	In terms of concrete & steel	Overestimates Moderately due Neg. Moment	Largely Overestimates Thickness	Basis

62

4.4   SENSITIVITY ANALYSIS OF MAT FOUNDATION

Various parameters relevant to mat foundations are selected for sensitivity analysis which is performed on some selected items at selected locations.

The selected parameters are :

a) Mat thickness

b) Modulus of subgrade reaction

c) Ultimate strength of concrete

d) Column spacing

e) Column size

f)   Width of overhanging portion

The selected items for parametric study are :

Items	Location
Displacement	Under the columns
Positive moment	At column faces
Negative moment	In between the columns
Flexural Shear	At column faces

For the study the same mat problem is selected. (Fig 4.8)

a) Effect of mat thickness :

The thickness of mat has been increased from 2 ft. to 4 ft.

The results of various items are tabulated in Table 4.13 and the variations are plotted in Fig 4.18- 4.20.

Table 4.13. Variation of displacement, moment and shear w.r.t. mat thickness t, when t is increased from 2.00 ft to 4.00 ft.

Location	Displace-ment	Positive moment	Negative moment*	Flexural shear
C1 {C1-C2*}	-25.9%	-6.8%	+20.9%	-0.08%
C2 {LINE1 CL*}	-20.4%	-22.1%	+50.2%	-11.9%
C3 {C3-C4*}	-18.5%	+2.9%	+27.9%	+14.8%
C4 {LINE2 CL*}	-7.2%	-20.2%	+74.7%	-0.18%

*   Locations for negative moments are given within curly brackets

As thickness increases

- Displacements decreases at a very good rate. Sensitive at corner columns.

- Positive moment decreases slightly. Sensitive to central columns

- Negative moment increases tremendously. Sensitive to in between central cols.

- Flexural shear has very little change at all.

- Punching shear remains almost constant.

So in reverse as thickness of mat decreases.

- Displacements increases with a very good rate. Sensitive at corner columns.

- Positive moment increases slightly. Sensitive to central columns

- Negative moment decreases tremendously. Sensitive to in between central cols.

- Flexural shear has very little change at all.

- Punching shear remains almost constant.

b) Effect of modulus of subgrade reaction :

Modulus of subgrade reaction ranges from 100 kcf to 500 kcf. The results of various items are tabulated in Table 4.14 and the variations are plotted in Fig. 4.21-4.23
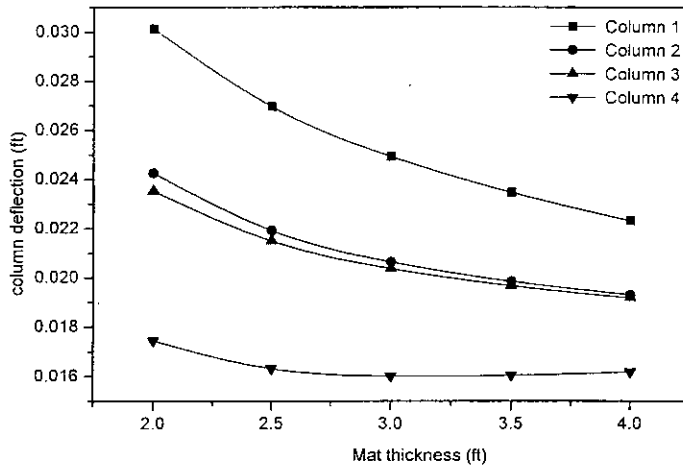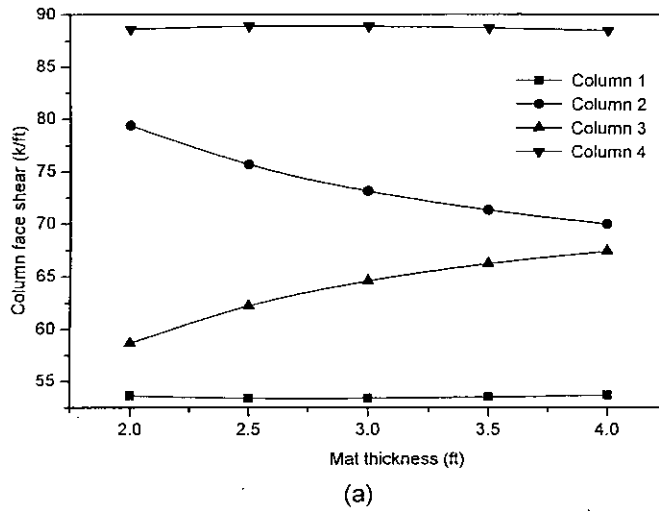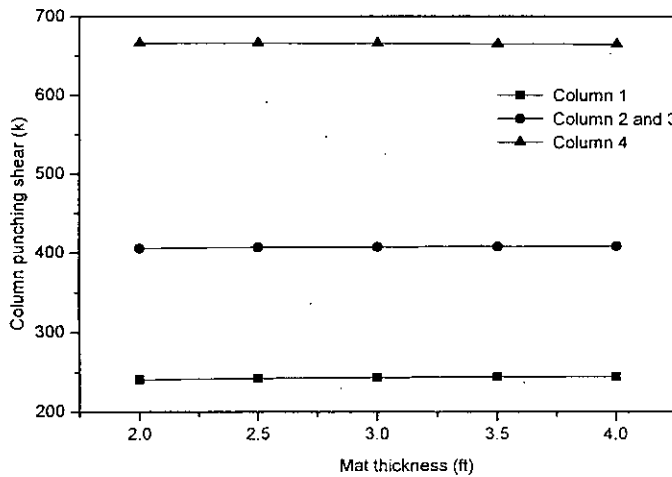
Fig. 4.18 : Effect of mat thickness on column deflection (mat thickness 3 ft)

(a)

(b)

Fig. 4.19 : Effect of mat thickness on (a) flexural and (b) punching shear
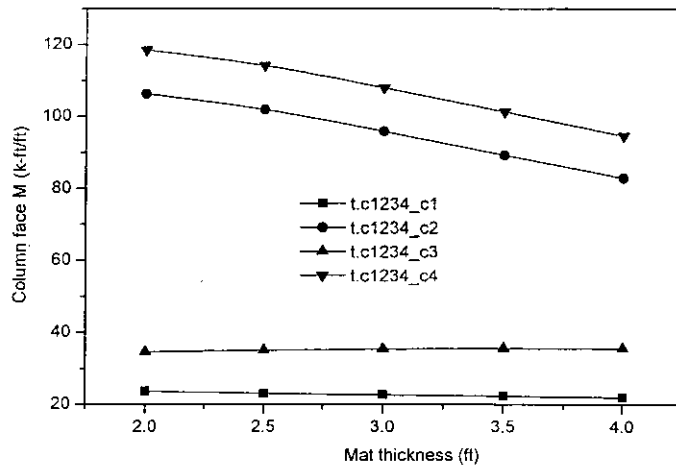
(a)
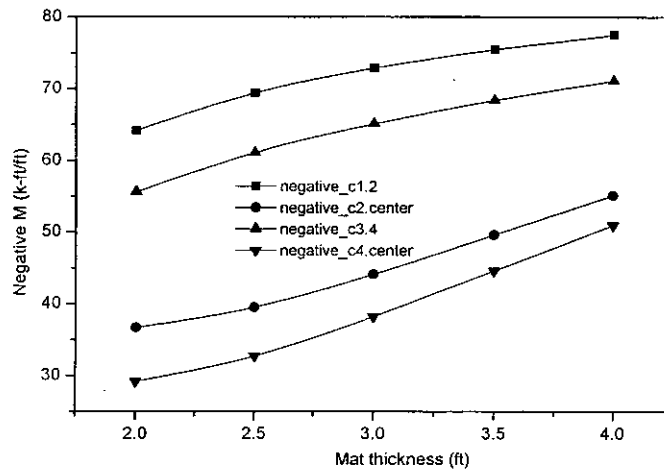
(b)

Fig. 4.20 : Effect of mat thickness on (a) positive and
(b) negative bending moment
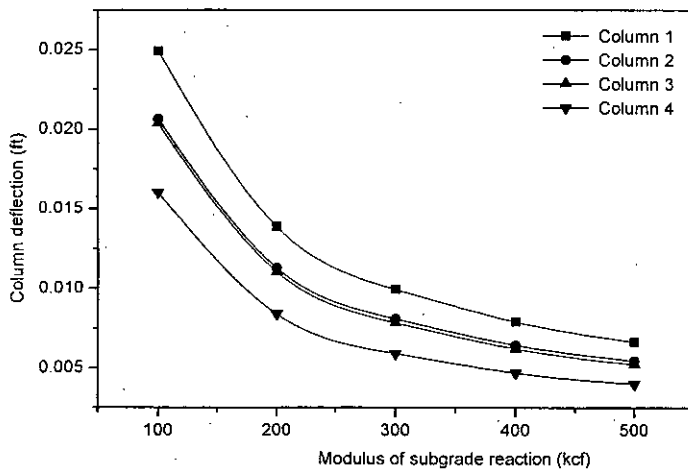
Fig. 4.21 : Effect of modulus of subgrade reaction on column
deflection (mat thickness 3 ft)
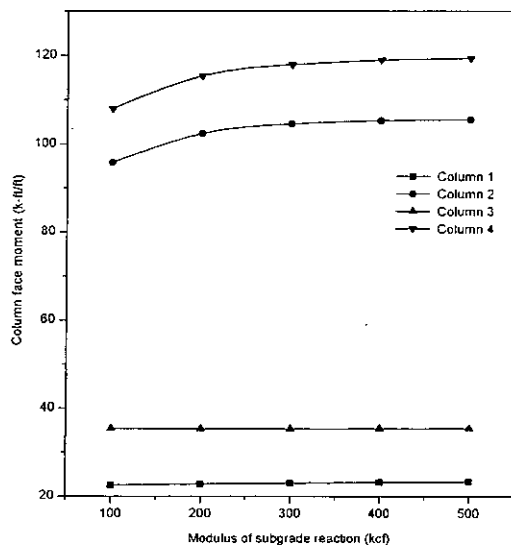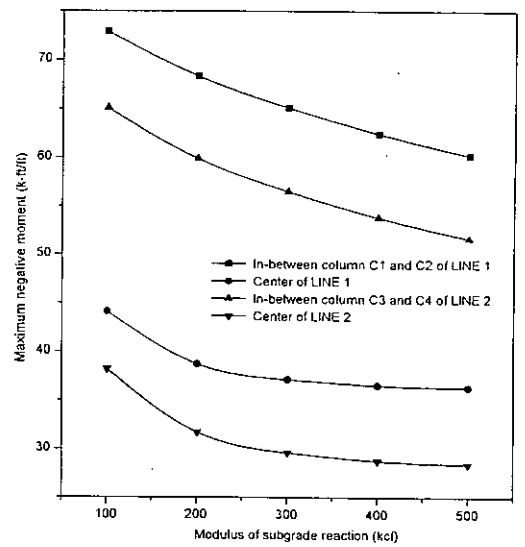
Fig. 4.22 : Effect of modulus of subgrade reaction on (a) positive
and (b) negative bending moment (mat thickness 3ft)
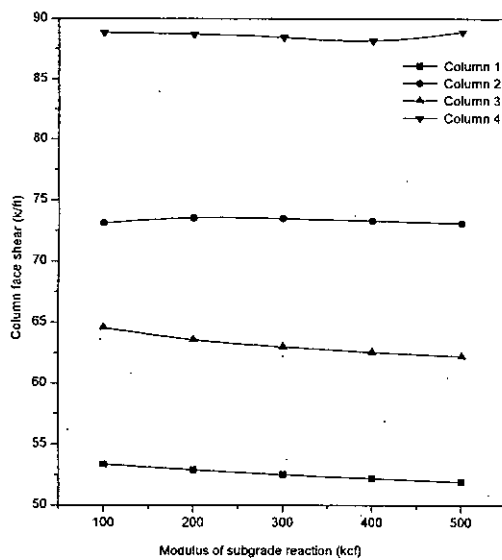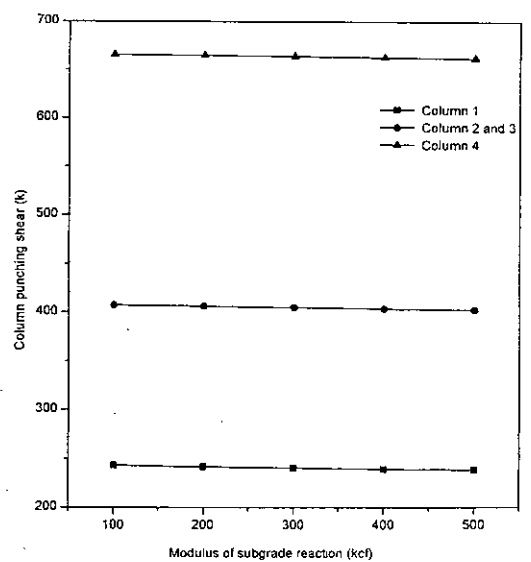
Fig. 4.23 : Effect of modulus of subgrade reaction on (a) flexural
and (b) punching shear (mat thickness 3ft)

Table 4.14   Variation of displacement, moment and shear w.r.t. modulus of subgrade reaction k, when k is increased from 100 kcf to 500 kcf.

Location (Table 4.2)	Displace-ment	Positive moment	Negative moment*	Flexural shear
C1 {C1-C2*}	-73.4%	+3.4%	-17.3%	-2.8%
C2 {LINE1 CL*}	-73.7%	+10.2%	-17.6%	-0.03%
C3 {C3-C4*}	-74.4%	+0.3%	-20.5%	-3.6%
C4 {LINE2 CL*}	-75.2%	+10.5%	-25.6%	+0.1%

*   Locations for negative moments are given within curly brackets

As modulus of subgrade reaction increases

- Displacements decreases considerably at a very faster rate. Sensitive at central columns.
- Positive moment increases slightly. Sensitive to corner columns
- Negative moment decreases moderately.   Sensitive to in between corner columns.
- Flexural shear has very little change at all.
- Punching shear remains almost constant.

c) **Effect of concrete strength**

The parameter is tested in the following range f_c' = 2 ksi to 4 ksi. The results of various items are shown in table 4.15 and the variations are plotted in Fig.4.24- 4.26.

Table 4.15.   Variation of displacement, moment and shear w.r.t. concrete strength f_c', when f_c' is increased from 2.00 ksi to 4.00 ksi.

Location (Table 4.2)	Displace-ment	Positive moment	Negative moment*	Flexural shear
C1 {C1-C2*}	-7.6%	-0.7%	+4.7%	+0.7%
C2 {LINE1 CL*}	-5.8%	-6.4%	+6.3%	-0.8%
C3 {C3-C4*}	-5.3%	+0.3%	+13.0%	+1.3%
C4 {LINE2 CL*}	-1.9%	-6.2%	+18.4%	0.0%

*   Locations for negative moments are given within curly brackets

Fig. 4.24 : Effect of ultimate concrete strength on column
deflection (mat thickness 3 ft)

(a)
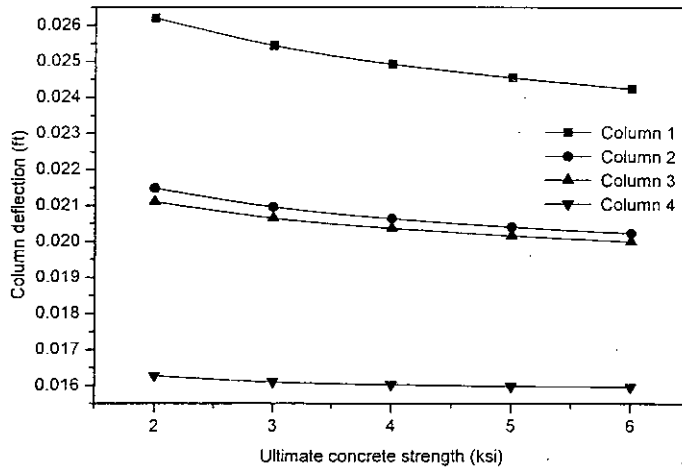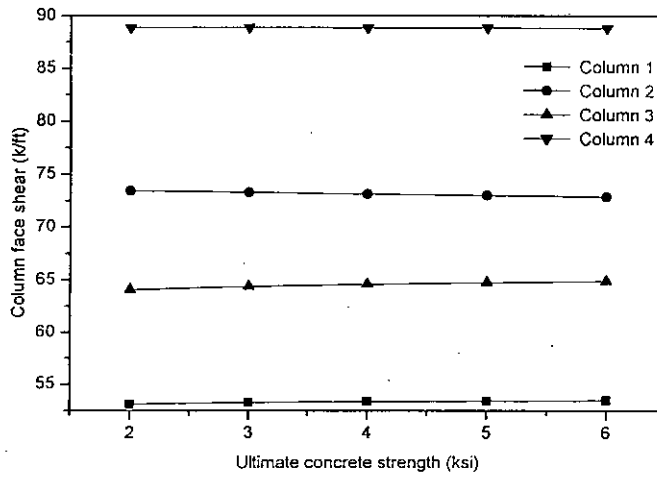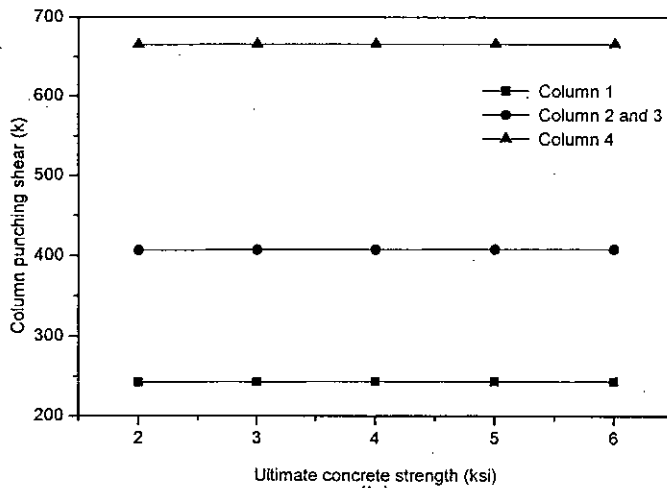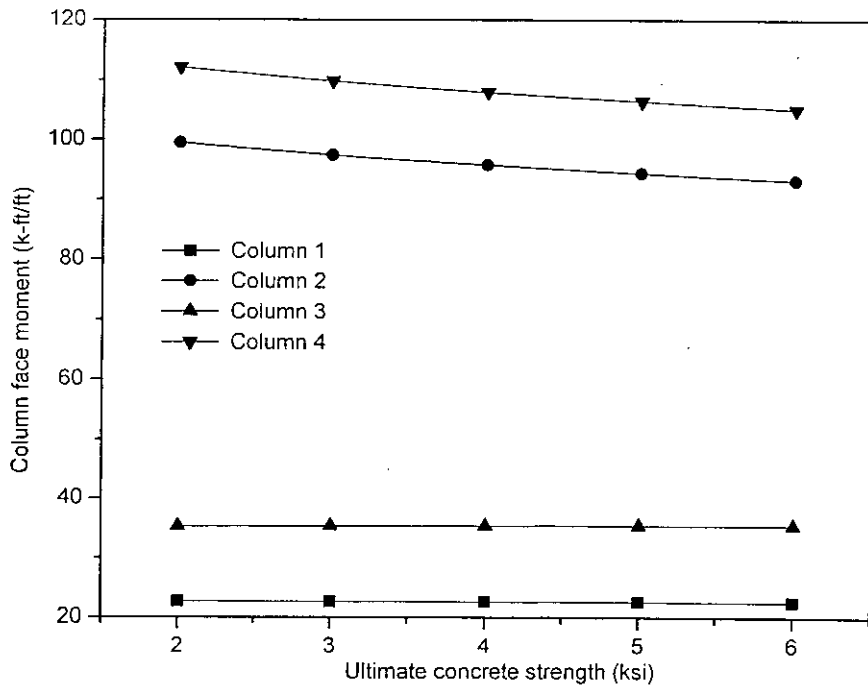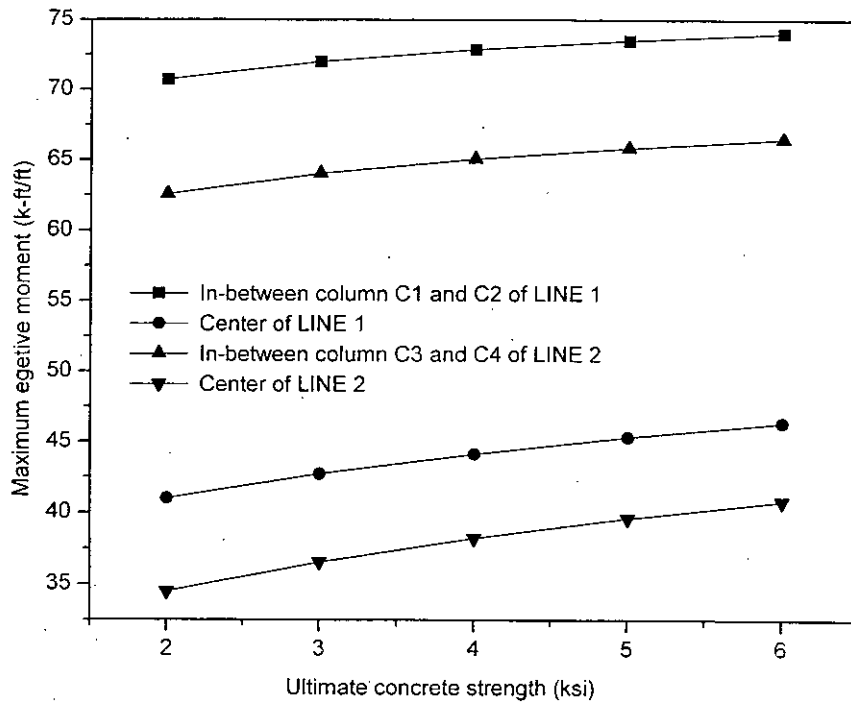

(b)

Fig. 4.25 : Effect of ultimate concrete strength on (a) flexural
and (b) punching shear force (mat thickness 3 ft)

(a)

(b)

Fig. 4.26 : Effect of concrete strength on (a) positive and
(b) negative moment (mat thickness 3 ft)

As ultimate strength of concrete increases

- Displacements decreases slightly. Little sensitive at corner columns.

- Positive moment decreases very slightly. Sensitive to corner columns

- Negative moment increases moderately. Sensitive to in between central cols.

- Flexural shear has very little change at all.

- Punching shear remains almost constant.

(d) Effect of column size

Since column loads are distributed over the respective column cross sectional areas, smaller cross sections of columns mean greater intensity of column loads. This increase in force concentration is expected to increase deflection, bending moment and shear force magnitudes in the vicinity of the columns. The columns are square in cross-section and ranging in dimension from 1.00 ft to 2.00 ft. Results are presented in Fig. 4.27 through Fig. 4.29. The moment and shear diagrams for columns with larger sizes remain aligned with those for narrower column cross-sections, except for a reduction in the peak values of moments and shears at the faces the columns. This indicates that analysis with one size of columns may well be applicable if column sizes are slightly increased or changed later for any reason.

(e) Effect of Column spacing

Reduction in column spacing means more columns to transfer the same load means a more uniform load distribution, which in turn means a reduction in deflections, bending moments and shear forces. To do this a 20′ x 20′ grid, a 15′ x 20′ grid and a 12′ x 20′ grid is taken. Total load carried by these mats are kept the same. Results are presented in Fig. 4.30 through Fig. 4.32.

(f) Effect of width of overhanging portion

Overhanging portion is the part of any mat projected outside the exterior most column line on any side of the mat. For the present study, its width is defined as the
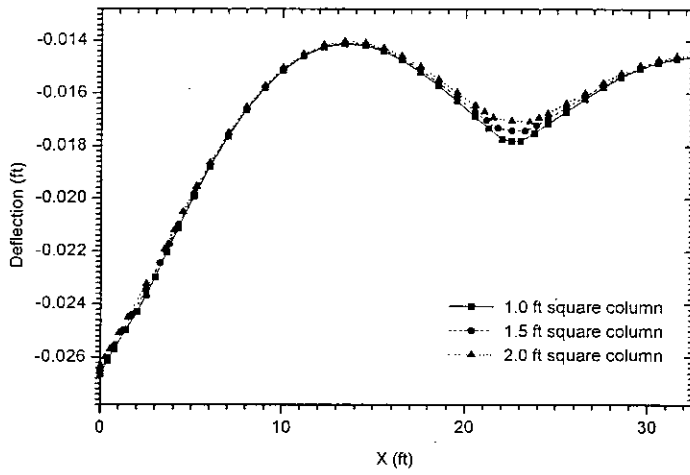
Fig. 4.27 : Deflection diagrams of LINE 2 for different
column sizes (mat thickness 3 ft)
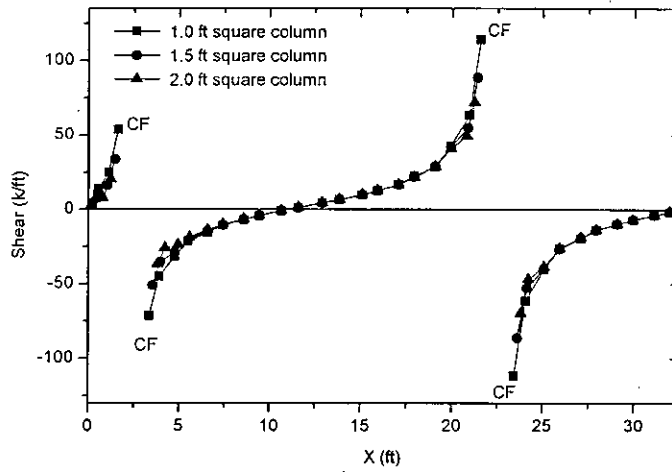
Fig. 4.28 : Shear force diagrams of LINE 2 for different
column sizes (mat thickness 3 ft)
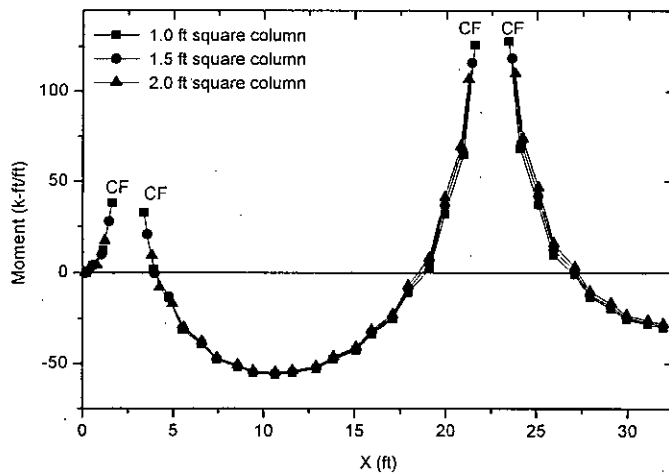
Fig. 4.29 : Bending moment diagrams of LINE 2 for
different column sizes (mat thickness 3 ft)
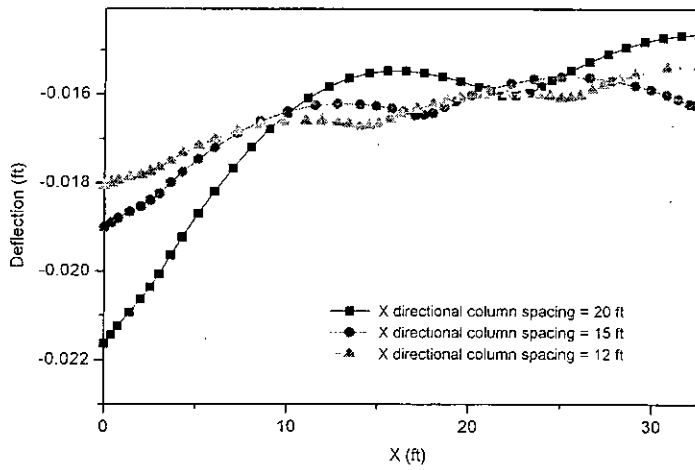
Fig. 4.30 : Deflection diagrams for different column spacing of LINE 2
(mat thickness 3 ft and column size 1.5 ft square)
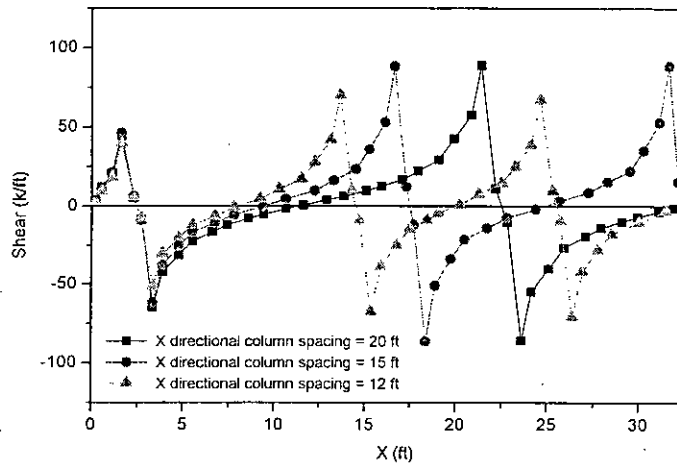
Fig. 4.31 : Shear force diagrams of LINE 2 for different column spacing
(mat thickness 3 ft and column size 1.5 ft square)
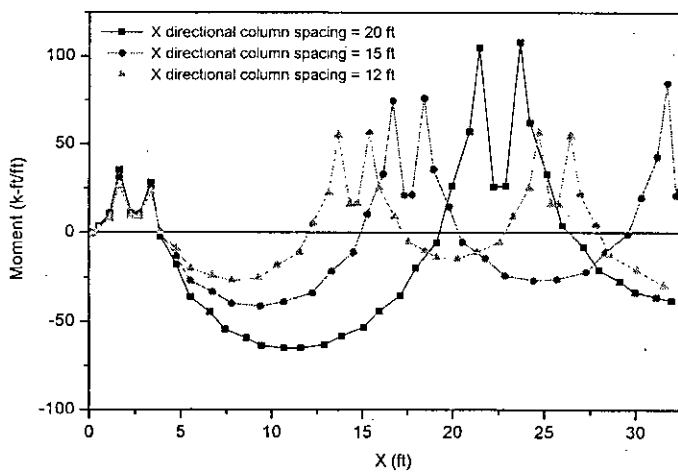
Fig. 4.32 : Bending moment diagrams of LINE 2 for different column spacing
(mat thickness 3 ft and column size 1.5 ft square)
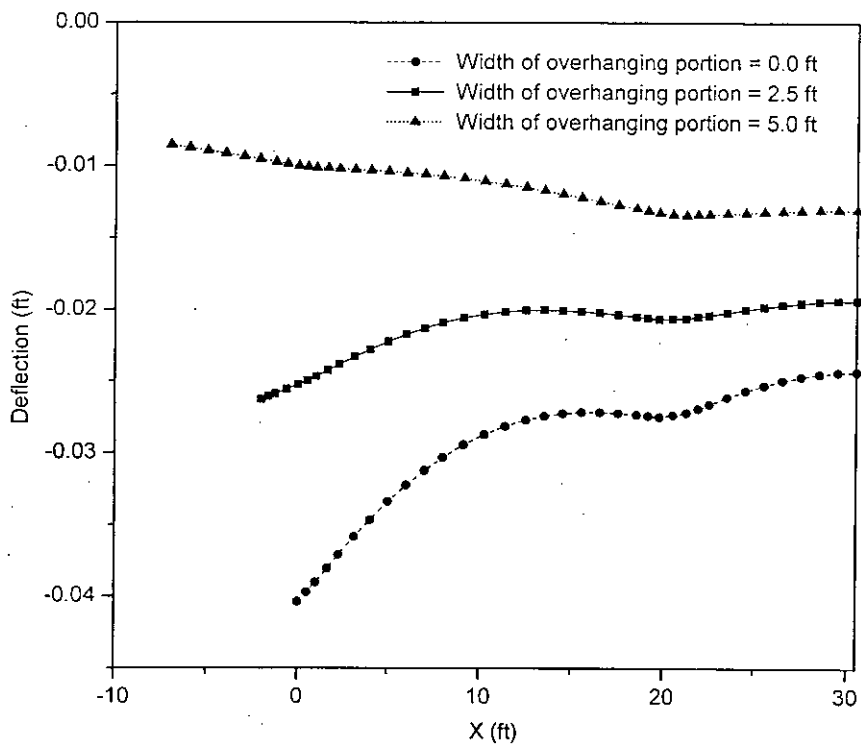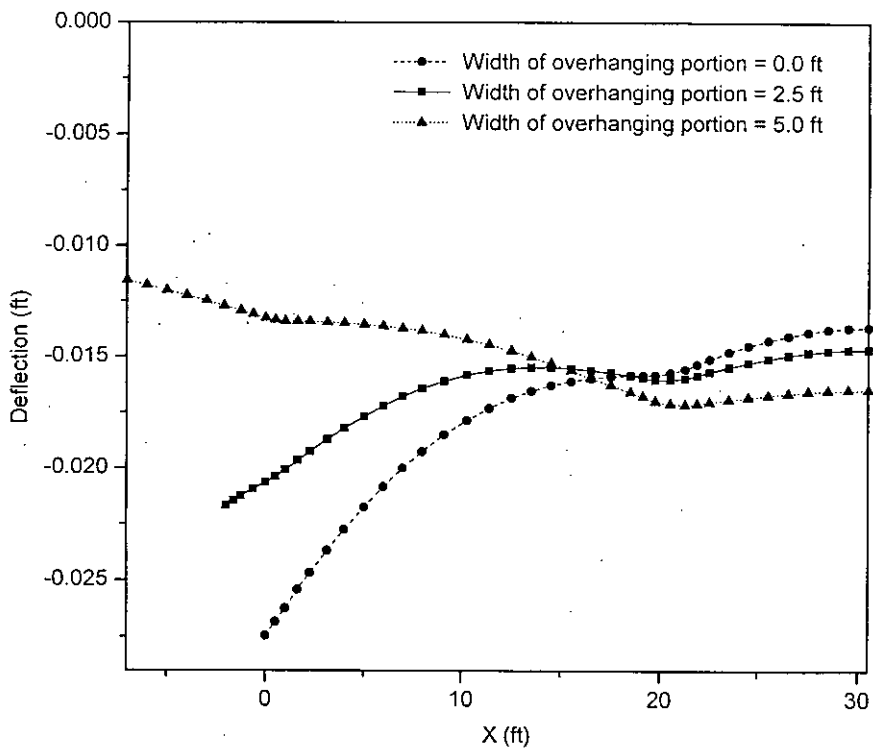
Fig. 4.33 : Deflection diagrams of (a) LINE 1 and (b) LINE 2 for
different widths of overhanging portions (mat thick-
ness 3 ft)
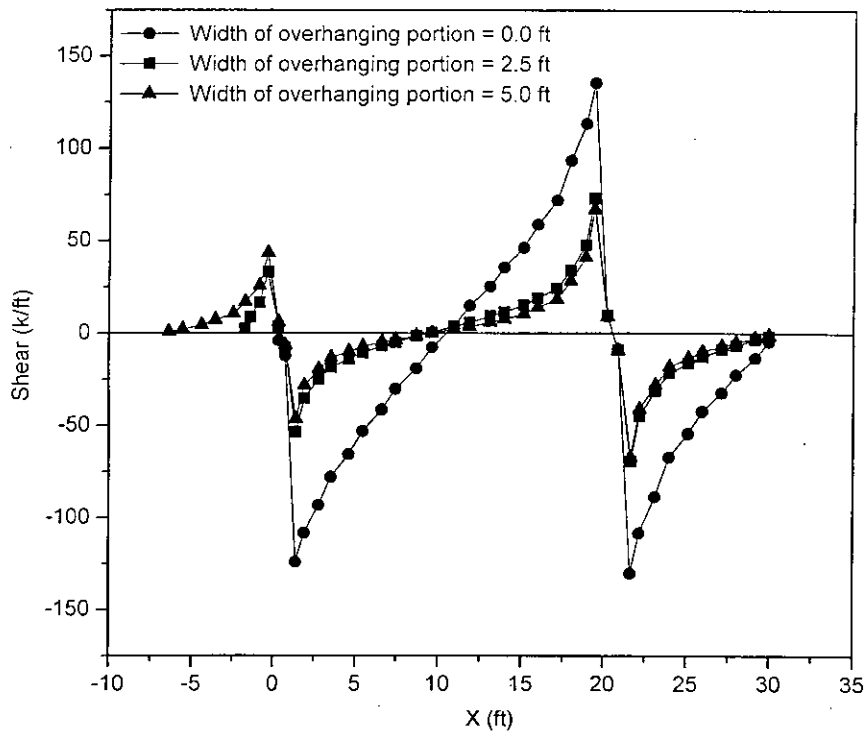
(a)
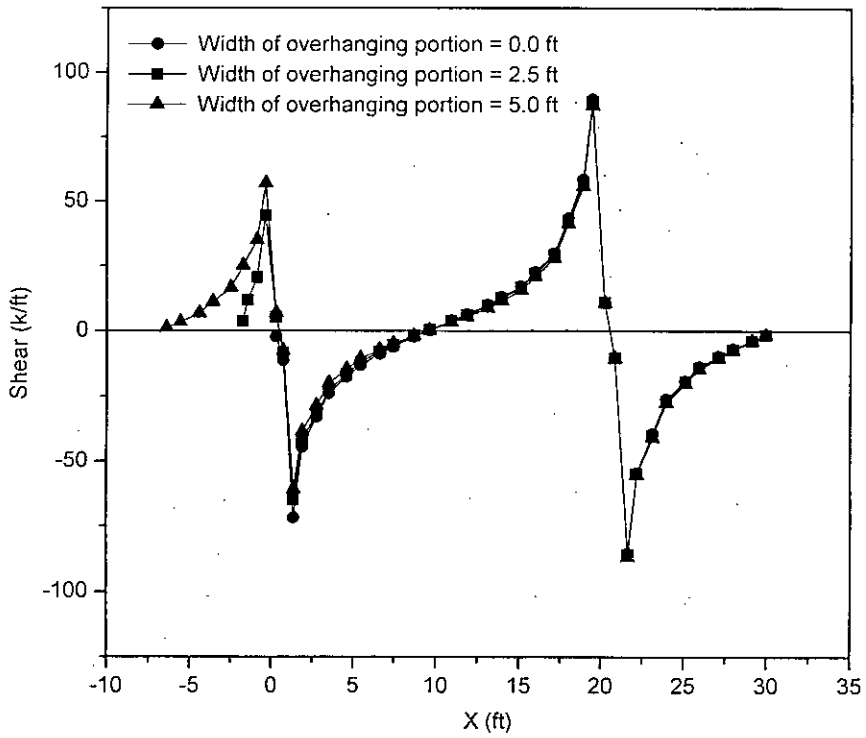
(b)

Fig. 4.34 : Shear force diagrams for different widths of overhanging
portions of (a) LINE 1 and (b) LINE 2 (mat thickness 3 ft)
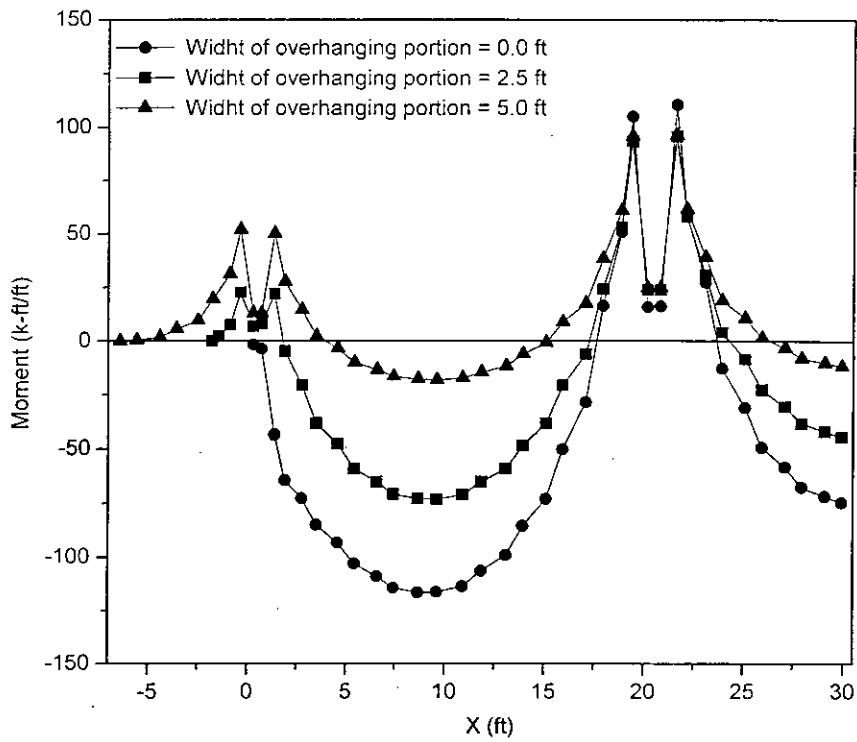
(a)
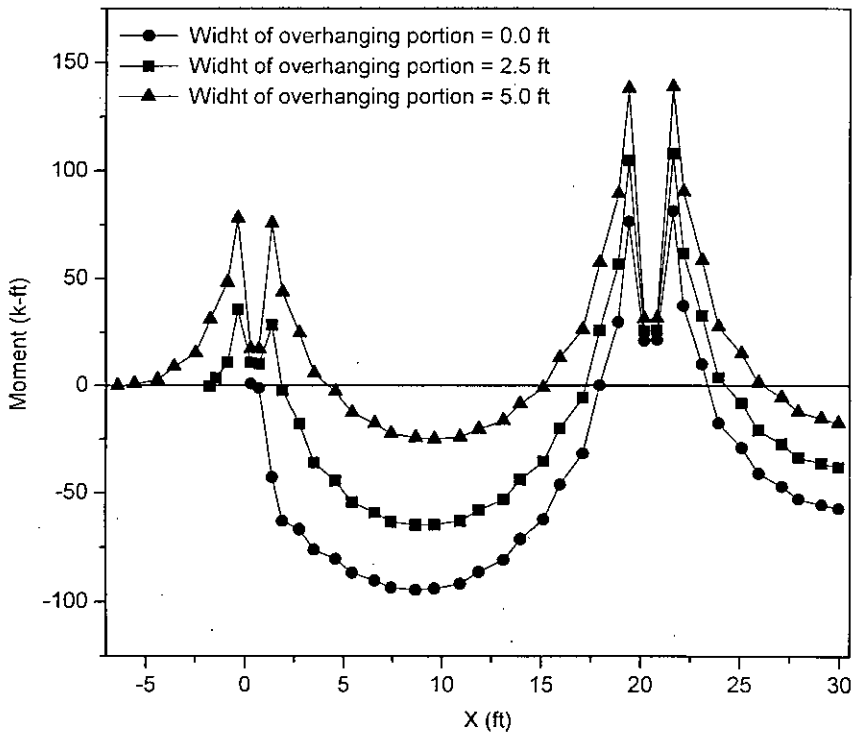
(b)

Fig. 4.35 : Bending moment diagrams of (a) LINE 1 and (b) LINE 2
for different widhts of overhanging portion (mat thick-
ness 3 ft)

distance between the center of the exterior most column line and the nearest edge of the mat (Fig. 4.8). Effect of the width of overhanging portion on mat behavior is depicted in Fig. 4.33 through Fig. 4.35. The graphs are obtained by analyzing the example mat of Fig. 4.8 by varying its width of overhanging portion from 0.00 ft to 7.50 ft.

As the width of overhanging portion is increased

- Deflection pattern changes with the maximum deflection of any column line being shifted from the end towards the center of the column line. Deflection pattern becomes more uniform with a reduction in magnitude.
- An increase in the magnitude of positive moment is observed.
- A decrease in the magnitude of negative moment is observed.
- Shear force is not much affected by this parameter.

The summary of the sensitivity analysis of mat is shown in Table 4.16

Table 4.16 Summary of Sensitivity Analysis of Mat

Parameter	Displacement	Positive moment	Negative moment	Flexural Shear	Punching shear
Mat thickness Increases	Decreases with a very good rate. Sensitive at corner columns	Decreases slightly. Sensitive to central columns	Increases tremendously. Sensitive to in between central columns.	Flexural shear has very little change	Punching shear remains almost constant
Modulus of subgrade reaction increases	Displacement decreases tremendously at a very faster rate.	Positive moment increases slightly. Sensitive to corner columns	Negative moment decreases moderately. Sensitive to in between corner columns.	Flexural shear has very little change.	Punching shear remains almost constant
Ultimate strength of concrete increases	Displacement decreases slightly.	Positive moment decreases very slightly. Sensitive to corner columns	Negative moment increases moderately. Sensitive to in between central columns.	Flexural shear has very little change	Punching shear remains almost constant.
Column spacing increases	Decreases	Decreases	Decreases	Decreases	Decreases
Column size increases	Very slight reduction in the values	Reduction in the peak values	Reduction in the peak values	Reduction in the peak values	Reduction in the peak values
Width of overhanging portion increases	Pattern becomes more uniform with a reduction in magnitude	Increase	Increase	Not affected	Not affected

CHAPTER 5

MAT FOUNDATION WITH NON-UNIFORM THICKNESS

5.1   GENERAL

Normally mat foundations with uniform thickness all over are designed. This kind of mats are always heavily overdesigned which is also the result of uncertainty in analysis procedure. Since Finite element technique is the most powerful and versatile of all the available numerical analysis techniques, so it is possible now to look at other economic configurations of mat. In Fig. 1.1 several mat foundation configurations were shown. There is no method or guideline for analysis or design of these kinds of mat. In the present study mat foundation with the plate thickened under columns termed *non-uniform mat* hereafter is analysed, designed and all parameters related to it are critically reviewed. Ultimately a design guideline is proposed after doing several mat problems.

5.2   JUSTIFICATION OF MAT WITH NON-UNIFORM THICKNESS

From the sensitivity analysis of mat thickness on various items of mat it has been found that as the thickness of mat decreases
- Displacements increases with a good rate. Sensitive at corner columns.
- Positive moment increases slightly. Sensitive to central columns
- Negative moment decreases considerably.   Sensitive to in between central columns.
- Flexural shear has very little change at all.
- Punching shear remains almost constant.

The increase of displacement will not pose any problem since mat is capable of taking high differential settlements. As already seen in the last chapter that positive moment steel is always governed by minimum steel requirements so the slight increase in positive moment will not be of much significance. Punching shear remains almost constant so the thickness provided under column will not change. Due to change in thickness flexural shear does not change much. The flexural shear decreases rapidly away from the column face, it is therefore possible to reduce mat thickness in those areas. Finally considerable decrease in negative moment occurs in the central region of mat due to thickness reduction. This will save cost and substantial economy can be achieved. The reduction of thickness of mat away from columns will also result in savings of steel in the negative moment areas.

5.3   PERFORMANCE OF MAT WITH NON-UNIFORM THICKNESS

To examine the performance of mat with non-uniform thickness, the previous mat of Fig. 4.8 is modified to design a new problem with non-uniform thickness. Greater thickness is maintained around column peripheries. Typical cross-sections along LINE 1 and 2 (Fig. 4.8) of mats with uniform and non-uniform thickness are shown in Fig. 5.1. Every other aspect of the previous mat is kept the same. Results of the analysis are plotted in Fig. 5.2 through Fig. 5.4.

It is important to note that when checking flexural shear, in addition to the usual locations (*d* distance away from column faces) sections *A, B* and *C,* which will be referred to as *neck sections* later on, must be given due attention for mats with non-uniform thickness.

Important design data are presented in Table 5.1 through Table 5.5. Based on these data, MAT I and II are designed separately. In the comparison of the design of MAT I and II, *weighted average thickness of mat* $(t_{avg,})$, is used which is calculated as follows :

70

$$t_{avg} = \frac{\sum t \times A_t}{\sum A_t}$$

(5.1)

where

t   = mat thickness,

A_t = plan area of mat having thickness t.

2 ft thick throughout

2.5'   20'   10'

CL

MAT I

2' thick   1.25' thick   2' thick   1.25' thick

A   B   C

CL

0. 5'   4.25' 1.25'   12.5'   1.5'   5'   1.5'   6'

MAT II

Center line →

10'

C3 (1.5' × 1')   C4 (1.5' × 1.5')   LINE

☐   435.5 k   ☐   697.0 k

20'

Width of overhanging portion

C1 (1' × 1')   C2 (1.5' × 1')   LINE 1

268.0 k   435.5 k

☐   ☐

2.5'

2.5'   20'   10'
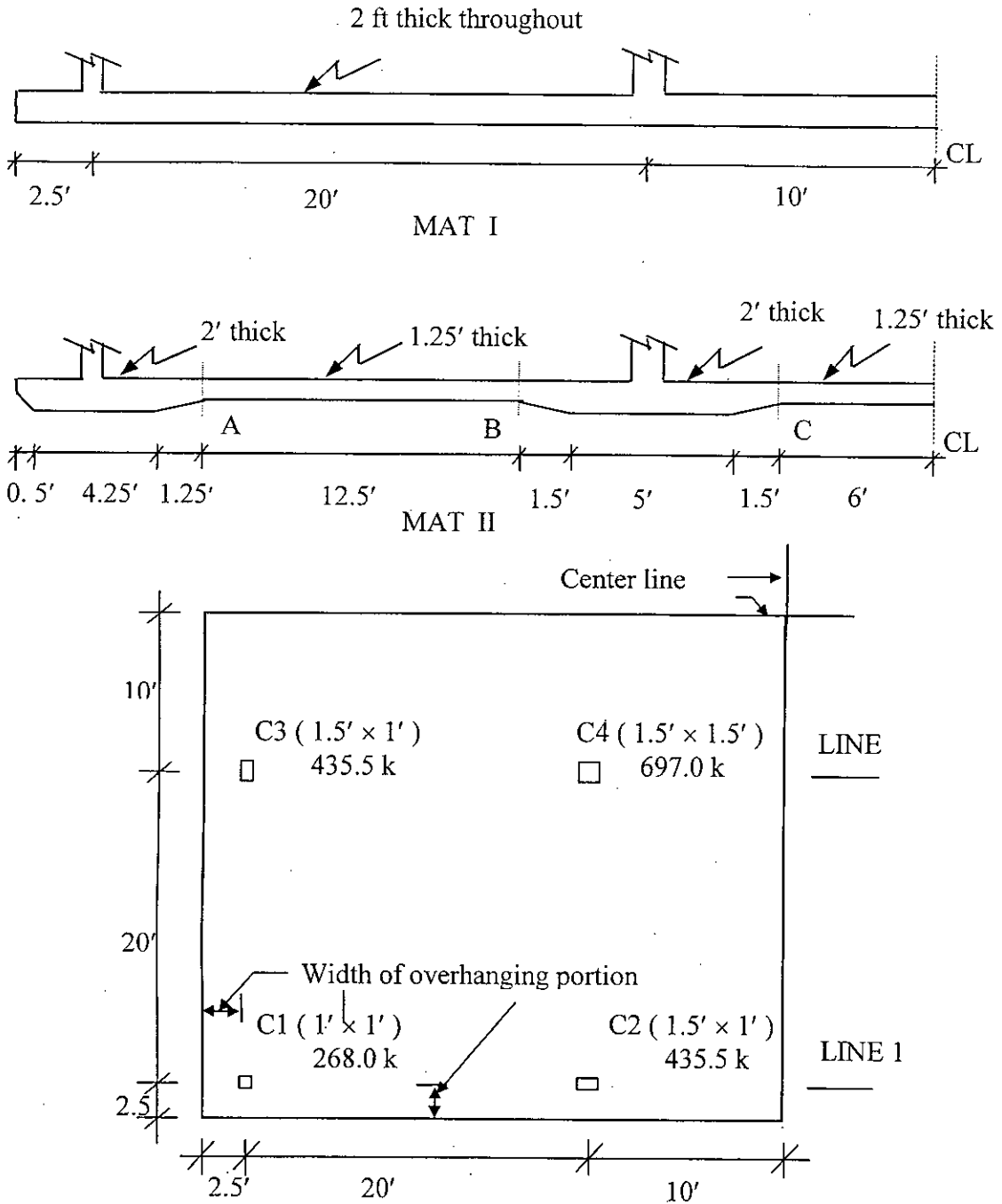
Fig. 5.1. Mats with uniform and non-uniform thickness (CL = center line).
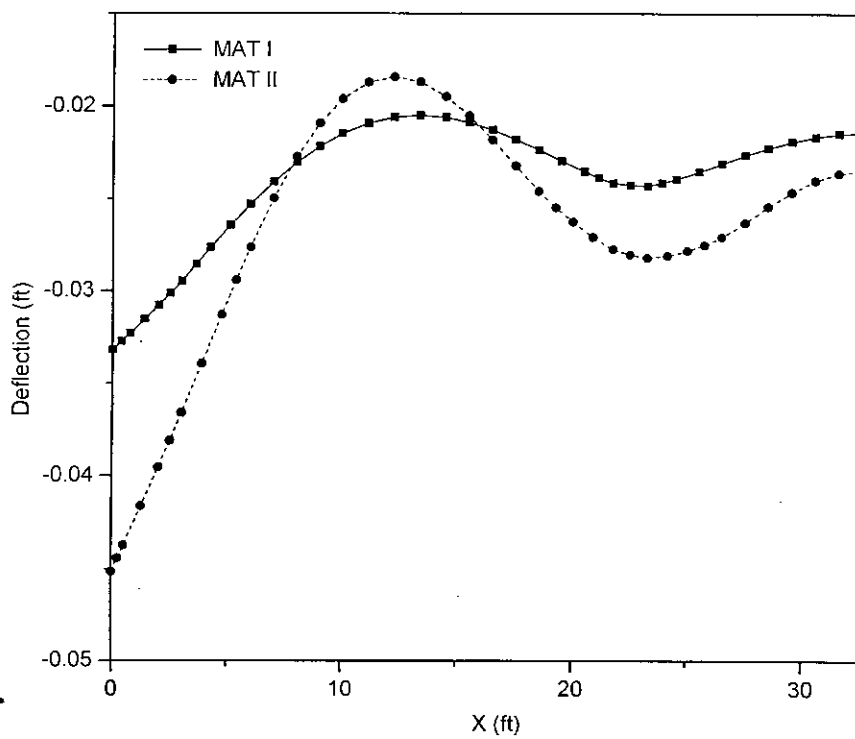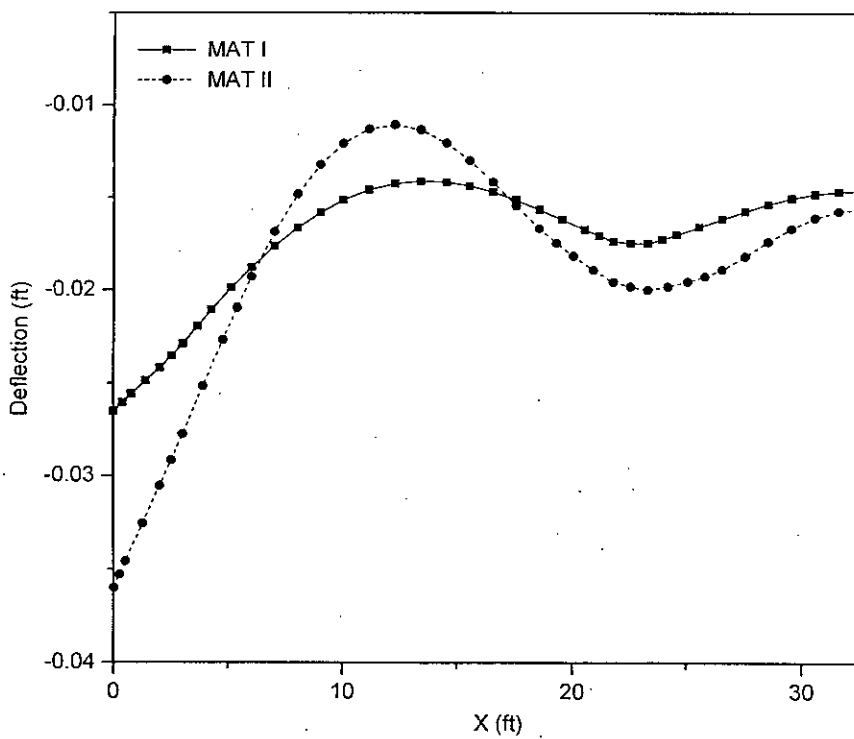
Fig. 5.2 : Comparison of deflection diagrams of (a) column strip 1
and (b) column strip 2 for MAT I and MAT II
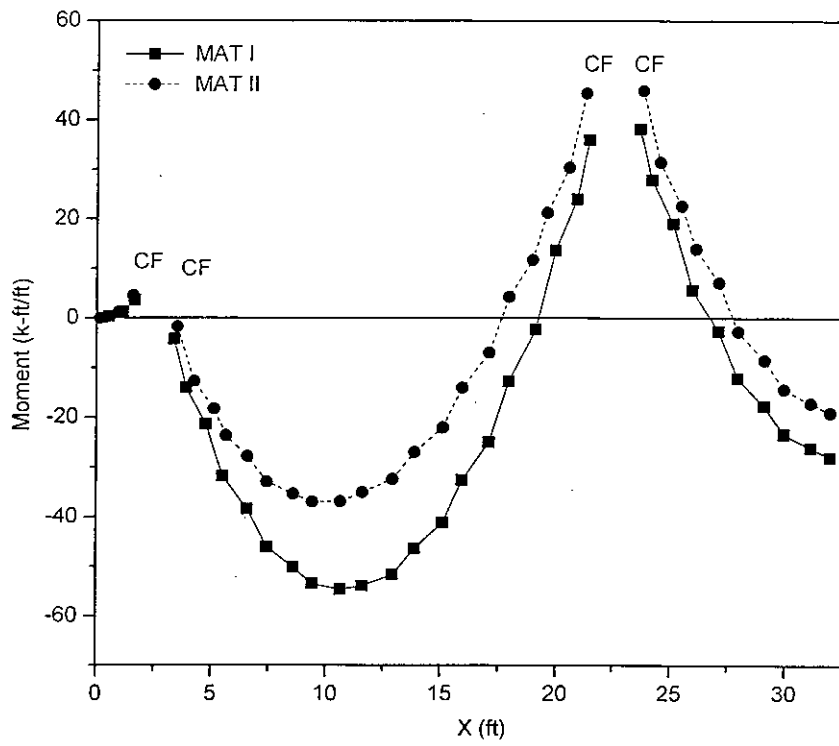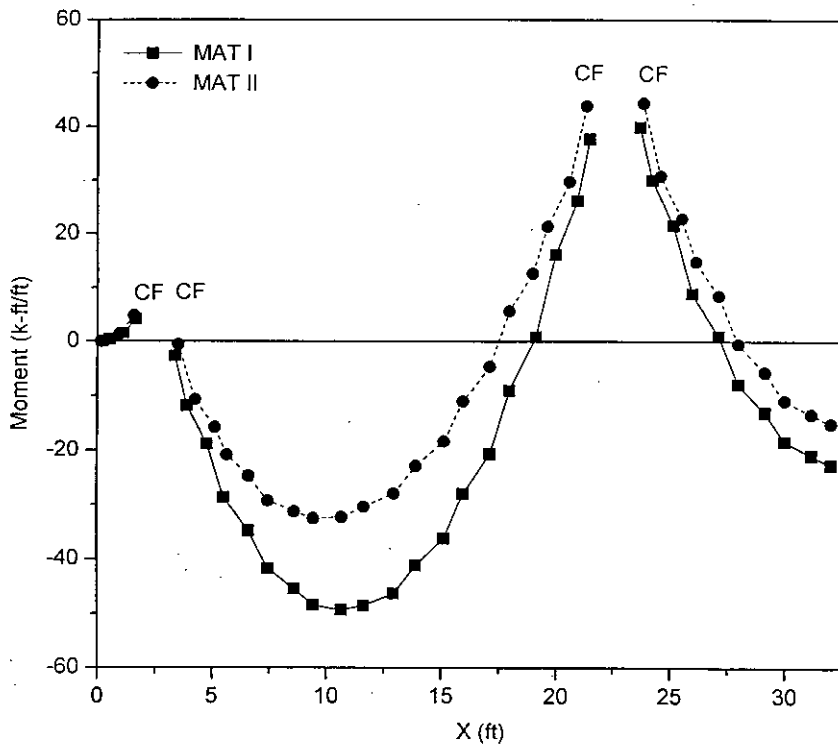
Fig. 5.3 : Comparison of bending moment diagrams of (a) column strip 1 and
(b) column strip 2 for MAT I and MAT II
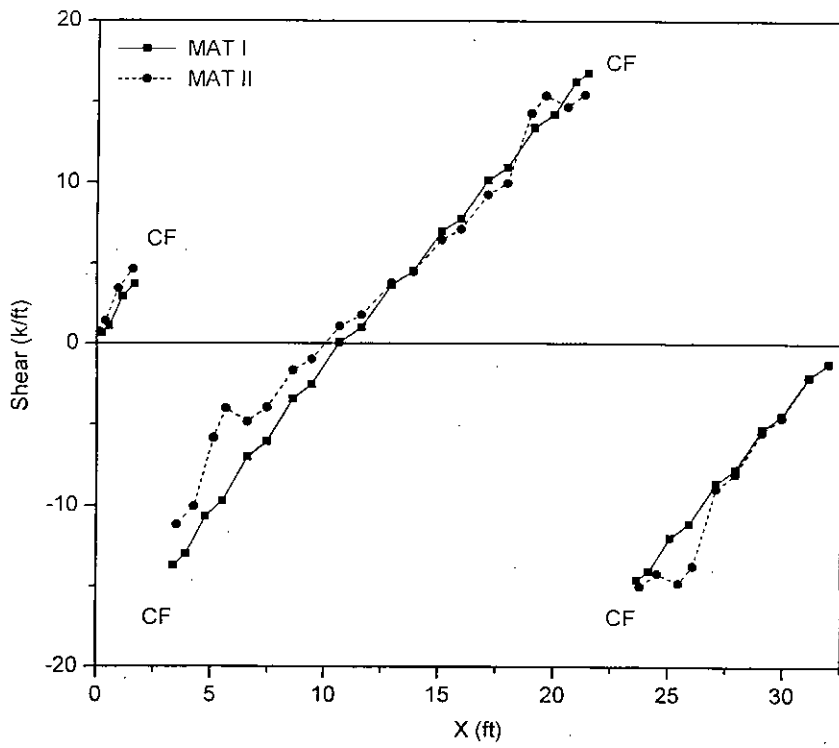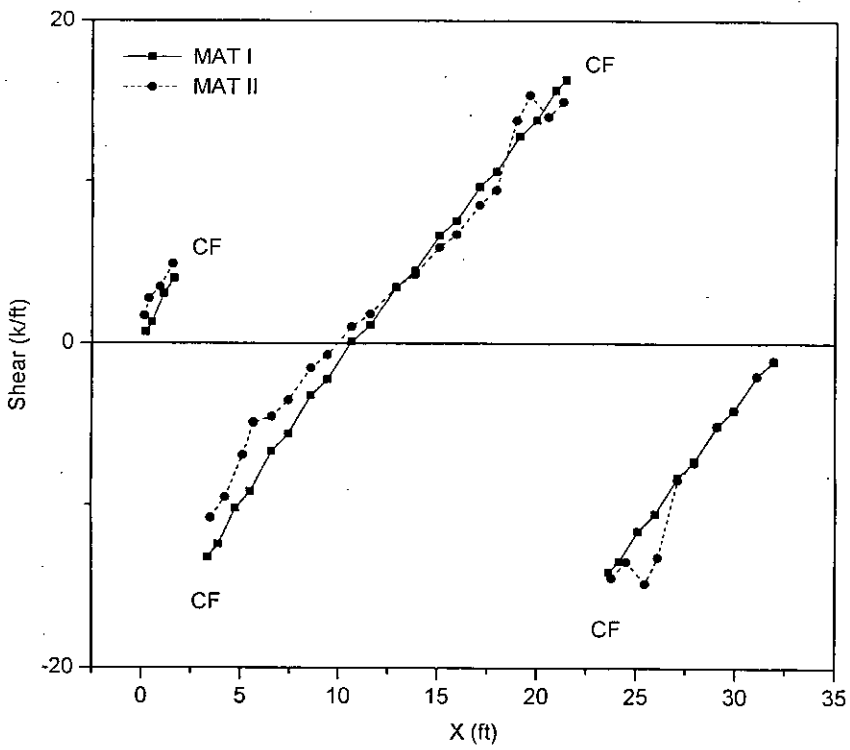
Fig. 5.4 : Comparison of shear force diagrams of (a) column
strip 1and (b) column strip 2 for MAT I and MAT II

Table 5.1.   Column displacements of MAT I and II (Fig. 5.1).

Mat Type	Column C1	Column C2	Column C3	Column C4
I	0.36"	0.29"	0.28"	0.21"
II	0.46"	0.34"	0.35"	0.24"

Table 5.2.   Punching shears of MAT I and II (Fig. 5.1).

Mat Type	Column C1	Column C2	Column C3	Column C4
I	240.2 k	405.8 k	405.8 k	666.3 k
II	233.9 k	401.4 k	401.4 k	665.5 k

Table 5.3.   Column face positive moments of MAT I and II (Fig. 5.1).

Mat Type	Column C1	Column C2	Column C3	Column C4
I	3.6 k-ft/ft	36.0 k-ft/ft	4.2 k-ft/ft	37.7 k-ft/ft
II	4.6 k-ft/ft	46.0 k-ft/ft	4.9 k-ft/ft	44.5 k-ft/ft

Table 5.4.   Maximum column strip negative moments of MAT I and II (Fig. 5.1).

Mat Type	Between C1-C2	Center of strip 1	Between C3-C4	Center of Strip 2
I	54.5 k-ft/ft	27.9 k-ft/ft	49.3 k-ft/ft	22.7 k-ft/ft
II	36.9 k-ft/ft	19.0 k-ft/ft	32.5 k-ft/ft	15.1 k-ft/ft

Table 5.5.   Critical flexural shears of MAT I and II (Fig. 5.1).

Mat Type	d distance away from column C2 (V_{C2})	At section B of strip 1 (V_B)
I	16.0 k/ft	12.2 k/ft
II	14.8 k/ft	12.3 k/ft

Table 5.1 shows that column deflections found by FE analysis are below the allowable limits by a substantial margin for the two mats considered even though weak clayey soil has been used in these examples. It can be concluded that differential settlement will not cause any problem when thickness is non-uniform.

Punching shear does not change significantly (Table 5.2) due to the reduction of mat thickness away from the columns. This implies that thickness requirement in the vicinity of columns will not change significantly and the same thicknesses at those locations, as obtained from uniform thickness solution, can be maintained without further revision.

Flexural shears change mainly near the columns. At the neck sections A, B or C (Fig. 5.1 and Table 5.5), practically there is no change in flexural shear which means that the magnitude of thickness reduction can be estimated from the uniform thickness solution. This is because at the locations where change of thickness occurs, punching shear will be of no concern for thickness design. Rather flexural shear will control thickness requirement at the neck sections. And as neck flexural shear can be estimated from the uniform thickness solution, thickness requirement at the neck sections can be calculated directly. So the magnitude of thickness reduction may be estimated.

In regions where transition from higher to lower thickness takes place (these regions will be referred to as *transition zones* subsequently), shear magnification is observed in the central regions of the column strips (Fig. 5.4). This phenomenon should be given due attention since this magnification occurs in contrast to the flexural shear capacity reduction of mat associated with thickness reduction at those locations.

Reduction of negative moments due to lower thickness in-between the columns is noteworthy (Fig. 5.3 and Table 5.4). It is observed to be as high as 32% for MAT II. This reduction increases with the lowering of thickness, a very positive advantage. In

73

the USD method of reinforced concrete design, maximum moment capacity of a section is very high and this substantial reduction in negative moment implies that if flexural shear permits, quite a thin section may be used in the negative moment regions with lower reinforcement cost.

Increase in positive moment due to the reduction of mat thickness away from the columns is also significant (Fig. 5.3 and Table 5.3) and is found to be up to 31%. However, thickness is high at the locations where positive moments occur. As a result, positive moments remain below the minimum moment capacity despite amplification. Evidently, making thickness non-uniform allows a more efficient and economic use of material strength near the columns since minimum steel must always be provided there.

MAT II comes out to be an acceptable design in terms of both concrete and steel requirements. A comparative evaluation of the design of MAT I and II is made in Table 5.6 to Table 5.8.

Table 5.6.   Design values of MAT I and II (Fig. 5.1).

Mat Type	$t_{required}$ for punching shear (in)	$t_{required}$ for flexural shear V_{C2} (in)	$t_{required}$ for neck flexural shear V_B (in)	A_s for column face positive moment (in^2/ft)	A_s for negative moment C1-C2 (in^2/ft)	A_s for negative moment LINE 1 center (in^2/ft)	A_s for negative moment C3-C4 (in^2/ft)	A_s for negative moment LINE 2 center (in^2/ft)
I	23.8	15.9	13.0	0.821	0.821	0.821	0.821	0.821
II	23.7	15.0	13.1	0.821	0.748	0.460	0.655	0.460

Table 5.7. Economic evaluation and comparison of the design of MAT I and II.

Mat Type	t_{avg} (in)	Positive A_s^{avg} (in²/ft)	Negative A_s^{avg} (in²/ft)	Economy in concrete cost w.r.t. MAT I	Economy in reinforcement cost w.r.t. MAT I
I	24.0	0.821	0.821	Not Applicable	
II	16.2	0.616	0.614	32.5%	25.0%

Table 5.8. Comparison of acting moments and shears with respective moment and shear capacities for MAT II with non-uniform thickness.

Column Strip	Maximum column face positive moment (k-ft)		Maximum shear at a distance d^* away form column face (k)		Maximum kink shear (k/ft)	
	Acting	Capacity	Acting	Capacity	Acting	Capacity
1	563.4	663.5	183.90	241.30	15.40	18.10
2	900.60	1031.20	299.70	376.10	15.50	17.30

* d = Effective depth.
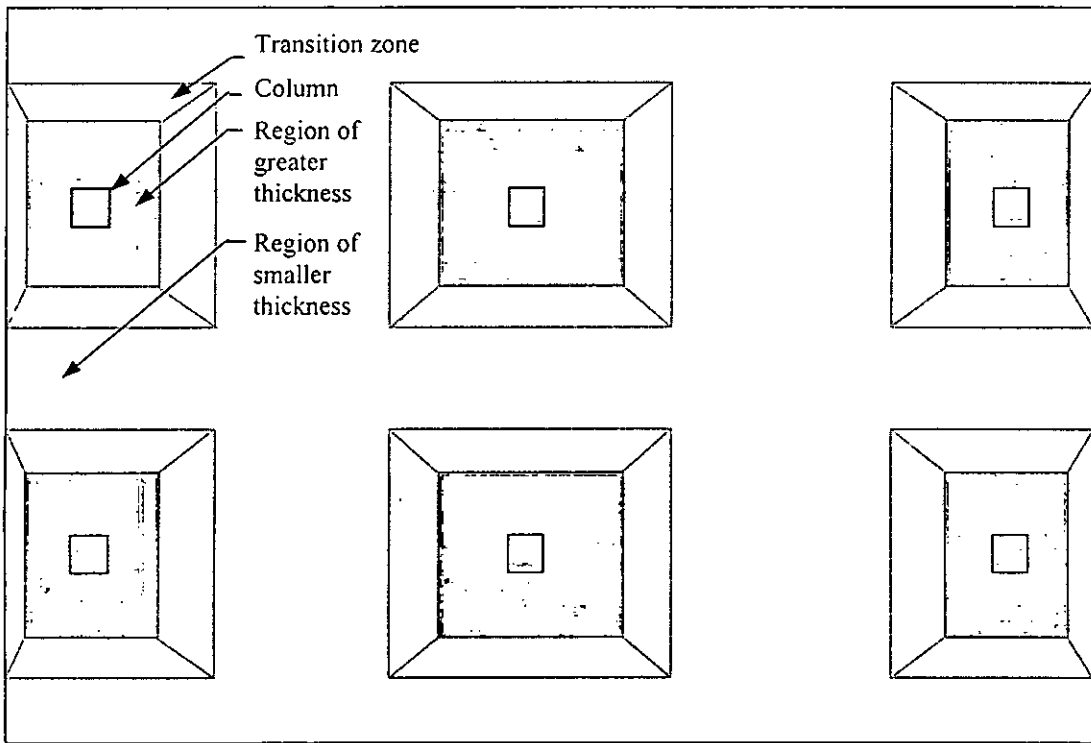
(b)
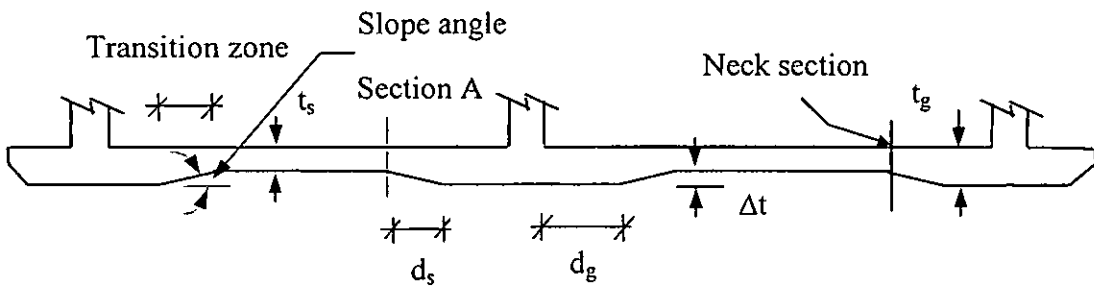
(a)

Fig. 5.5. Various important properties of mat with non-uniform thickness : :
(a) typical plan. and (b) typical cross-section

76

5.4   SENSITIVITY ANALYSIS OF MAT WITH NON-UNIFORM THICKNESS

It has been established in the previous article, mat with different thicknesses at different locations has been found to be a better design than mat with uniform thickness.

For the non-uniform thickness solution, to formulate a general guideline certain geometrical parameter of the new mat is considered. Effects of these parameters on the mat is studied i.e. the distance over which the change in thickness should be implemented (d_s), the lateral extent of greater thickness around the columns (d_g) and the amount of reduction in mat thickness away from the columns (Δt) (Fig. 5.5). Of the above items, Δt can be realized in terms of t_g and t_s. For the convenience of further discussion these items are named as follows :

d_s =   *Slope width,*

d_g =   *Width of greater thickness,*

t_g =   *Greater thickness,*

t_s =   *Smaller thickness,*

Δt =   *Change in thickness.*

5.4.1   Effect of Slope Width (d_s)

To examine the effect of slope width, MAT II of Fig. 5.1 is analyzed by varying its d_s from 0.75 ft to 2.00 ft. Variation of column displacements, column face positive bending moments, maximum negative bending moments, column face flexural shears and *kink shears* (those in the transition zones) are shown in Fig. 5.6 through Fig. 5.8 and tabulated in Table 5.9.
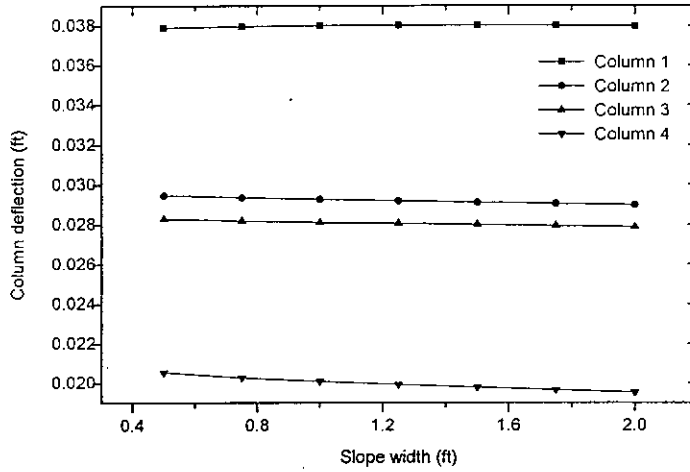
(a)
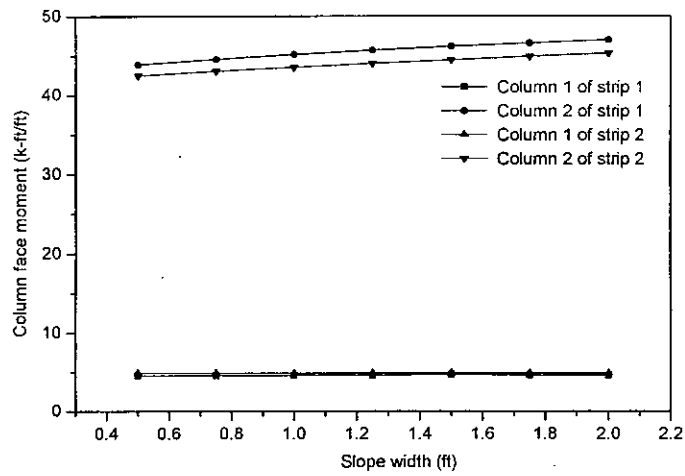
(b)
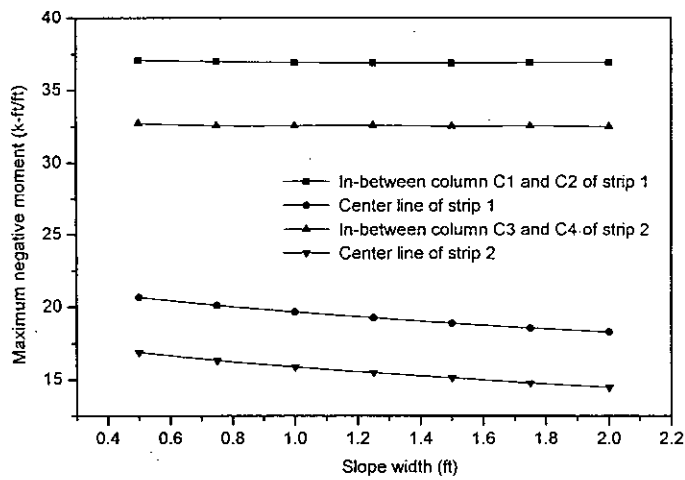
(c)

Fig. 5.6 : Effect of slope width on (a) column deflection, (b) positive
and (c) negative bending moment (MAT II)
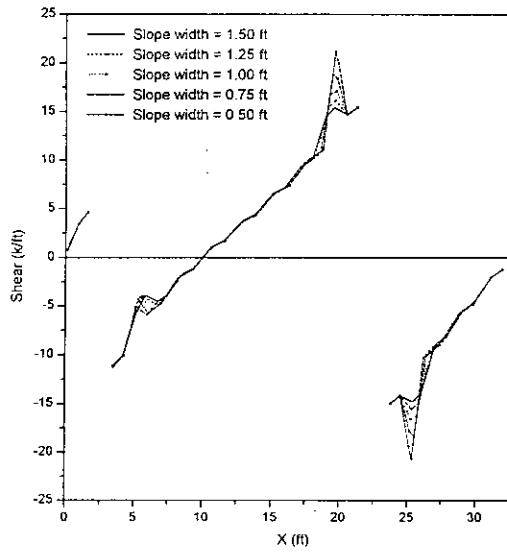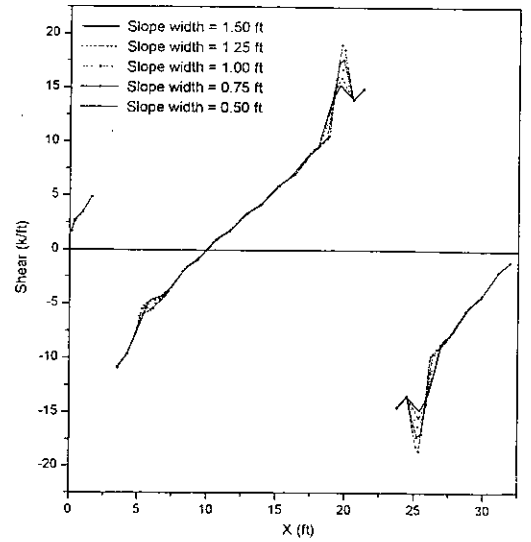
Fig. 5.7   : Shear force diagrams for different slope widths of
(a) column strip 1 and (b) column strip 2 (MAT II)
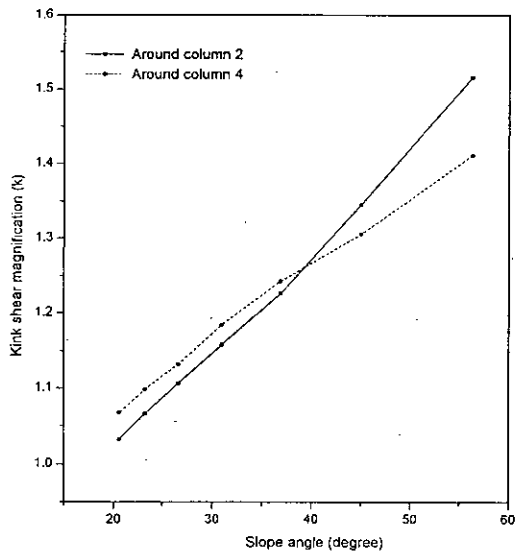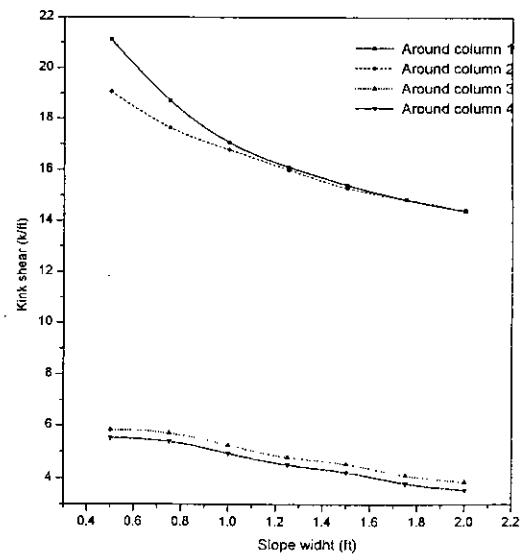
Fig. 5.8   : Effect of slope width on kink shear as a function of
(a) slope width and (b) slope angle (MAT II)

As slope width increases

- Deflection of column decreases by very small amount (5% at C4)
- Column face moment increases by very small amount (6.7% at C4)
- Negative moment decreases slightly (14.3% at centre of strip 2)
- Punching shear does not change at all.
- High flexural shear concentration occurs in the transition zone near the centre of the column strip.

Effect of slope width on flexural shear is noticeable. Fig 5.7 shows that high shear concentration occurs in the transition zones (Fig. 5.5) near the center of the column strips. Near the ends of the column strips, flexural shears decrease in the transition zones. A plot of the ratio of the magnified shear to the shear at the corresponding points in case of uniform thickness, against slope width (Fig. 5.8) shows that the ratio, which will be designated as *kink shear magnification* later on, tends to unity as slope width is increased. When considered in terms of the angle of the slope (Fig. 5.8), the ratio comes close to unity as the slope flattens out.

Final selection of the slope depends on the optimization between the flexural shear capacity of the transition zone and the degree of kink shear magnification. But sharp change in thickness should be avoided when possible.

5.4.2   Effect of Change in Thickness (Δt)

For the same problem (MAT II of Fig. 5.1) change in thickness (Δt) is varied from 0.00 to 1.00 ft, keeping the greater thickness t_g (Fig. 5.5) fixed at 2 ft. Variation of different items thus observed is depicted in Fig. 5.9 through Fig. 5.12.

As the smaller thickness is decreased or Δt is increased,

- Deflection increases rapidly but differential settlement is within tolerable limits.
- Reduction of negative moments occurs in regions away from the columns.
- Column face moment is increased moderately.
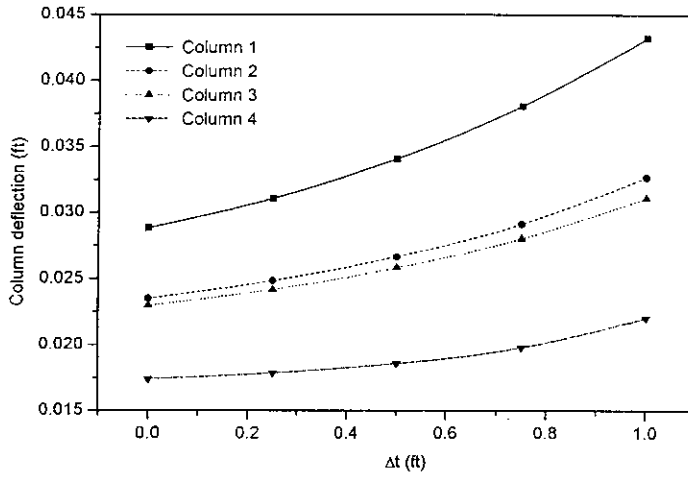
Fig. 5.9 : Effect of Δt on column deflection (MAT II)
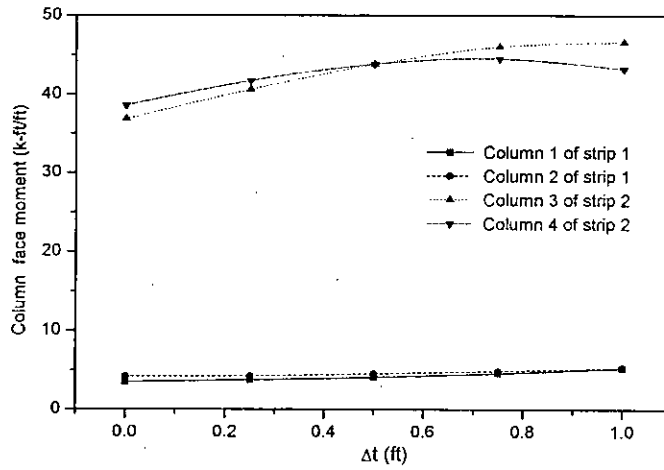
(a)

(b)
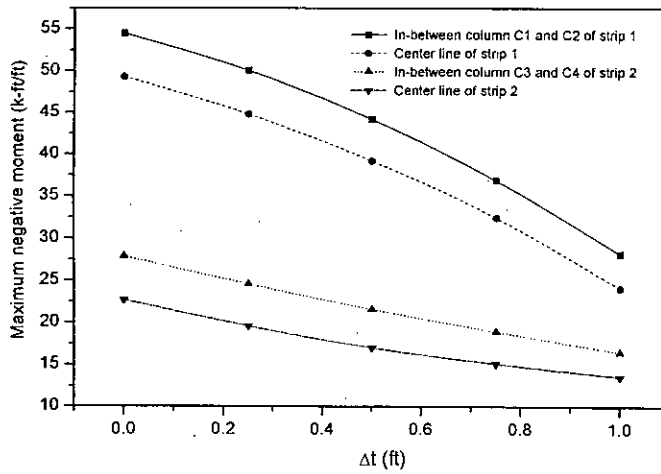
Fig. 5.10 : Effect of Δt on (a) positive and (b) negative bending
moment (MAT II)
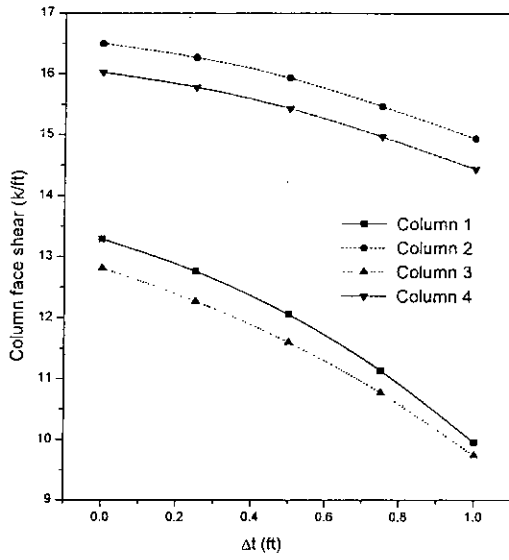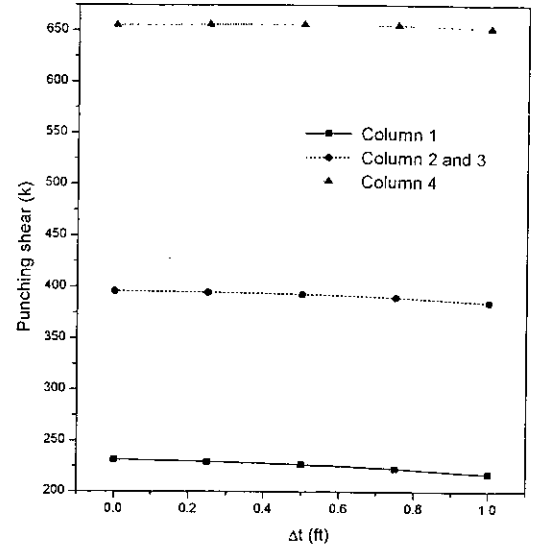
Fig. 5.11 : Effect of Δt on (a) column face shear and (b) punching
shear (MAT II)
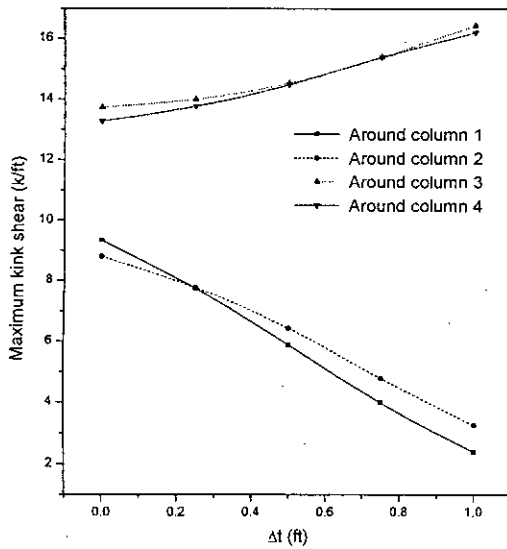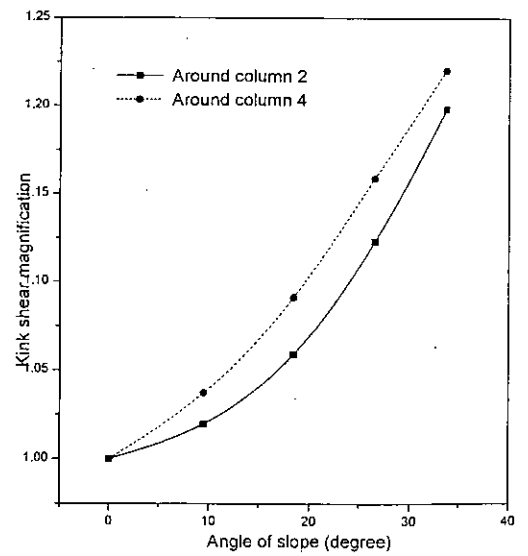
Fig. 5.12 : Effect of Δt on kink shear as a function of (a) Δt
and (b) slope angle (MAT II)

- Kink shear increases as the slope of the transition zones gets steeper (with greater change in thickness, slope of the transition zones gets steeper).

Table 5.9.   Variation of mat response with the change of Δt from 0.00 ft to 1.00 ft.

Location*	Column face +ve Moment	Maximum Negative Moment*	Punching Shear	Column Deflection	Kink Shear	Column Face Shear
C1	+49.5%	-48.3%	-6.1%	+50.0%	+74.4%	-25.1%
C2	+26.4%	-40.8%	-2.6%	+39.0%	+19.8%	-9.5%
C3	+26.5%	-51.1%	-2.6%	+35.4%	-63.0%	-24.0%
C4	+11.9%	-40.0%	-0.4%	+26.5%	+22.0%	-9.9%

*   respective locations for negative moments are in-between columns C1 & C2, center of LINE 1, in-between columns C3 & C4 and center of LINE 2.

A plot of kink shear w.r.t. to the zero *slope angle* (Fig. 5.5) solution verses slope angle (Fig. 5.12) shows as before that kink shear magnification becomes less prominent as the slope flattens out.

5.4.3   Effect of Width of Greater Thickness (d_g)

MAT II (Fig. 5.1) is analysed by varying only d_g in the range of 15.00 inches to 27.00 inches. Final results are graphically compared to investigate the effect of d_g on mat behavior. The graphs are shown in Fig. 5.13 through Fig. 5.16.

As the width of greater thickness is increased
- Column deflection decreases by a very small amount (5.5% at C4).
- Column face positive moment does not change appreciably.
- Negative moment at centre of strips decreases moderately (13%).
- Flexural shear is lowered. Column face shear decreases slightly (by 3-8%).

79
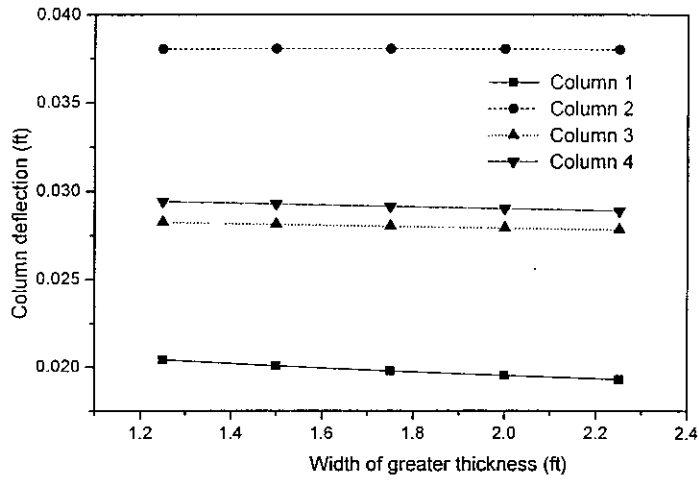
Fig. 5.13 : Effect of width of greater thickness on column
deflection (MAT II)
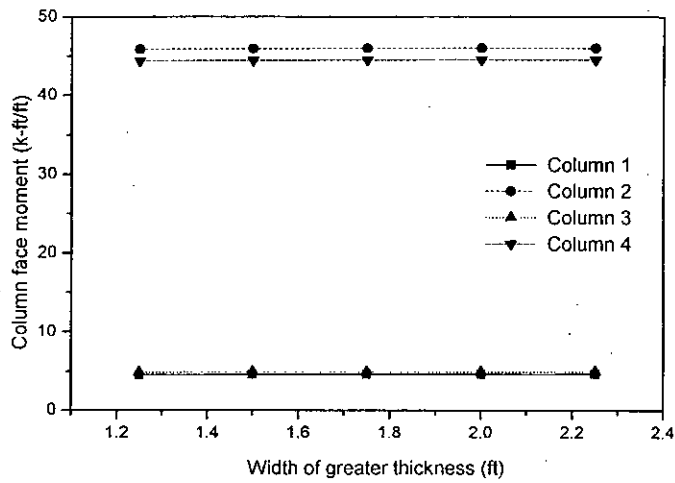
(a)
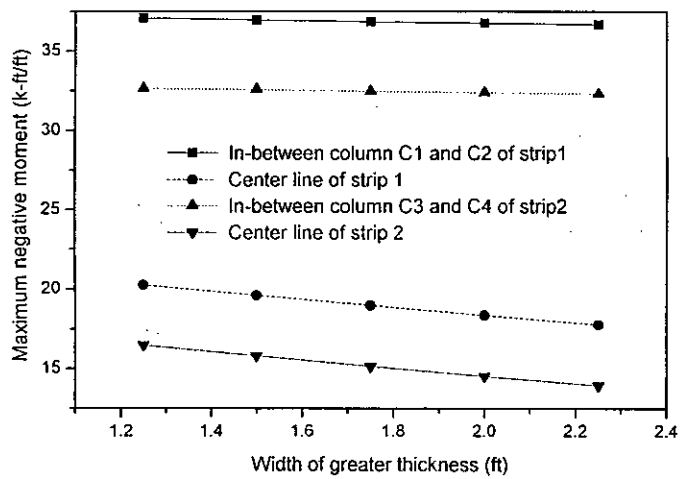
(b)

Fig. 5.14 : Effect of width of greater thickness on (a) positive
and (b) negative moment (MAT II)
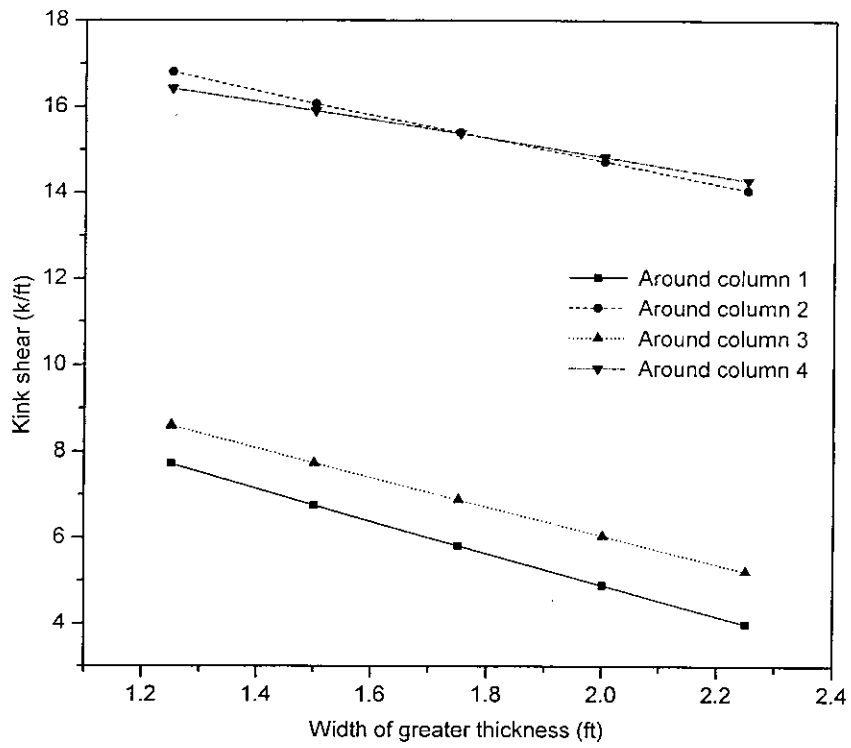
(a)
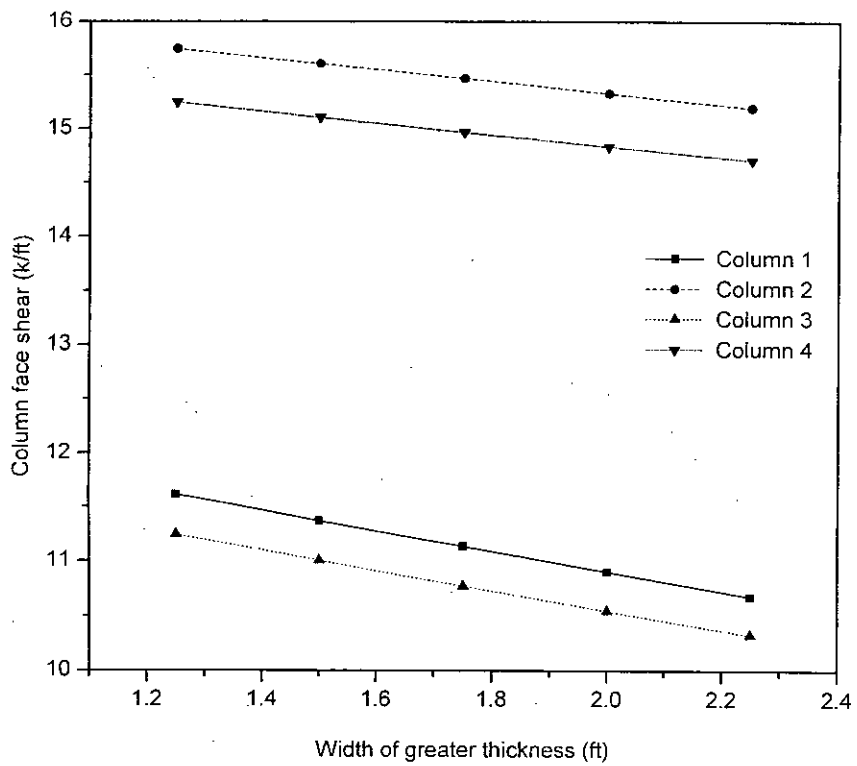
(b)

Fig. 5.15 : Effect of width of greater thickness on (a) kink shear
and (b) column face shear (MAT II)
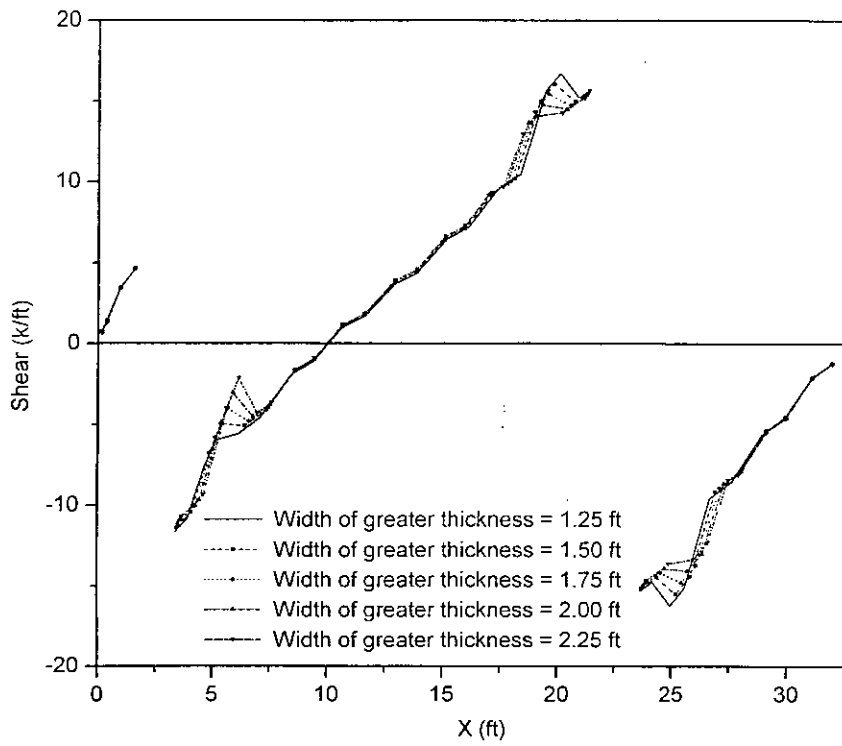
(a)
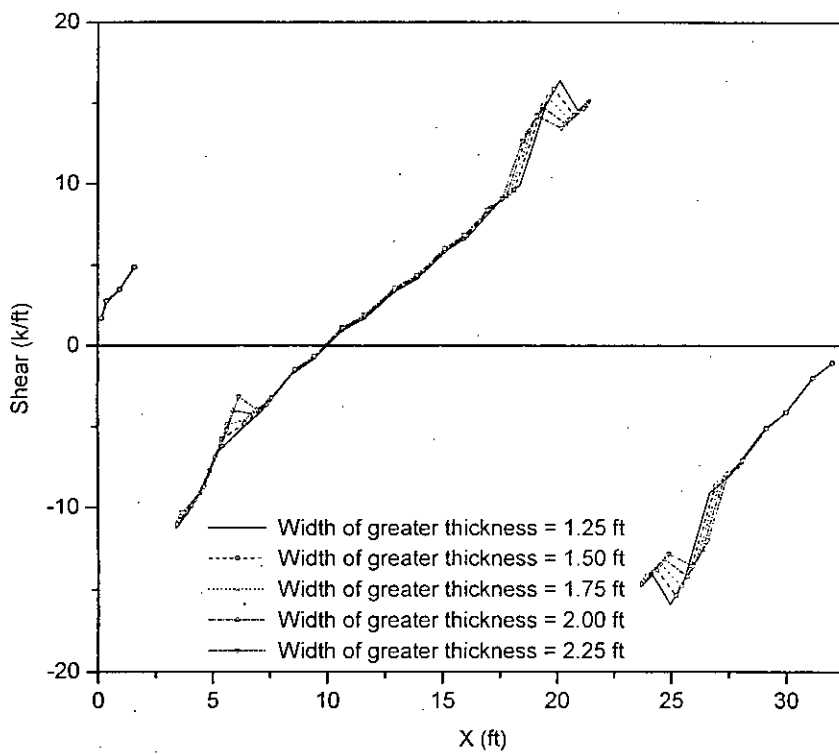
(b)

Fig. 5.16 : Shear force diagrams of (a) column strip 1 and (b) column
strip 2 for different widths of greater thickness (MAT II)

With the widening of thicker regions, transition zones move away from the faces of the columns towards lower flexural shear regions. Consequently kink shear reduction is observed which, due to the change in their locations, are not comparable. But since flexural shears do not govern the thickness design near the columns, this reduction in the magnitude of column face shear forces do not offer any additional advantage.

5.5   FINDINGS FROM THE SENSITIVITY ANALYSIS

Mat with non-uniform thickness offers a way of attaining substantial economy.

- Greater thickness under the columns will be designed from maximum punching shear .

- The smaller thickness will be designed from flexural shear at the neck sections. Then this thickness should be reinforced for negative moments.

- With the reduction of thickness in the low shear and high negative moment regions, column face positive moments increases. But since greater thickness is provided in the positive moment and high shear regions, this amplification does not pose any threat. Column face positive moments, after being averaged across column strip widths, come out to be much lower than the moment capacities of mat at those sections. Reinforced throughout with the minimum steel is required for the greater thickness.

- Reduction of thickness is associated with the reduction of moment capacity. As negative moments decrease with the decrease of thickness, reduction of moment capacity of mat at the corresponding locations does not change to that extent.

- Width over which change of thickness should be made .i.e. slope width is not very critical as long as the slope of the transition zones is kept as flat as practicable.

- But since greater thickness is required for punching shear purpose and since in the calculation of the punching shear capacity, flexural shear cracks are assumed to propagate downward from the column face at an angle of 45°, a width equal to the effective depth corresponding to the greater thickness seems to be rational.

5.6 .DESIGN GUIDELINE FOR MAT WITH NON-UNIFORM THICKNESS

The sensitivity analysis reveals that the design of regular shaped mats with non-uniform thickness follow some well defined trends. Based on these findings, a design approach for mat with non-uniform thickness is recommended as follows :

$P_{DL+LL\,(max)}$ = Maximum column axial load due to live load and dead load

t_g = thickness required to encounter $0.95\ P_{DL+LL\,(max)}$ as punching shear,

t_s = $2t_g\,/\,3$,

d_g = effective depth corresponding to t_g,

d_s = $t_g/\sqrt{3}$.
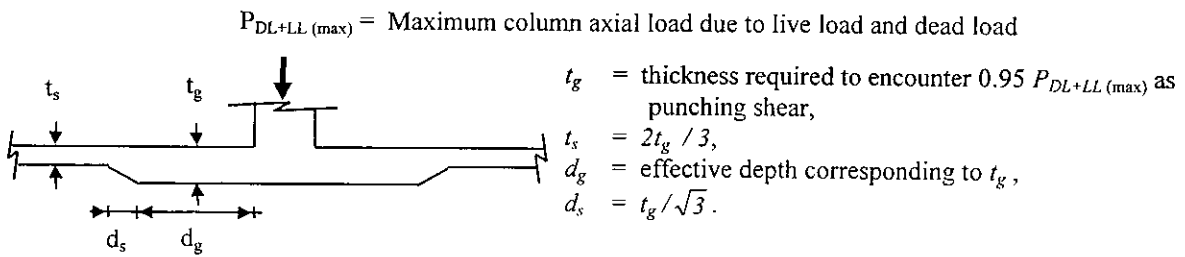
Fig. 5.17. Guideline for selecting cross-sectional geometry for the first trial solution of mat with non-uniform thickness.

(i)   The problem should be solved first with a non-uniform thickness geometry selected from the guideline shown in Fig. 5.17. Column punching shear should be estimated as 0.95 x column axial force.

t_g = *Greater thickness*, calculate from this punching shear

t_s = *Smaller thickness*, = 66% of t_g

d_g = *Width of greater thickness*, = effective depth corresponding to t_g

d_s = *Slope width*, = $t_g/\sqrt{3}$

Slope angle $\cong 30°$

(ii)   A mat analysis is performed regarding this geometry. Now the Greater thickness (t_g) under the columns should be designed from the column punching shear found from analysis.

(iii) The greater thickness (t_g) should be provided around the column peripheries over a distance equal to the effective depth corresponding to the greater thickness itself.

(iv) Smaller thickness should be calculated from the maximum flexural shear, found from the solution, at the neck sections.

(v) Width of the transition zones (for gradual reduction of thickness) should be such that slope angle of the underside of mat in these zones be between 30° to 35°.

(vi) The problem should be analyzed again with the new geometry just selected in order to calculate reinforcements. Finally a check on the adopted geometry using the shear forces diagrams and punching shears found from the *new solution*.

(vii) Minimum reinforcement required for the zone of greater thickness should be provided as bottom reinforcement under the columns across the entire widths of column strips. Again, the new solution may be used to check the adequacy of these reinforcements.

(viii) Reinforcements for negative moments in-between the columns should be designed using the new solution.

(ix) Bottom reinforcements in-between the columns (negative moment zones) and top reinforcements under the columns (positive moment zones) should be calculated as per minimum requirements specified by ACI code.

Case studies reveals that mat thickness away from the column faces can be reduced by about 40%. But to be in the safe side here 34% reduction is suggested.

5.7   DESIGN EXAMPLE I

To evaluate the performance of mat with non-uniform thickness compared to mat with uniform thickness. This mat is a 81.50 ft square one with 3.25 ft overhanging portion. There are 16 columns arranged in a 4×4 grid, each 30 inches square in cross-section and spaced 25.00 ft apart. Due to the symmetry of the problem, only

half of the mat is analyzed. Material properties are kept fc' = 4 ksi and fy = 60 ksi, modulus of subgrade reaction 100 pcf. Plan of the mat is drawn in Fig. 5.18. Loads are calculated for a 15 story building and the analysis for column loads is made using a frame analysis software. Two loading cases are considered. These are :

DL = 150 pcf, LL = 60 psf, Floor finish = 30 psf., Partition wall = 30 psf.

LOADING I = 1.4 × Dead Load + 1.7 × Live Load

LOADING II = 0.75 × (1.4 × Dead Load + 1.7 × Live Load +

1.7 × Wind Load)

Column loads obtained from the analysis are listed in Table 5.10.

Table 5.10.   Column loads for LOADING I and II.

Column	LOADING I		LOADING II	
Column No	Axial Force (k)	Base Moment (k-ft)	Axial Force (k)	Base Moment (k-ft)
C1	742.05	-40.87	383.14	586.55
C2	1288.6	-2.33	964.77	642.01
C3	1288.6	2.33	968.13	644.11
C4	742.05	40.87	729.87	643.67
C5	1295.2	-78.21	624.64	1175.7
C6	2341.1	-4.46	1752.5	1284.2
C7	2341.1	4.46	1759.3	1288.1
C8	1295.2	78.21	1318.1	1284.7

Estimated Punching shear = 0.95 x 2341.1 = 2224 kips

$$d_{punch} = \frac{1}{2}(-c + \sqrt{c^2 + 4.65 \times V_p}) \text{ in},   V_p \text{ in k/ft and } c \text{ in inches},   V_p$$

= punching shear = 2224, c = Column dimension = 30

d_{punch} = 36 in.   Greater thickness t_g = 36 + 5.5 = 41.5 in. take = 3.5 '

So the geometry is selected shown in Fig. 5.18 by following guideline of Fig. 5.17.
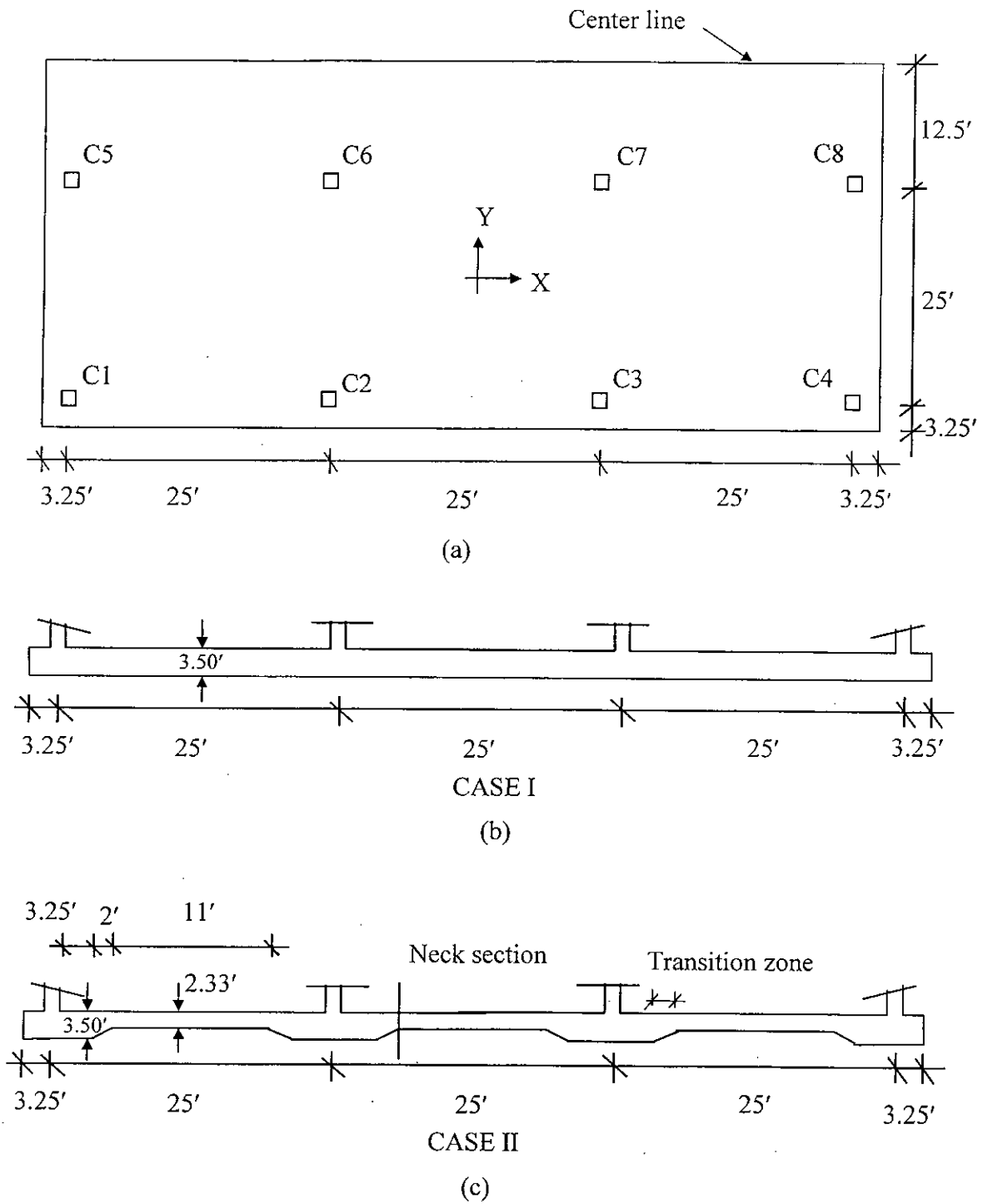
Fig. 5.18. (a) Plan of the mats of CASE I and II.

(b) Cross sections of the mat of CASE I (uniform thickness) and

(c) Cross sections of the mat of CASE II (non-uniform thickness)
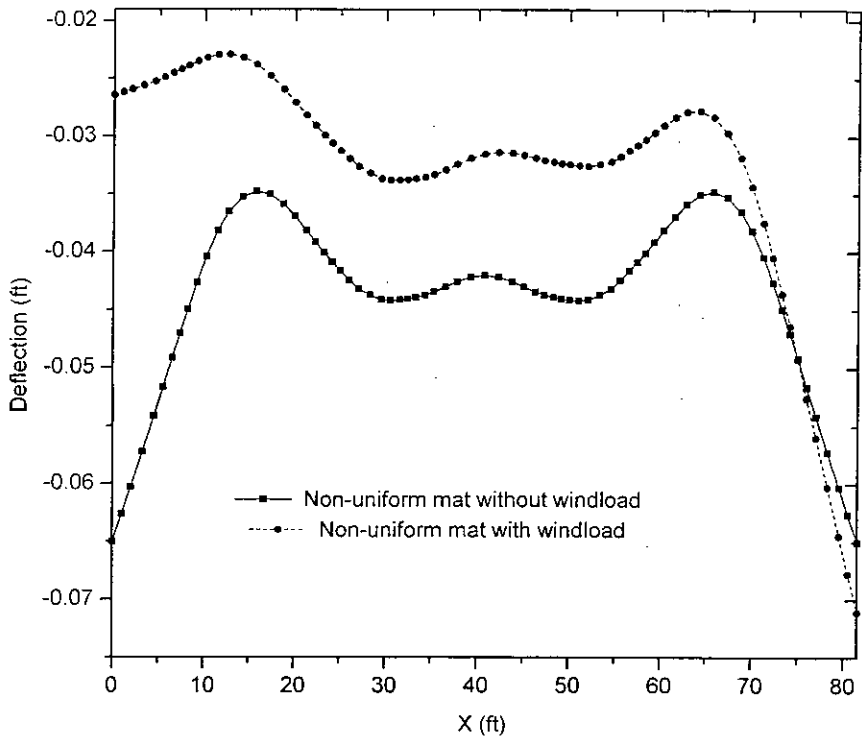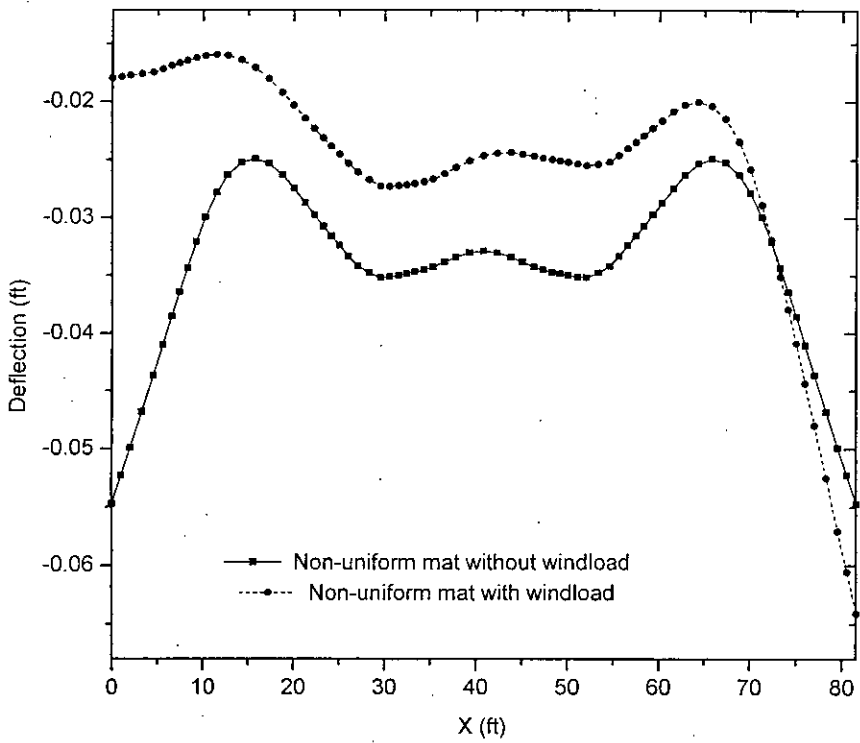
Fig. 5.19 : Deflection diagrams of X directional Column strip (a) C1-C4 and
(b) C5-C8 for CASE II under LOADING I and LOADING II
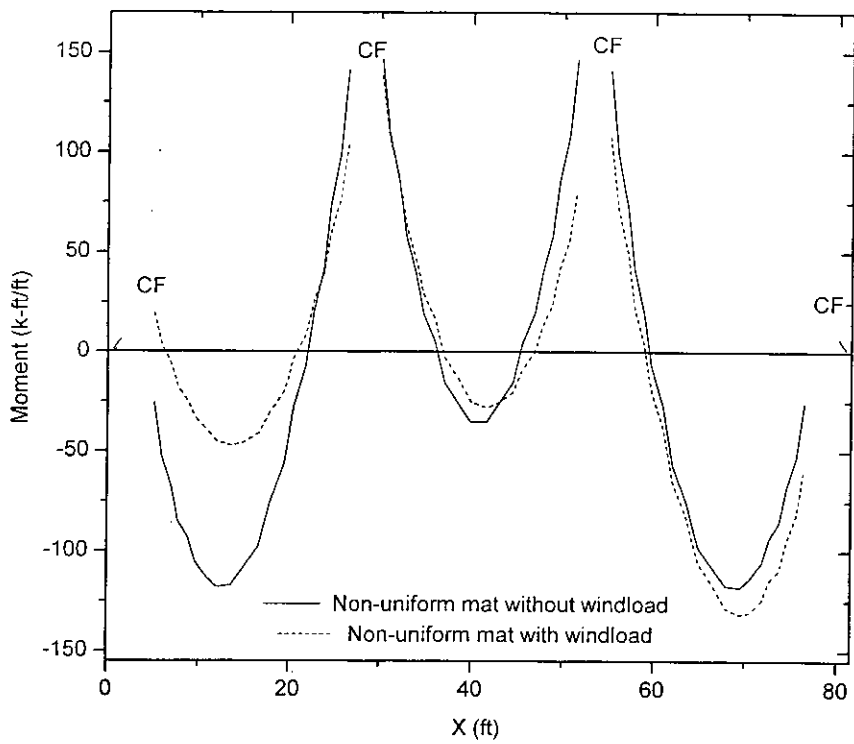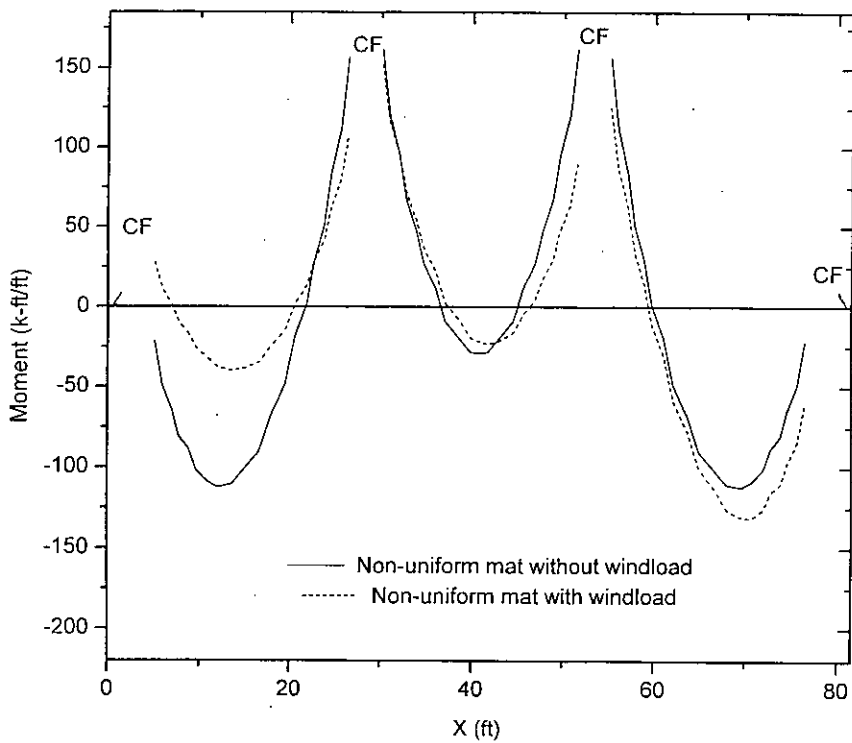
Fig. 5.20 : Bending moment diagrams of X directional Column strip (a) C1-C4 and (b) C5-C8 for CASE II under LOADING I and LOADING II
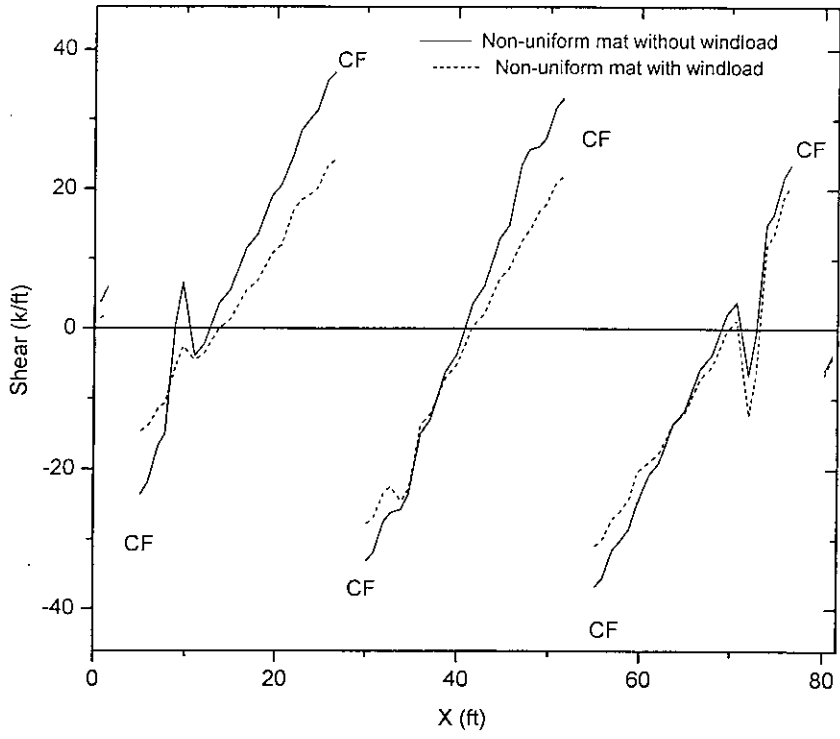
(a)
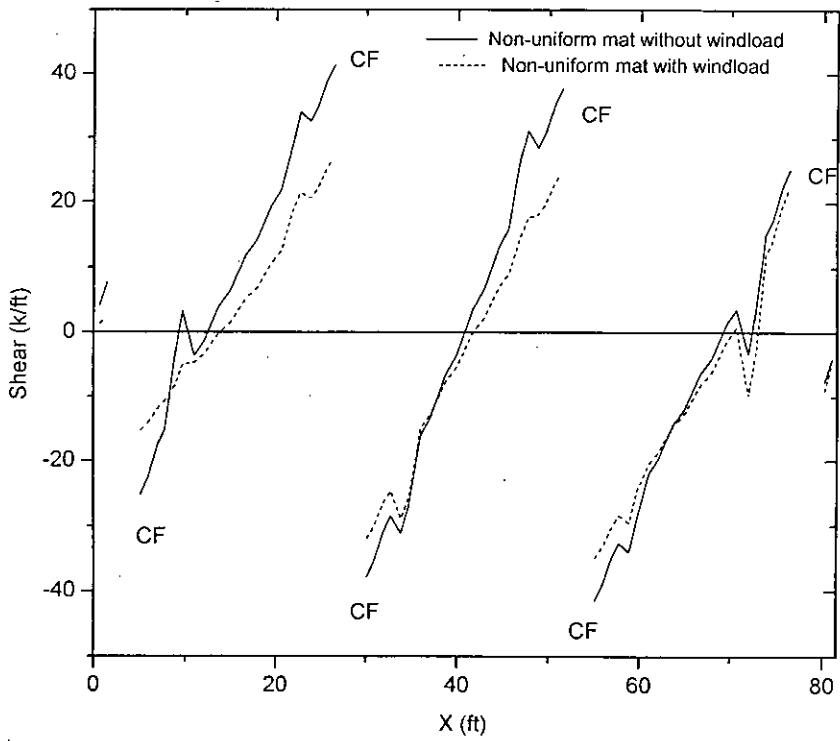
(b)

Fig. 5.21 : Shear force diagrams of X directional Column strip (a) C1-C4 and (b) C5-C8 for CASE II under LOADING I and LOADING II

LOADING I gives higher column axial forces and lower column base moments whereas LOADING II gives lower axial forces and much higher base moments. So analysis is performed using both the loading cases. Results of column strips C1-C4, C5-C8 in Fig 5.19. through Fig. 5.21. Design values of column deflections, punching shears, flexural shears, column face positive moments and negative moments are listed in Table 5.11 through Table 5.19. Design thicknesses, reinforcements and relative economic evaluation of CASE I and II are presented in Table 5.20 and Table 5.21.

Table 5.11. Column deflections of CASE I and II for LOADING I and II.

Column	CASE I		CASE II	
	LOADING I	LOADING II	LOADING I	LOADING II
C1	0.58 in	0.24 in	0.68 in	0.32 in
C2	0.46 in	0.34 in	0.52 in	0.41 in
C3	0.46 in	0.35 in	0.52 in	0.38 in
C4	0.53 in	0.55 in	0.68 in	0.72 in
C5	0.48 in	0.19 in	0.56 in	0.22 in
C6	0.42 in	0.30 in	0.42 in	0.32 in
C7	0.42 in	0.32 in	0.42 in	0.31 in
C8	0.48 in	0.52 in	0.56 in	0.62 in

Table 5.12.   Column punching shears of CASE I and II   for LOADING I and II.

Column	CASE I		CASE II	
	LOADING I (k)	LOADING II (k)	LOADING I (k)	LOADING II (k)
C1	620	325	581	308
C2	1170	878	1151	861
C3	1170	877	1151	866
C4	620	605	581	564
C5	1175	585	1156	589
C6	2210	1656	2212	1654
C7	2210	1658	2212	1664
C8	1175	1191	1156	1167

Table 5.13. Column face positive moments of CASE I and II for LOADING I and II.

Column	CASE I (k-ft/ft)				CASE II (k-ft/ft)			
	LOADING I		LOADING II		LOADING I		LOADING II	
	M_X	M_Y	M_X	M_Y	M_X	M_Y	M_X	M_Y
1	4.6	4.6	16.6	5.1	6.3	6.5	17.5	7.0
2	100.1	101.3	126.2	102.4	145.6	147.6	137.4	149.8
3	100.1	101.3	42.3	102.4	145.6	147.6	107.9	149.8
4	4.6	4.6	4.7	5.1	6.4	6.5	7.1	7.0
5	6.7	6.6	25.3	5.6	8.4	8.4	26.2	6.7
6	125.1	125.8	149.4	99.2	160.1	162.0	152.4	122.0
7	125.1	125.8	64.9	99.2	160.1	162.0	124.6	122.0
8	6.7	6.6	7.8	5.6	8.4	8.4	10.2	6.7

Table 5.14. Design positive moments for CASE I and II .

CASE	C1 (k-ft/ft)	C2 (k-ft/ft)	C5 (k-ft/ft)	C6 (k-ft/ft)
I	16.6	126.2	25.3	149.4
II	19.5	149.8	26.2	162.0

Table 5.15. In-between-column maximum negative moments of CASE I and II for LOADING I and II.

Location (In bet^n columns)	CASE I (k-ft/ft)				CASE II (k-ft/ft)			
	LOADING I		LOADING II		LOADING I		LOADING II	
	M_X	M_Y	M_X	M_Y	M_X	M_Y	M_X	M_Y
C1-C2	166.6	164.9	59.6	158.7	116.9	116.7	47.1	111.7
C2-C3	80.1	80.3	65.4	84.3	34.3	35.7	27.9	38.5
C3-C4	166.6	164.9	190.1	158.7	117.9	116.7	131.4	111.7
C5-C6	161.4	158.9	52.6	127.3	112.2	110.4	39.7	86.7
C6-C7	72.4	72.1	59.8	60.7	28.6	28.7	23.1	23.4
C7-C8	161.4	158.1	189.3	127.3	112.2	110.4	131.1	86.7

Table 5.16.   Design negative moments for CASE I and II .

CASE	C1-C2	C2-C3	C5-C6	C6-C7
I	190.1 k-ft/ft	84.3 k-ft/ft	189.3 k-ft/ft	72.4 k-ft/ft
II	116.9 k-ft/ft	38.5 k-ft/ft	131.1 k-ft/ft	28.7 k-ft/ft

Table 5.17.   Column strip flexural shears of CASE I and II for LOADING I and II

Column	CASE I (k/ft)				CASE II (k/ft)			
	LOADING I		LOADING II		LOADING I		LOADING II	
	V_X	V_Y	V_X	V_Y	V_X	V_Y	V_X	V_Y
1	19.9	20.0	11.9	19.8	15.0	15.2	10.5	15.0
2	31.0	31.1	23.4	31.2	30.3	30.4	22.4	30.5
3	31.0	31.1	27.4	31.2	30.3	30.4	26.1	30.5
4	19.9	20.0	18.0	19.8	15.0	15.2	12.0	15.0
5	20.5	20.5	11.9	15.8	15.1	15.2	10.6	11.5
6	34.3	34.0	26.0	25.7	32.6	25.7	24.6	24.5
7	34.3	34.0	30.2	25.7	32.6	25.7	28.4	24.5
8	20.5	20.5	18.8	15.8	15.1	15.2	12.0	11.5

Table 5.18.   Design flexural shears of CASE I and II .

CASE	C1 (k)	C2 (k)	C5 (k)	C6 (k)
I	20.0	31.2	20.5	34.3
II	15.2	30.5	15.2	32.6

Table 5.19. Neck flexural shears for CASE I and II .

Column	CASE I (k/ft)				CASE II (k/ft)			
	LOADING I		LOADING II		LOADING I		LOADING II	
	V_X	V_Y	V_X	V_Y	V_X	V_Y	V_X	V_Y
2	20.2	20.2	15.2	20.2	20.3	20.3	13.7	20.6
3	20.2	20.2	18.6	20.2	20.3	20.3	18.9	20.6
6	22.3	20.2	16.9	16.7	21.4	21.5	14.9	16.4
7	22.3	20.2	20.6	16.7	213	21.5	20.3	16.4
Design	22.3 k/ft				21.5 k/ft			

Table 5.20. Design requirements for CASE I and II .

CASE	$t_{punching}$ (in)	$t_{flexural}$ (in)	t_{neck} (in)	A_s^{+ve} col. face (in²/ft)	A_s^{-ve} C1-C2 (in²/ft)	A_s^{-ve} C2-C3 (in²/ft)	A_s^{-ve} C5-C6 (in²/ft)	A_s^{-ve} C6-C7 (in²/ft)
I	41.9	30.6		1.52	1.52	1.52	1.52	1.52
II	41.9	29.2	20.8	1.52	1.38	0.80	1.54	0.80

Table 5.21. Relative economic evaluation of CASE I and II .

CASE	t_{avg} (in)	+ve A_s^{avg} (in²/ft)	-ve A_s^{avg} (in²/ft)	Concrete Saving w.r.t. CASE I	Steel Saving w.r.t. CASE I
I	42	1.52	1.52	Not applicable	
II	29	1.23	1.24	30%	19%

Now column strip flexural shear and neck shear is checked to see whether the thickness there is adequate or not. It is found quite adequate.

Once again, economy of mat with non-uniform thickness is significant (Table 5.21). It is of interest to note that despite application of heavy loads, differential deflections are well below the allowable limits, even when wind load is considered (Table 5.11).

One other important thing to be noted is the column punching shear. Presence of column base moments does not affect column punching shears much. Mainly axial column loads determine punching shears. In this regard, a list of punching shears w.r.t. respective column axial loads is presented in Table 5.22 for both LOADING I and II. Table 5.22 shows that the percent column axial load encountered as punching shear remarkably matches for both LOADING I and LOADING II. Also it reveals that guideline of estimated punching shear of 95% is very good.

Table 5.22.   Punching shears as a percentage of respective column axial loads for CASE I and CASE II .

	CASE I		CASE II	
Columns	LOADING I	LOADING II	LOADING I	LOADING II
C1	83.5%	84.9%	78.3%	80.4%
C2	90.8%	90.9%	89.3%	89.2%
C3	90.8%	90.6%	89.3%	89.4%
C4	83.5%	82.9%	78.3%	77.2%
C5	90.7%	93.6%	89.3%	94.3%
C6	94.4%	94.5%	94.4%	94.4%
C7	94.4%	94.3%	94.4%	94.6%
C8	90.7%	90.4%	89.3%	88.6%

LOADING I governs all shear criteria while moment criteria are mainly governed by LOADING II. Once again, whether thickness is lowered away from the columns or not, positive moments are found to be low enough to be covered by minimum

89

reinforcement. Near the column faces, 1.52 in^2/ft steel (minimum requirement for 3.50 ft thickness) is provided across the entire column strip widths. This gives total moment capacities of 3173.00 k-ft and 4706.00 k-ft for strips C1-C4 and C5-C8 respectively, against acting maximum moments of 2360.00 k-ft and 4053.00 k-ft respectively. Flexural shear capacity of strip C1-C2 and C5-C6 at a distance d, for 3.50 ft thickness, away from the faces of column C2 and C6 respectively are 621.20 k and 923.80 k respectively, against a maximum acting total shear of 480.40 k and 815.00 k respectively, which are considerably higher than requirements. In the transition zones, average mat thickness of column strip 1 and 2 are 30.90 inches and 29.70 inches respectively, giving flexural shear capacities equal to 35.30 k/ft and 33.80 k/ft respectively thereby. The respective maximum acting kink shears are 28.40 k/ft and 33.90 k/ft respectively and it is clear that no further reduction of slope width can be performed.

Reduction of the thickness of mat away from the columns produces shear magnification in the transition zones in the central region of mat as before. For MAT II kink shear magnification has been found to be dependent on slope of the transition zone. So a study is made by varying the slope width of CASE II from 1.00 ft to 3.00 ft. A plot of kink shear magnification versus slope angle is presented in Fig. 5.22.

However in the transition zones, average thickness, and hence average shear capacity, of mat will be higher than the acting shears if slope angle is not too high there. As a matter of fact, slope angle much higher than 20° will be acceptable because of this excess shear capacity in the transition zones, which will take care of the resulting shear magnification. In the previous examples, namely MAT II of Fig. 5.1 and CASE II of Fig. 5.18, slope angle equal to 26.6° and 30.32° respectively has been used without any possibility of shear failure in the transition zones.

90
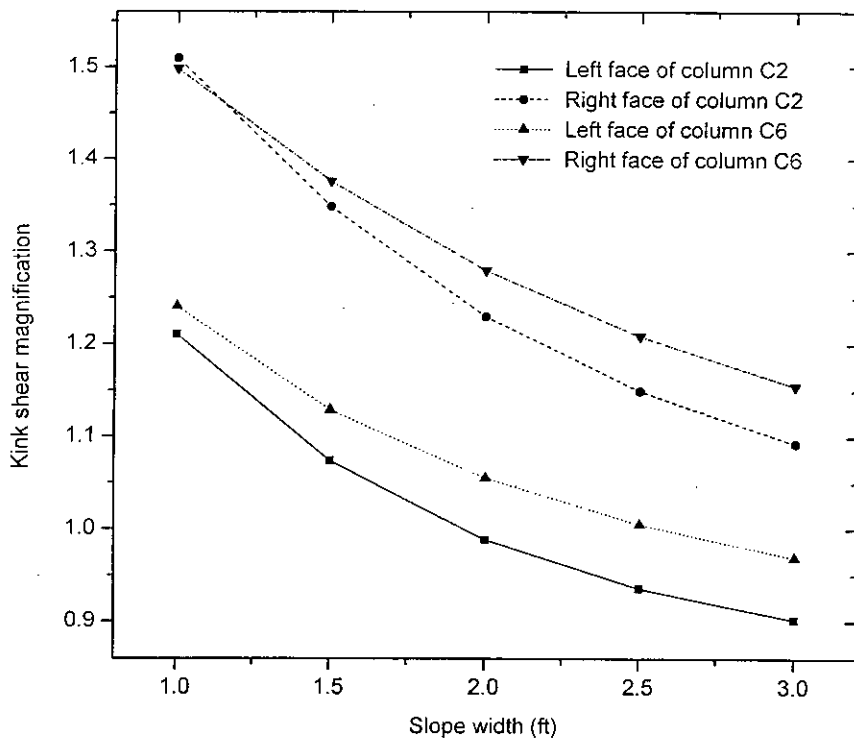
(a)
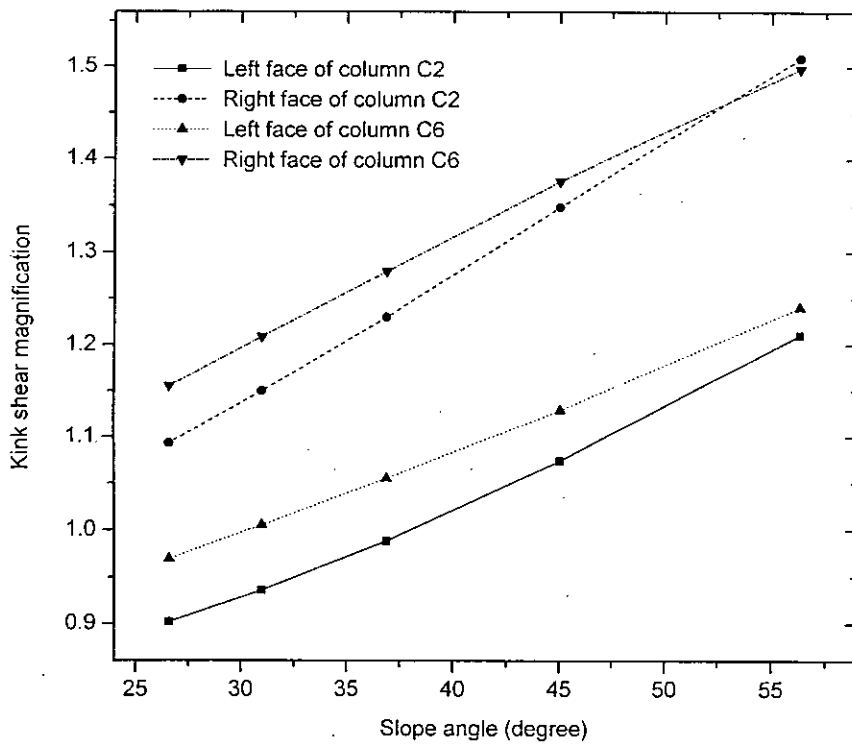
(b)

Fig. 5.22 : Effect of slope width on kink shear as a function of (a) slope width
and (b) slope angle (CASE II and LOADING I)

5.8 DESIGN EXAMPLE II

A second design example is done using the guide line. A 10 storied building with 5 bay each of 18 ft. and story height of 10 ft. (Fig. 5.23) is selected for the study. A 100 ft. square mat is selected with 5.00 ft overhanging portion. There are 36 columns arranged in a 6×6 grid, each 2.5 ft. square in cross-section and spaced 18.00 ft apart.

Due to the symmetry of the problem, only quarter of the mat is analyzed. Material properties are fc' = 4 ksi and f_y = 60 ksi, modulus of subgrade reaction 100 pcf. Plan of the mat is drawn in Fig. 5.23. Loads are calculated for a 10 story building The loads considered are :

DL = 150 pcf, LL = 80 psf, Floor finish = 30 psf., Partition wall = 30 psf.
LOADING = 1.4 × Dead Load + 1.7 × Live Load

The frame is analysed for the loads considered. The column loads obtained from the analysis are listed in Table 5.23.

Table 5.23.   Column loads for the loading

Column No.	Axial Load (kips)	Base Moment (kip-ft)
C1	335.8	-23.51
C2	585.16	-3.26
C3	592.16	-0.88
C4	671.59	-47.02
C5	1170.33	-6.51
C6	1184.33	-1.75
C7	671.59	-47.02
C8	1170.33	-6.51
C9	1184.33	-1.75

Estimated Punching shear = 0.95 x 1184.33 = 1125 kips
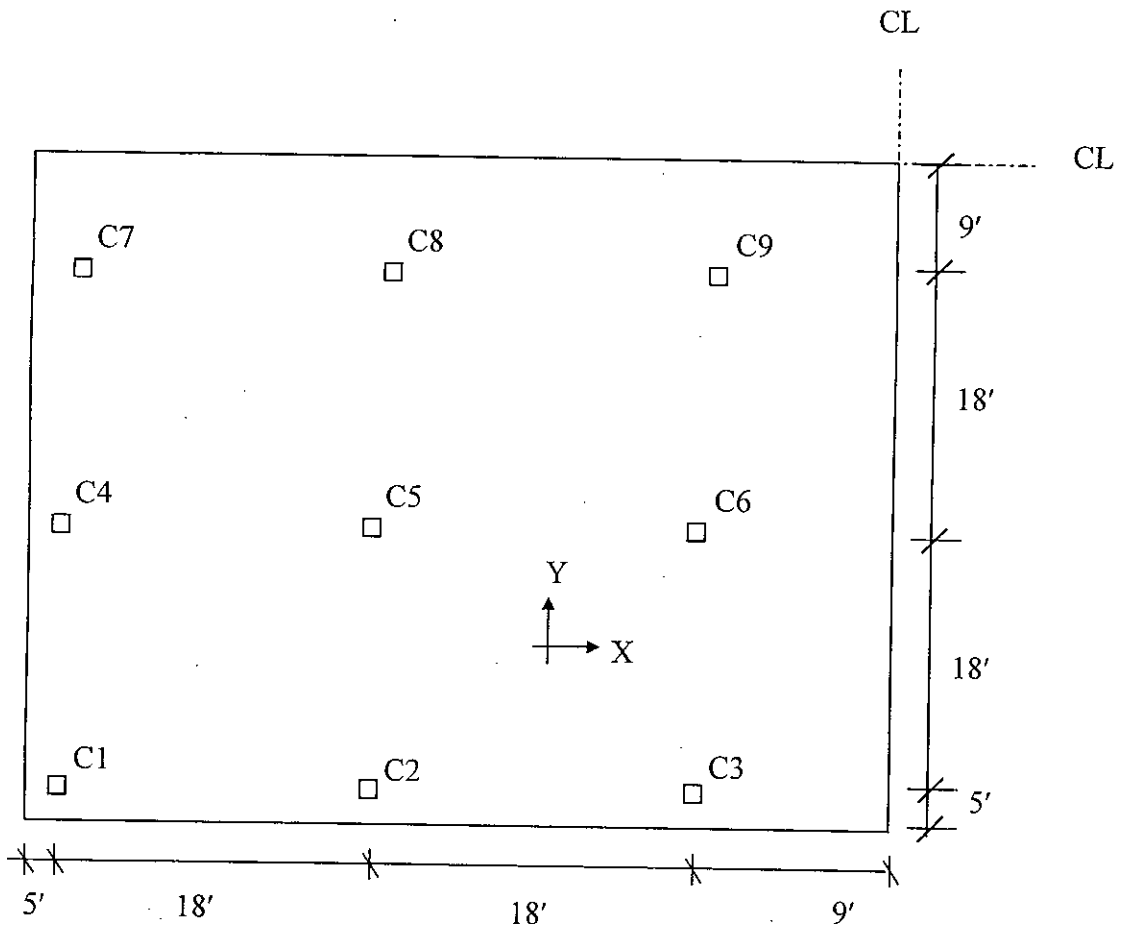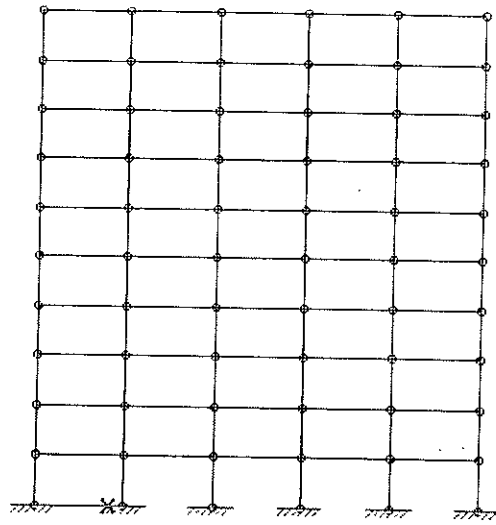
Fig. 5.23 (a) Frame of the 10 storied building   (b) Plan of the mat.

If uniform mat is designed then

$$d_{punch} = \frac{1}{2}(-c + \sqrt{c^2 + 4.65 \times V_p}) \text{ in}, \quad V_p \text{ in k/ft and c in inches},$$

V_p = punching shear = 1125 k , c = Column dimension = 30″

∴ d_{punch} = 24.2 in.

Thickness t_g = 24.2 + 3.5 = 27.7 ″ Take 28″

So the geometry is selected shown in Fig. 5.24 by following guideline of Fig. 5.17.

For mat with non-uniform thickness

∴ t_g = *Greater thickness* = 28 ″

t_s = *Smaller thickness,* = 66% of t_g = 18.5 ″

d_g = *Width of greater thickness,* = 24.5 ″ ≈ 2′

d_s = *Slope width,* = $t_g/\sqrt{3}$ = 16.2 ″ ≈ 1.35 ′

CASE I

(a)

CASE II

(b)
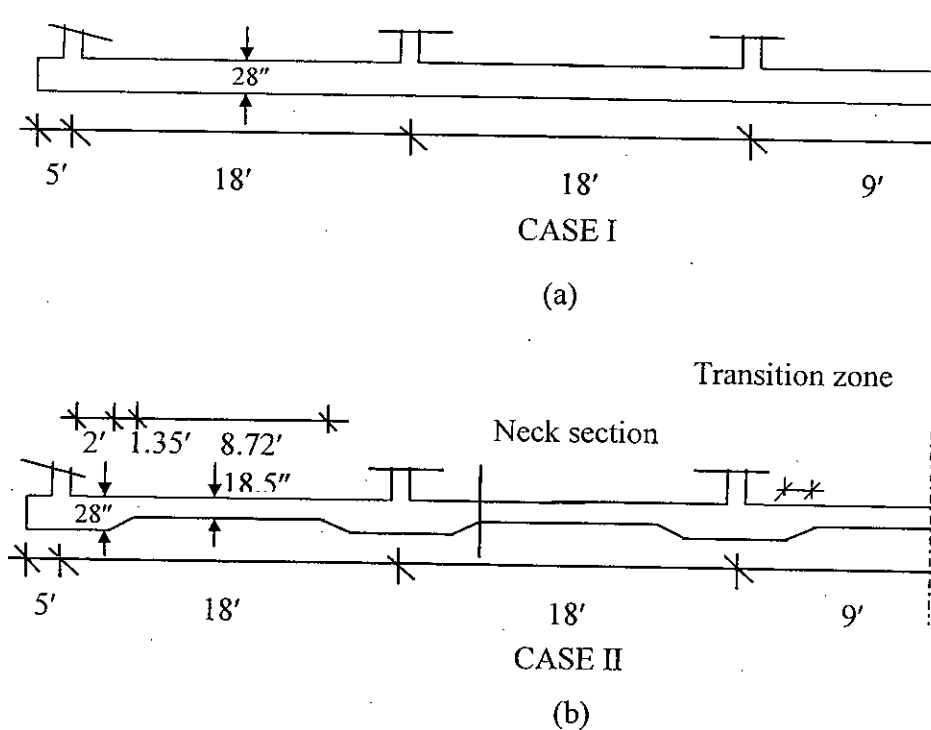
Fig. 5.24. (a) Cross sections of the mat of CASE I (uniform thickness) and
(b) Cross sections of the mat of CASE II (non-uniform thickness)

Now selecting this geometry, the mat is analysed.

Punching Shear

Punching shear in columns from the are as tabulated in Table 5.24

Table 5.24 Punching shear around columns

Column	Axial Load	Punching shear Case I	% of column load	Punching shear Case I	% of column load
C1	335.8	279.88	83	275.96	82
C2	585	513.81	88	512.66	88
C3	592	515.02	87	513.34	87
C4	671	590.24	88	588.08	88
C5	1170	1066.11	91	1066.3	91
C6	1184	1072.65	91	1072.4	91
C7	671	583.87	87	581.71	87
C8	1170	1058.26	90	1059	91
C9	1184	1064.05	90	1064.35	90

Maximum punching shear is 1072 kip. Already thickness has been calculated using 1125 kip. So thickness is adequate.

Flexural shear

Flexural shear in columns from the are as tabulated in Table 5.25

Table 5.25 Flexural shear in columns.

Column No.	Flexural shear (k/ft) Case I	Flexural shear (k/ft)Case II
C1	10.87	4.5
C2	18.5	15.8
C3	18.3	15.02
C4	12.5	11.32

C5	22	23
C6	21.14	22.75
C7	13.1	11.42
C8	22.2	23.9
C9	21.41	23.04

Maximum Flexural shear is at C8 = 23.9 k/ft

$\therefore$ Effective Depth required = 0.775 x 23.9 = 18.52 ''   (See Art. 4.3)

Thickness = 18.52 + 3.5 = 22.2 '' < 28 '' $\therefore$ Adequate.

Neck Flexural shear

Neck Flexural shear for Case II are tabulated in Table 5.26

Table 5.26   Neck Flexural shear for Case II (Mat with non-uniform thickness)

Column No.	Neck Flexural Shear (kip/ft)
C1	6.8
C2	12.5
C3	11.78
C4	10.03
C5	18.5
C6	17.39
C7	10.3
C8	18.97
C9	17.71

Maximum Neck Flexural shear is at C8 = 18.97 kip/ft.

$\therefore$ Effective Depth required = 0.775 x 18.97 = 14.7 ''   (See Art. 4.3)

Thickness = 14.7 + 3.5 = 18.2 '' < 18.5 '' $\therefore$ Adequate.

Design for Column face positive moment

As per guideline reinforcement for positive moment in the column region will be governed by minimum reinforcement

A_s (+ve) $= 0.48 \times d = 0.48 \times 24.5'' = 0.98 \ in^2 / ft$

To verify it Column face positive moment are checked. The results are tabulated in Table 5.27.

Table 5.27   Column face positive moment (k-ft/ft)

Column no.	Case I (Uniform thickness)	Case II (Non-uniform thickness)
C1	10.10	11.23
C2	41.20	48.09
C3	37.56	43.79
C4	18.18	19.47
C5	63.64	69.04
C6	59.63	63.79
C7	17.27	18.91
C8	64.02	70.22
C9	59.68	64.61

Maximum positive moment for case II $= 70.22$ k-ft/ft

Steel ratio $\rho = \dfrac{1}{17.7}(1 - \sqrt{1 - \dfrac{0.6556 \times 70.22}{24.5^2}}) = 0.0022 < \rho_{min} \ (= 0.0033)$

$\therefore$ Minimum reinforcement governs.

Design for Negative moment in region in between columns

Reinforcement for negative moment in between column region will have to be calculated. The results are tabulate in Table 5.28

Table 5.28.   In-between-column maximum negative moments of CASE I and II

Location(In between columns)	CASE I (kip-ft/ft)	CASE II (kip-ft/ft)
C1-C2	36.47	26.05
C2-C3	25.25	16.09
C4-C5	43.6	31.75
C5-C6	29.37	20.66
C7-C8	47.25	34.63
C8-C9	31.41	22.52

Maximum Negative Moment $=$ 34.63 kip-ft/ft

Steel ratio $\rho = \frac{1}{17.7}(1 - \sqrt{1 - \frac{0.6556 \times 34.63}{15^2}}) = 0.0029 < \rho_{min}(= 0.0033)$

$\therefore A_s(-ve) = 0.60$ in^2/ft

Design thicknesses, reinforcements and relative economic evaluation of CASE I and II are presented in Table 5.29 and Table 5.30.

Table 5.29.   Design requirements for CASE I and II .

CASE	$t_{punching}$ (in)	$t_{flexural}$ (in)	t_{neck} (in)	A_s^{+ve} col. face (in^2/ft)	A_s^{-ve} In between columns (in^2/ft)
I	26.85	20.7		0.98	0.98
II	26.85	22	18.2	0.98	0.60

Table 5.30.   Relative economic evaluation of CASE I and II .

CASE	t_{avg} (in)	+ve A_s^{avg} (in^2/ft)	-ve A_s^{avg} (in^2/ft)	Concrete Saving w.r.t. CASE I	Steel Saving w.r.t. CASE I
I	28	0.98	0.98	Not applicable	
II	20	0.66	0.60	29 %	38%

It may be mentioned that thickness was calculated from 1125 k instead of 1072 k. For 1072 kip the calculated thickness is 27″, means that economy would be more if greater thickness was 27″ was selected.

From the results it is seen that the column strip C7-C9 is the controlling strip. So variation of deflection, shear force and bending moment are plotted in Fig. 5.25 to 5.27.

The example problems demonstrates the effectiveness of the proposed guideline.
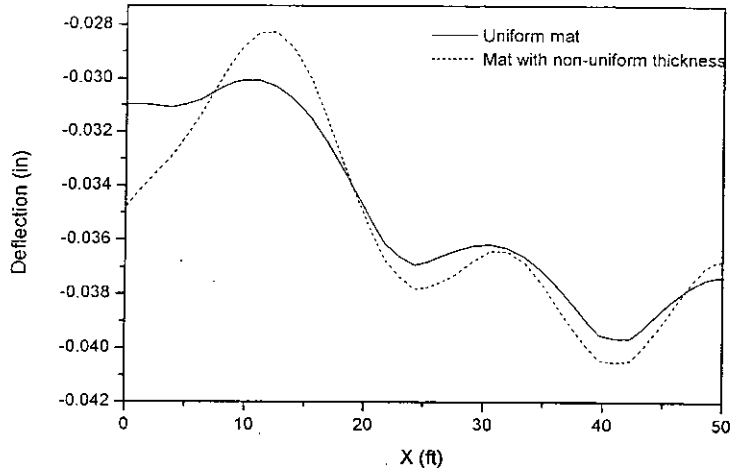
Fig 5.25 Deflection diagram of X directional column strip C7-C9
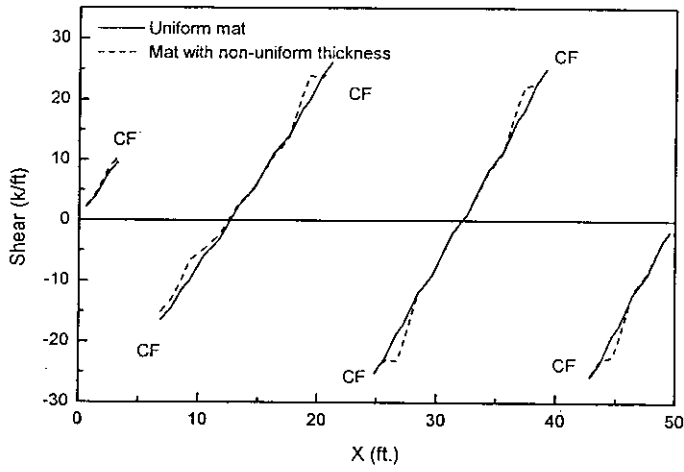
Fig. 5.26 Shear Force diagram of X directional column strip C7-C9
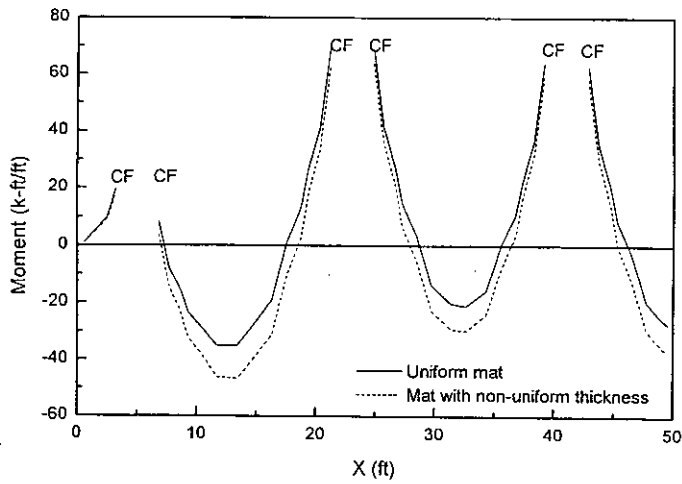
Fig. 5.27 Bending Moment Diagram of X directional strip C7-C9

CHAPTER 6

DEVELOPMENT OF SOFTWARE **MATFEA**

6.1   GENERAL

For general use for the civil engineering community a windows based user friendly computer software has been developed. This software can analyse uniform and non-uniform mat foundation, The data input procedure is very simple and clear. After execution of the program, graphs for deflection, shear force and bending moment are generated automatically.

6.2   FEATURES OF THE CORE COMPUTER PROGRAM

The core program was in FORTRAN77 written by Ahmad [1969]. It can analyze any plate or shell type structure using 8 noded or 12 noded Ahmad's thick shell element. The shell elements may be curved or plane on both or any one of its faces and may be of uniform or variable thickness. Later Morshed [1997] modified the program to analyse mat foundation.

6.3   MODIFICATION OF THE CORE PROGRAM

The core program, with the desired modifications and development of supporting programs for data generation and result interpretation, has been turned into a versatile mat analysis software. Attributes of the software are as follows.

(i)   The program takes mat dimensions, material properties, element mesh features, information about loads, items of output and location and type of result interpretation etc. as its input.

(ii)   It gives nodal displacements, stresses, moments and shears as output. Displacements will always be at nodes but moments and shears may be at the nodal points or at the Gauss points upon request.

(iii)   The program can analyze a full mat or, in case of symmetric problems, half or quarter of a mat.

(iv)   Column axial loads and column base moments can be applied as concentrated or distributed loads.

(v)   In case of distributed column axial loads and column base moments, an element is taken under the concerned column and that element can be made more rigid than the other portion of the mat.

(vi)   Elements near the loads can be taken of smaller dimensions than the other elements away from the columns.

(vii)   Thickness of mat under the columns may be higher than that elsewhere.

(viii)   Strips of thickness greater than the thickness of mat elsewhere can be incorporated along the column lines.

(ix)   Punching shear for each column can be calculated.

(x)   As for boundary condition, the program can attach horizontal soil springs along the edges, can fix the edges horizontally or can fix only the corner nodes horizontally.

(xi)   Self weight of mat may be neglected or considered.

(xii)   Detailed or specified output items may be obtained upon request.

(xiii)   Modulus of subgrade reaction may be uniform or zoned.

(xiv)   Element dimensions may be generated by the program itself or may be given by the user.

(xv)   Due to the limitation of the operating system, only sixty output files can be opened by a program. So the program has the option of being specifically instructed about the locations for which graph data are required. The graph files for displacements, moments and shears are automatically generated for those locations.

(xvi)   Bending moments and shear forces along the column lines may be given for a strip of width equal to unity, the widths of the column strips or any specified width after averaging over the width requested.

(xvii) Besides these, the software has many other features for fine-tuning.

A limitation of the software is that it can handle only mats with rectangular plan area.

6.4   FORMS OF THE SOFTWARE

The present sofware is named MATFEA. It is a windows based software. It takes datas through some forms. Few radiobuttons has to be checked by mouse in order to specify the type of modeling and various data.   The forms in order are presented below.

MATFEA

VER 1.O

Finite Element Structural Analysis Software
for Uniform and Non-uniform Mat foundation

Developed by   :   Dr. Sohrabuddin Ahmad ,   Dr. Abdul Muqtadir
                       A.S.M. Monzurul Morshed ,   Abk Sutradhar

Special Thanks to :   Md. Badre Ehan

Warning : This software is protected by copyright law and international treaties. Unauthorized reproduction and distribution is strictly prohibited.
Copyright © 1999

MATFEA

VER 1.0

Matfea is a finite element analysis based software for design and analysis of mat foundations. This softare can analyse both uniform and non-uniform thickness mat foundations. A design rationale based on research works at BUET is presented. Using this 30% savings in cost can be done in terms of concrete volume and reinforcement.

- ○ Input new data
- ○ Edit existing data
- ○ Execute Program
- ○ View Results
- ○ Plot and View Graphs
- ○ Design Rationale

Next

MATFEA 2

Analyse part of the mat? (In case of bisymetric mat)   ● Yes   ○ No

Half portion analysis?   ● Yes   ○ No

Half of the mat will be analysed considering one way symmetry.

X dimension (feet): `31`   Y dimension (feet): `25.25`   Mat depth (feet): `1.5`

Finite Element Mesh :

X directional divisions : (Should not be greater than 45)   `11`

Y directional divisions : (Should not be greater than 112)   `8`

Cut boundary at   ● Top   ○ Bottom   ○ Left   ○ Right
(Specify which boundary is the centre line of the mat)

Next   **Cancel**

Matfea3

Modulus of Elasticity directly ?　　○ Yes　　● No

Value of E of mat material will be calculated using ultimate concrete strength.

Ultimate Concrete Strength (Ksi) :　　`4`

Poisson's ratio :　　`0.18`

Unit Weight (KCF)　:　　`145`

[**Back**]　　[**Next**]　　[**Cancel**]

Matfea4

Modulus of Subgrade Reaction (KCF) :　　`100`

Element springs to be lumped at nodes　:

　　○ Distribution by 12th part　　● Distribution by 16th part

Deflection, Moment and Shear Calculations will be based on　:

　　● Gauss Point Stresses　　○ Nodal Point Stresses

Sign Conventions :　　Column Load ::: Downward　= +ve
　　　　　　　　　　MX = Moment about x-axis ::: Counter clock wise　= +ve
　　　　　　　　　　MY = Moment about y-axis ::: Counter clock wise　= +ve

No. of Column Loads in the portion of mat to be analysed :　　`4`

Column No.	Left Division	Bottom Division	Vertical Load	X-X Moment	Y-Y Moment
1.	0	0	0	0	0
2	0	0	0	0	0

[**Back**]　　[**Next**]　　[**Cancel**]

Columns idealized by element ?   ⦿ Yes   ○ No

Column load will be distributed through element.

Calculate punching shear ?   ⦿ Yes   ○ No

Elements under columns more rigid ?   ⦿ Yes   ○ No

Column element thickness directly ?   ○ Yes   ⦿ No

Ratio of Column element stiffness to mat stiffness : |8

This effect is realized by increasing the value of the modulus of elasticity of the portions
of mat under the columns.

| Back | Next | Cancel |

Nonuniform thickness mat :   ⦿ Yes   ○ No

Element mid surface plane :   ⦿ Yes   ○ No

Thickness under all columns will be same ?   ○ Yes   ⦿ No

Column No.	Thickness under column (in ft.)
1	0
2	0
3	0
4	0

| Back | Next | Cancel |

Matfea 7   _ □ X

Same range of differential thickness under all column ?   ◯ Yes   ◉ No

Range of division of differential thickness away from columns :

Column No.	Left Div.	Right Div.	Bottom Div.	Top Div.
1	0	0	0	0
2	0	0	0	0
3	0	0	0	0
4	0	0	0	0

Back   Next   Cancel

Matfea 8   _ □ X

Strips of greater thickness :   ◉ Yes   ◯ No

Element mid surface plane :   ◉ Yes   ◯ No

Thickness of strips (in ft.) :   3

No. of Horizontal Strips :   2

No. of Vertical Strips :   2

Horizontal Strip	Div. No.	Vertical Strip	Div. No.
1	0	1	0
2	0	2	0

Back   Next   Cancel

Matfea 9

Horizontal Springs at Egde Nodes in each elements :   ⦿ Yes   ◯ No

Horizontal Modulus of Subgrade Reaction (in kcf.) :   `50`

Effective Depth spans over how many divisions around column ?   `1`

No. of Strip averaging width divisions on any side of column :   `0`

File for average strip moments and shears :   ⦿ Yes   ◯ No

No. of Horizontal Strips :   `2`   No. of Vertical Strips :   `2`

| Back | Next | Cancel |

Matfea 10

Self Weight :   ◯ Yes   ⦿ No

Output all details in file Mat.out ?   ⦿ Yes   ◯ No

Soil Spring Zoning :   ◯ Yes   ⦿ No

Coordinates :   Y from X :   ◯ Yes   ⦿ No

Horizontal Division	X- coordinate.	Vertical Division	Y- coordinate
1	0	1	0
2	0	2	0
3	0	3	0

| Back | Next | Cancel |

Matfea 11

Generate data files to draw all moment, shear, deflection graphs : ⦿ Yes   ○ No

Due to storage limitation graph files for all X and Y lines cannot be generated. So select nodal lines for graph. In case of Gauss analysis, gauss-lines will be around these selected nodal lines.

Graph for how many X lines ?   {Should be < 8}   [3]

X line no.		

Graph for how many Y lines ? [Should be < (16 – X line No.s)]   [3]

Y line no.		

Back	Generate Data File	Next	Cancel

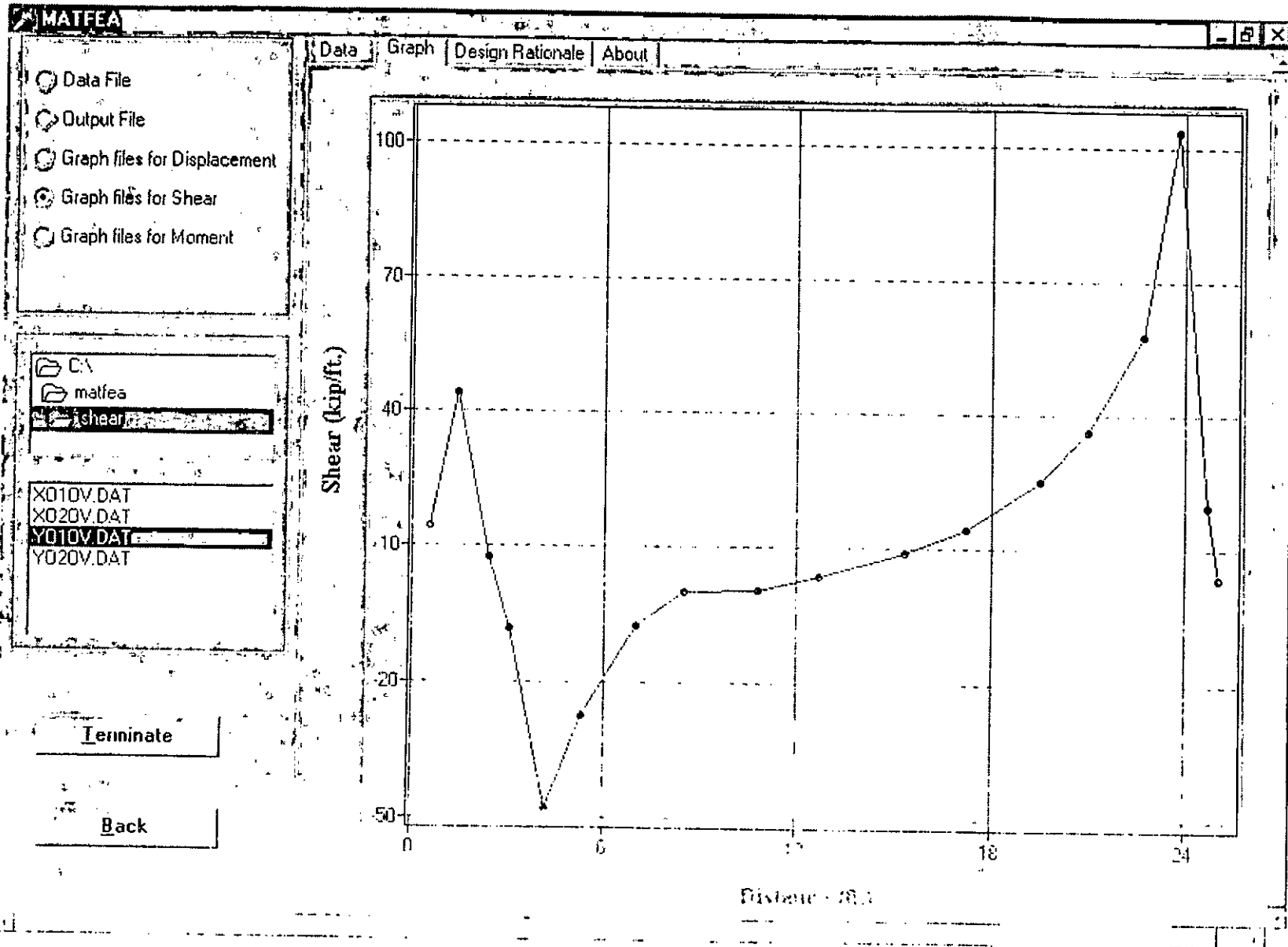## Form13

GENERATED DATA FILE

```
Y
Y
N
31
25.25
1.5
11
9
Y
Y
N
4
0.18
145
300
N
Y
4
1 1 483 0 -18
7 1 819 0 -2
1 8 388 0 -17
7 8 658 0 -2
Y
```
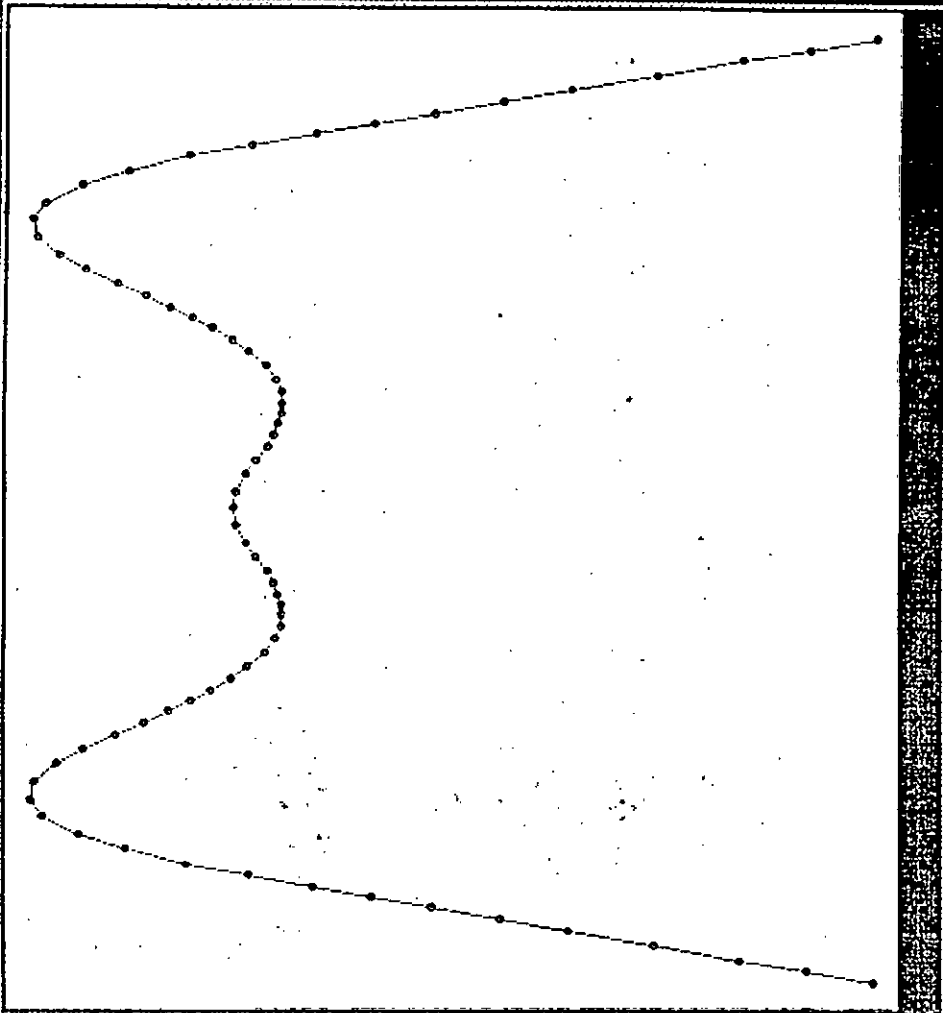
Edit	Save	Back	Execute Program	Next
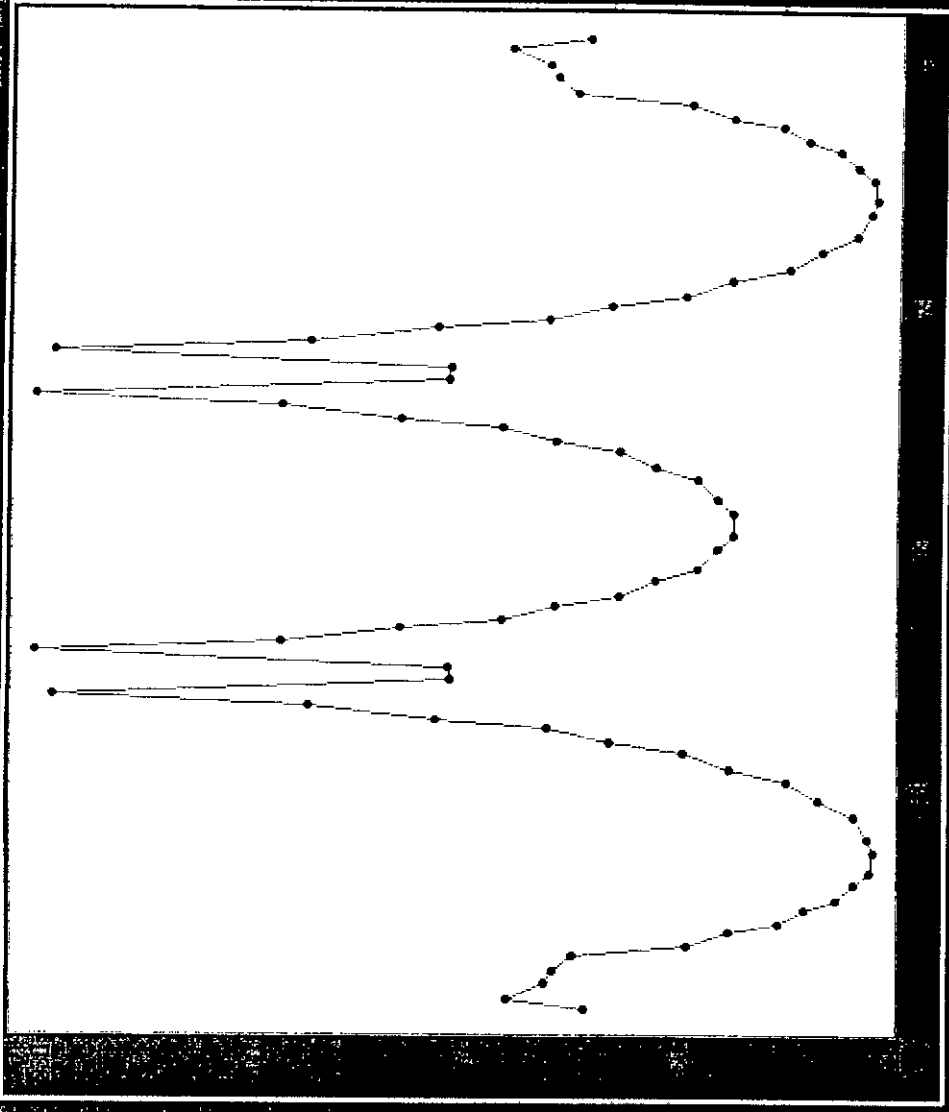
CHAPTER 7

CONCLUSIONS

7.1 GENERAL

A thorough study on mat foundation has been performed in this thesis. Comparison between Winkler foundation model and two parameter foundation model has been done. Critical review of the analysis methods has been performed. Parametric studies has been done on sensitive parameters of mat. To achieve economy, mat thickened under column, designated as non-uniform mat in this study, has been analysed and designed. The new parameters related to the non-uniform mat has been studied and their response on the mat has been investigated. Depending on this study and some example problems an economic design guideline for mat with non-uniform thickness has been established. For general use for the civil engineering community a windows based user friendly computer software has been developed.

7.2 COMPARISON BETWEEN WINKLER AND TWO PARAMETER MODEL

From the study it is evident that using two parameter model reduces deflection and also bending moment. A variation of 6-8 % is seen in deflection while 9-12 % in moment. So it proves that Winkler model with its simplicity can depict soil response as good as two parameter model. Thus Winkler model establishes itself as very good idealization for soil.

7.3 COMPARISON BETWEEN VARIOUS METHODS

Critical review has been done on the performances of Conventional method, ACI method and finite element method. Finite element method being the best one in terms of all aspects has exposed the short comings of other methods. From the present study the extent of the use of other methods has been depicted. In order to use a method the various limitations of it must be known. FE method has revealed it.

From the study it has been verified that conventional method is a crude method. It does not depict the actual behaviour of mat at all. It fails to predict any positive moment at the column face of the column. Deflection can not be calculated by this method. Apparently it may seem that since mat can take substantial differential settlement so deflection will not pose any problem. But if it requires any review after construction then it will pose an uncertainty. The same applies in case of flexural shear also. Conventional method gives very low flexural shear. For most cases punching shear governs the thickness determination but in some cases flexural shear governs the thickness determination. In such problems use of this method will be fatal.

ACI method involves extensive calculation but it causes overestimation of thickness due to overestimation of flexural shear as well as reinforcements due to overestimation of negative moments.

Economy of various methods are evaluated by parameter such as concrete volume and steel requirements. From the preceding study it reveals that in ACI method the thickness governed by flexural shear will be high w.r.t. FE method. Also in Conventional method the steel required by negative moment will be more w.r.t. FE method. So FE method will result in substantial economy than both ACI and Conventional Method. It is also implied that this economy will increase with high column loads. The summary of different methods are given in Table 4.12 which will be very useful for designers during design.

7.4 FINDINGS OF THE PARAMETRIC STUDY

The material parameters associated with mat foundation are modulus of subgrade reaction and concrete strength. The main geometric parameter of mat is its thickness. However, other geometric parameters include column spacing, column dimension and width of overhanging portion.

Mat deflection has been found to be the most sensitive item of all to its parameters. However, mat deflection has also been found to be the least significant item of all from design point of view.

Mat shear has been found to be insensitive to most of its parameters. The only noticeable variation of flexural shear is that near mat edges with respect to mat thickness. However, since critical flexural shears usually occur near central columns, this variation will seldom be of any practical significance.

Positive moments are less sensitive to mat parameters than negative moments and this sensitivity is confined in the central portion of mat. Since positive moments are small enough to be usually covered by minimum steel, its variation with mat parameters is expected to be of no practical significance. Modulus of subgrade reaction and mat thickness have the most significant effects on negative moments.

Closer column spacing produces more uniformity in load application resulting in lower deflections, moments and shears. Reduction of positive and negative moments is particularly significant. Bending moment and shear force diagrams for different column sizes remain more or less aligned with some reduction in the peak values with the increase of column sizes. Width of overhanging portion has significant effect on mat deflections and negative moments. With wider overhang, deflection pattern becomes concave and negative moments reduce sharply. An increase in central positive moments also occurs. The summary of parametric study is depicted in Table 4.16 which is expected to be very useful to designers during design.

7.5   DESIGN OF NON-UNIFORM MAT FOUNDATION

Mat foundation is a relatively heavy and costly structure. Economy in mat is an engineers dream for many years. This was not possible for lack of appropriate design method and guideline. Possibility of economy has been hinted by several authors in the form of changing the configuration of mat geometry. In fig 1.1 such configurations are shown. Since we have the most powerful tool FE in our hand so it is our privilege to discover economy in such configurations.

In this study successfully a well verified guideline for design of mat with non-uniform thickness has been presented. Such type of mat foundation offers a way of attaining substantial economy. Sensitivity analysis of all relevant parameters have been performed. It has been found that

- Greater thickness under the columns has to be designed from maximum punching shear .

- The smaller thickness has to be designed from flexural shear at the neck sections. Then this thickness should be reinforced for negative moments.

- With the reduction of thickness in the low shear and high negative moment regions, column face positive moments increases. But since greater thickness is provided in the positive moment and high shear regions, this amplification does not pose any threat. Column face positive moments, after being averaged across column strip widths, come out to be much lower than the moment capacities of mat at those sections. Reinforced throughout with the minimum steel is required for the greater thickness.

- Reduction of thickness is associated with the reduction of moment capacity. As negative moments decrease with the decrease of thickness, reduction of moment capacity of mat at the corresponding locations does not change to that extent.

- Width over which change of thickness should be made i.e. slope width is not very critical as long as the slope of the transition zones is kept as flat as practicable.

106

- Greater thickness is required for punching shear purpose and since in the calculation of the punching shear capacity, flexural shear cracks are assumed to propagate downward from the column face at an angle of 45°, a width equal to the effective depth corresponding to the greater thickness seems to be reasonable.

After critical review and in-depth verification the following guideline has been established.

$P_{DL+LL\,(max)}$ = Maximum column axial load due to live load and dead load

t_g = thickness required to encounter $0.95\ P_{DL \cdot LL\,(max)}$ as punching shear,
t_s = $2t_g\,/\,3$,
d_g = effective depth corresponding to t_g,
d_s = $t_g/\sqrt{3}$.
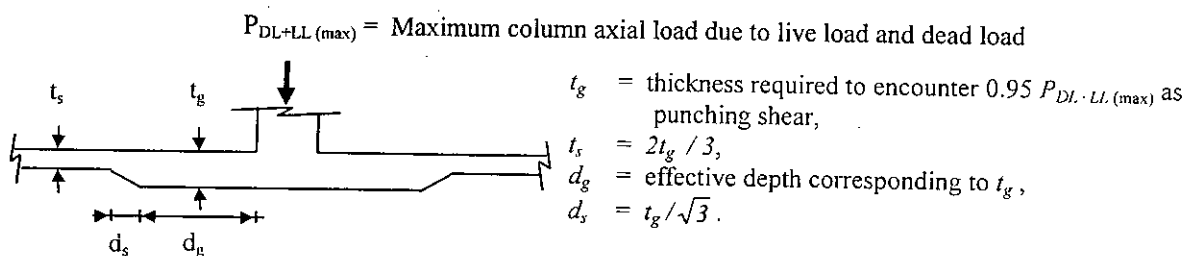
Fig. 7.1 Guideline for selecting cross-sectional geometry for the first trial solution of mat with non-uniform thickness.

(i)   The problem should be solved first with a non-uniform thickness geometry selected from the guideline shown in Fig. 7.1. Column punching shear should be estimated as 0.95 x column axial force.

t_g = *Greater thickness*, calculate from this punching shear

t_s = *Smaller thickness*, = 66 % of t_g

d_g = *Width of greater thickness*, = effective depth corresponding to t_g

d_s = *Slope width*, = $t_g/\sqrt{3}$

Slope angle $\cong$ 30°

(ii)   A mat analysis is performed regarding this geometry. Now the Greater thickness (t_g) under the columns should be designed from the column punching shear found from analysis.

107

(iii)   The greater thickness (t_g) should be provided around the column peripheries over a distance equal to the effective depth corresponding to the greater thickness itself.

(iv)   Smaller thickness should be calculated from the maximum flexural shear, found from the solution, at the neck sections.

(v)   Width of the transition zones (for gradual reduction of thickness) should be such that slope angle of the underside of mat in these zones be between 30° to 35°. A simple trial will be sufficient to finalise steps (iii) and (iv).

(vi)   The problem should be analyzed again with the new geometry just selected in order to calculate reinforcements. Finally a check on the adopted geometry using the shear forces diagrams and punching shears found from the *new solution*.

(vii)   Minimum reinforcement required for the zone of greater thickness should be provided as bottom reinforcement under the columns across the entire widths of column strips. Again, the new solution may be used to check the adequacy of these reinforcements.

(viii)   Reinforcements for negative moments in-between the columns should be designed using the new solution.

(ix)   Bottom reinforcements in-between the columns (negative moment zones) and top reinforcements under the columns (positive moment zones) should be calculated as per minimum requirements specified by ACI code.

Using this guideline it has been revealed that thickness away from column can be reduced up to 35%. And economy achievable in terms of volume of concrete and reinforcement is about 20 to 30 % with respect to uniform thickness mats.

For facilitation of designing the non-uniform mat foundation a full pledged windows based software **MATFEA** has been developed. Working with this software is very friendly regarding data input and result interpretation. Graphs of displacements, flexural shears and bending moments are generated instantly and shown in screen.

7.6   RECOMMENDATIONS FOR FUTURE STUDY

The following recommendations are made for future investigation on mat foundation.

(i)   Behavior of irregularly shaped mat, mat with punches, mat with irregular column arrangements and mat with shear walls may be investigated.

(ii)   Both mat and supporting soil have been modeled as linearly elastic material in the current study. A non-linear analysis may be performed.

(iii) Dynamic mat-soil interaction can be analyzed using FE method.

(iv)   The integrated structure consisting of mat monolithically built with the building frame with and without shear walls may be analyzed for both static and dynamic response.

(v)   Rectangular and circular mats subject to peripheral line lodes, as are found under silos and oil tanks, may be analyzed.

REFERENCES

(1) Ahmad, S., *Curved Finite Elements in the Analysis of Solid, Shell and Plate Structures*, Ph.D. Thesis, University College of Swansea, 1969.

(2) Ahmad, S., "General Thick Shell Element Program - Part A and Part B ", Computer Program Report, No. 22, University of Wales, Swansea, October, 1969.

(3) Ahmad, S., Irons, B.M. and Zienkiewicz, O.C., "Analysis of Thick and Thin Shell Structures by Curved Finite Elements" , International Journal of Numerical Methods in Engineering , Vol. 2, 1970, pp. 419-451.

(4) Amanat, K.M., *A Design Rationale for Free Standing Stair Slab Based on Finite Element Analysis*, M.Sc. Thesis, BUET, Dhaka, September, 1993.

(5) Arora, K.R., *Soil Mechanics and Foundation Engineering*, 1st Ed., Standard Publishers and Distributors, New Delhi, 1992, pp. 948-975.

(6) Bathe, K.J., *Numerical Methods in Finite Element Analysis*, 1st Ed., Prentice Hall Inc., New Jersey, 1976.

(7) Bowels, J.E., *Foundation Analysis and Design* , 2nd Ed., McGraw Hill Book Co., New York, 1968, pp. 294-320.

(8) Bowels, J.E., *Analytical and Computer Methods in Foundation Engineering*, 1st Ed., McGraw Hill Book Co., New York, 1974, pp. 209-254.

(9) Bowels, J.E., "Mat Design" , ACI Journal, Vol. 83, No. 6, November-December, 1986, pp. 1010-1017.

(10) Bowels, J.E., *Foundation Analysis and Design* ,4th Ed., McGraw Hill Book Co., New York, 1988, pp. 436-470.

(11) Chilton, D.S. and Wekezer, J.W., "Plates on Elastic Foundation", Journal of Structural Engineering, ASCE, Vol. 116, No. 11, November, 1990, pp. 3236-3241.

(12) Das, B.M., *Advanced Soil Mechanics*, 1st Ed., Hemisphere Publishing Corporation, Washington, 1983, pp. 167-241 and 339-401.

(13) Deryck, N. and Severn, R.N., "Stresses in Foundation Rafts", Proceedings of the Institute of Civil Engineers (London), Part 1, Vol. 15, January, 1960, pp. 35-48.

(14) Deryck, N. and Severn, R.N., "Stresses in Foundation Rafts", Proceedings of the Institute of Civil Engineers (London), Part 2, Vol. 20, October, 1960, pp. 293-304.

(15) Gupta, A. and Patel, A.N., "Rational Analysis of Mat Foundations Using Finite Element Technique", Proceedings of the International Seminar on Civil Engineering Practice in the Twenty first Century, Roorkee, Vol. 1, February, 1996, pp. 149-159.

(16) Hemsley, J.A., "Elastic Solutions for Axisymetrically Loaded Circular Raft with Free or Clamped Edges Founded on Winkler Springs or a Half-space", Proceedings of the Institute of Civil Engineers (London), Part 2, Vol. 83, March, 1987, pp. 61-90.

(17) Hemsley, J.A., "Plane Elastostatic Flexure of an Infinite Plate on a Half space" , Proceedings of the Institute of Civil Engineers (London), Part 2, Vol. 85, December, 1988, pp. 629-664.

(18) Hemsley, J.A., "Comparative Flexure of an Infinite Plate on Winkler Springs and a Half-space", Proceedings of the Institute of Civil Engineers (London), Part 2, Vol. 85, December, 1988, pp. 665-687.

(19) Hetenyi, M., *Beams on Elastic foundation*, 1st Ed., University of Michigan Press, En Arbor, 1946, pp. 245-255.

(20) Hooper, J.A. and West, D.J., "Structural Analysis of Circular Raft on Yielding Soil", Proceedings of the Institute of Civil Engineers (London), Part 2, Vol. 75, June, 1983, pp. 205-241.

(21) Horvath, J.S., "New Subgrade Model Applied to Mat Foundations", Journal of Geotechnical Engineering, ASCE, Vol. 109, No. 12, December, 1983, pp. 1567-1587.

(22) Horvath, J.S., "Modulus of Subgrade Reaction : New Perspective", Journal of Geotechnical Engineering, ASCE, Vol. 109, No. 12, December, 1983, pp. 1591-1596.

(23) Horvath, J.S., "New Subgrade Model Applied to Mat Foundations", Journal of Geotechnical Engineering, ASCE, Vol. 119, No. 2, February, 1993, pp. 1567-1587.

(24) Hossain, T.R., *Comparative Study of the Analysis Techniques of Mat Foundation*, M.Sc. Thesis, BUET, Dhaka, November, 1993.

(25) Irons, B. and Ahmad, S., *Techniques of Finite Elements*, 1st Ed., Ellis Horwood Ltd., Chichester, 1980.

(26) Krishnamoorthy, C.S., *Finite Element Analysis : Theory and Programming*, 1st Ed., Tata McGraw Hill Publishing Co. Ltd., New Delhi, 1987.

(27) Mician, R., "Discussion on a Simplified Method for Design of Mat on Elastic Foundation (paper by Shukla, S.N.)" , ACI Journal, July-August, 1985, pp. 584-586.

(28) Molla, M.A.S., *Finite Element Analysis of Footings and Mat foundations*, M.Sc. Thesis, BUET, Dhaka, February, 1995.

(29) Nilson, A.H. and Winter, G., *Design of Concrete Structures*, 10th Ed., McGraw Hill Book Company, Singapore, 1986.

(30) Scott, R.F., *Foundation Analysis*, 1st Ed., Prentice Hall Inc., New Jersey, 1981, pp. 119-200.

(31) Shukla, S.N., "A Simplified Method for Design of Mats on Elastic Foundation" , ACI Journal , Vol. 81, No. 5, September-October, 1984, pp. 469-475.

(32) Singh, A., *Modern Geotechnical Engineering*, 3rd Ed., CBS Publishers and Distributors Pvt. Ltd., New Delhi, 1992, pp. 532-554.

(33) Sutradhar, A., *Analysis of Mat Foundations with Special Reference to Thick Shell Finite Elements*, B.Sc. Thesis, BUET, Dhaka, March, 1995.

(34) Teng, W.C., *Foundation Design*, 13th Ed., Prentice Hall of India Private Limited, New Delhi, 1992, pp. 159-191.

(35) Worsak, K.N., Somporn, A. and Sarun, U., *"MICROFEAP II : Analysis of 2D Truss, Frame and Wall"*, Module P1, Release 3.1, MICRO-ACE Club, Asian Institute of Technology, 1988.

(36) Steven C. Ball and James S. Notch, *"Computer analysis/design of large mat foundation"*, ASCE journal of structural engineering , Vol 110, No. 5, May 1984

(37) Liou Gin-show and Lai S.C. " Structural Analysis model for mat foundations", ASCE journal of structural engineering , Vol 110, No. 5, May 1984, Vol. 122, No. 9, Sept. 1996

(38) Selvadurai, A.P.S. 'Elastic Analysis of soil-foundation interaction', Developments in Geotechnical Engineering, VOL 17, Elsevier scientific publishing company.

(39) Yang T.Y. 'Flexible plate finite element on elastic foundation. J. Struct. Div., Proc. ASCE., 96 : ST10, 2083

(40) Yang T.Y., 'A finite element analysis of plates on a two parameter foundation model, Comput. Struct., pp. 593-614, 1970.

(41) Morshed, A. S. M. M. (1996). "A Design Rationale for Mat Foundation Based on Finite Element Analysis." M.Sc. thesis, Bangladesh Univ. of Engrg. and Technol., Dhaka, Bangladesh.

APPENDIX A

THICK SHELL ELEMENT

A.1 BRIEF DESCRIPTION OF THICK SHELL ELEMENT

The general thick shell finite element was developed by Ahmad (1969). Typical thick shell elements are shown in Fig. A.1. In thick shells, bending effect can be expected to be significant. The transverse shear deformation is also significant. In the element formulation, two assumptions were made. Firstly, the original normal to the middle surface are assumed to remain straight. Secondly, the distance of a point along the normal from the middle surface remains unaffected.

A.1.1 Geometric Definition of the Element

The external faces of the elements are curved, while the sections across the thickness are generated by straight lines. Pairs of points i_{top} and i_{bottom}, each with given Cartesian coordinates, describe the shape of the element.

If ξ and η be the two curvilinear coordinates in the middle plane of the shell element (Fig. A.2) and ζ be a linear coordinate in the thickness direction and further, if it is assumed that ξ, η and ζ vary between +1 and -1 on the respective faces of the element, then a relationship can be written between Cartesian coordinates of any point of the shell and the curvilinear coordinates in the form :

$$\begin{Bmatrix} x \\ y \\ z \end{Bmatrix} = \sum N_i(\xi,\eta)\frac{1+\zeta}{2}\begin{Bmatrix} x_i \\ y_i \\ z_i \end{Bmatrix}_{top} + \sum N_i(\xi,\eta)\frac{1-\zeta}{2}\begin{Bmatrix} x_i \\ y_i \\ z_i \end{Bmatrix}_{bottom} \qquad (A.1)$$

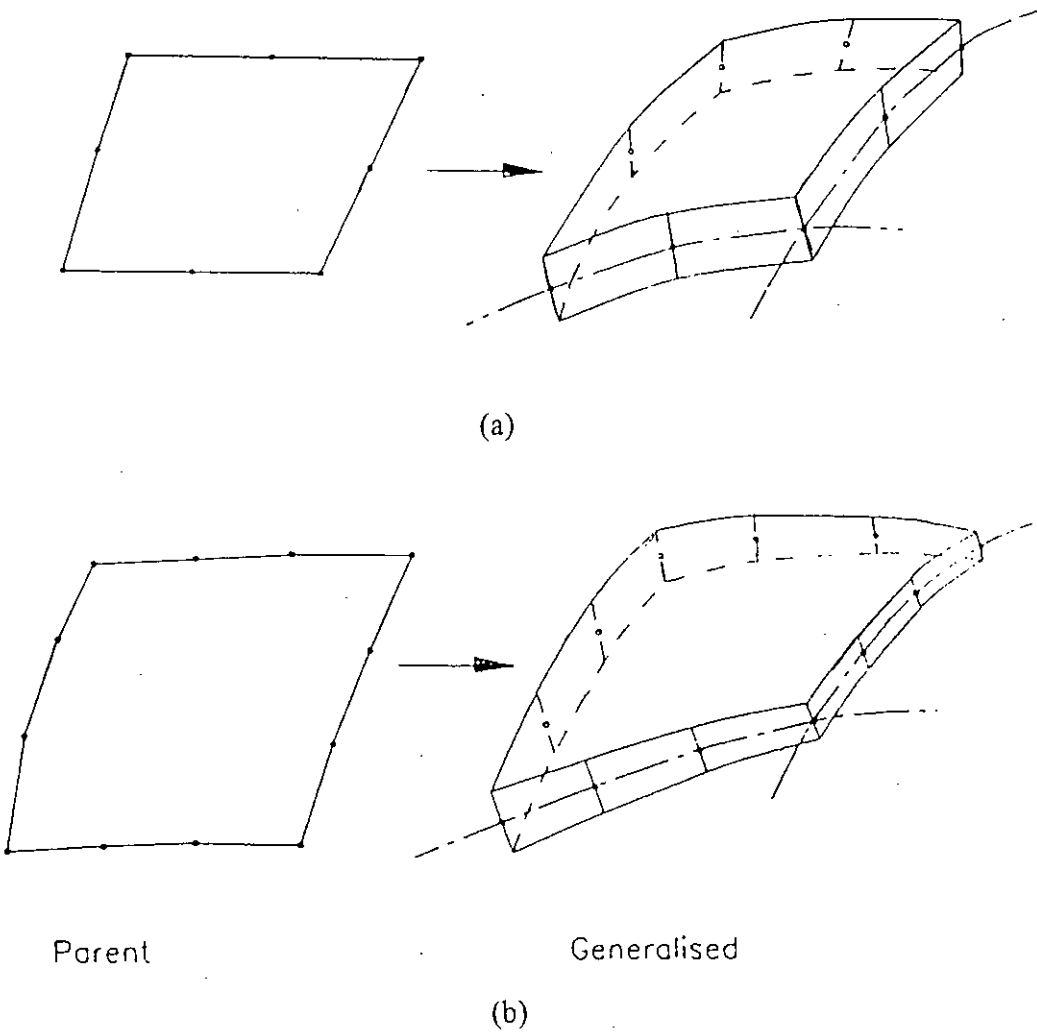Parent   Generalised

(b)

Fig. A.1. Thick shell elements : (a) parabolic element and (b) cubic element

Here, $N_i (\xi, \eta)$ are shape functions taking a value of unity at the nodes i and zero at all other nodes. If the basic functions, N_i are derived as shape functions of a parent two dimensional element, square or even triangular in plan and are so designed that compatibility is achieved at interfaces, then the curved shape elements will fit into each other. Arbitrarily curved shapes of the element can be achieved by using shape functions of different orders. Only parabolic and cubic types are shown in Fig. A.1. For the purpose of present analysis, a parabolic element has been used. By placing a larger number of nodes on the surfaces of the element, more elaborate shapes can be achieved if so desired. It should be noted that the ζ direction is only approximately normal to the middle surface of the element. The relationship between the Cartesian coordinates and the curvilinear coordinates can be written conveniently in a form specified by the vector connecting the upper and lower points (i.e. a vector of length equal to the shell thickness, t) and mid surface coordinates (Fig. A.3) as follows

$$\begin{Bmatrix} x \\ y \\ z \end{Bmatrix} = \sum N_i \begin{Bmatrix} x_i \\ y_i \\ z_i \end{Bmatrix}_{mid} + \sum N_i \frac{\zeta}{2} \bar{v}_{3i} \qquad (A.2)$$

and

$$\bar{v}_{3i} = \begin{Bmatrix} x_i \\ y_i \\ z_i \end{Bmatrix}_{top} - \begin{Bmatrix} x_i \\ y_i \\ z_i \end{Bmatrix}_{bottom} \qquad (A.3)$$

Here $\bar{v}_{3i}$ is a vector whose length is equal to the shell thickness.

A.1.2 Displacement Field

Since strains in the direction normal to the mid surface is assumed to be negligible, the displacement throughout the element will be taken to be uniquely defined by the three mid surface nodal displacements in the directions of the three Cartesian
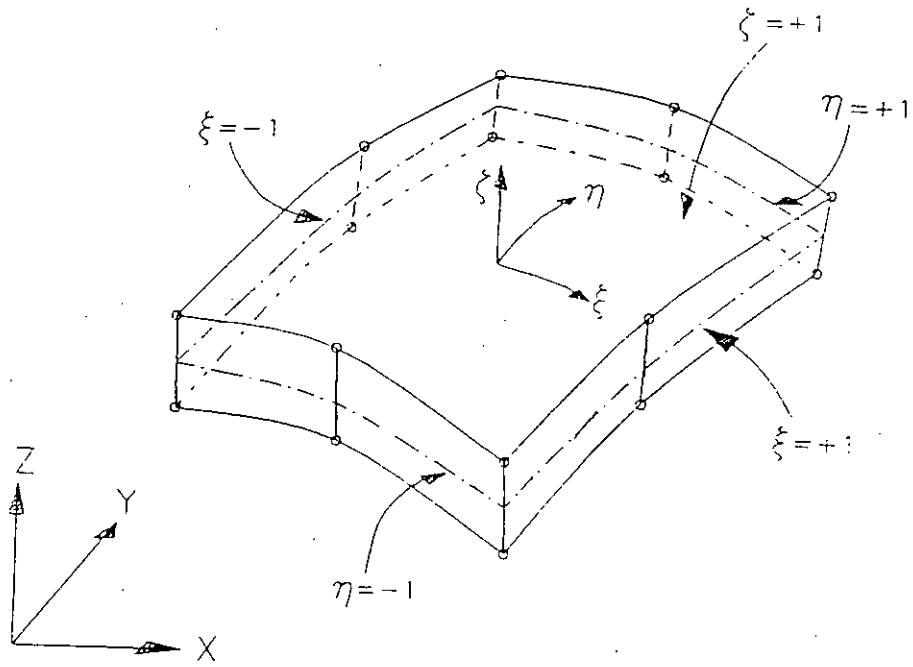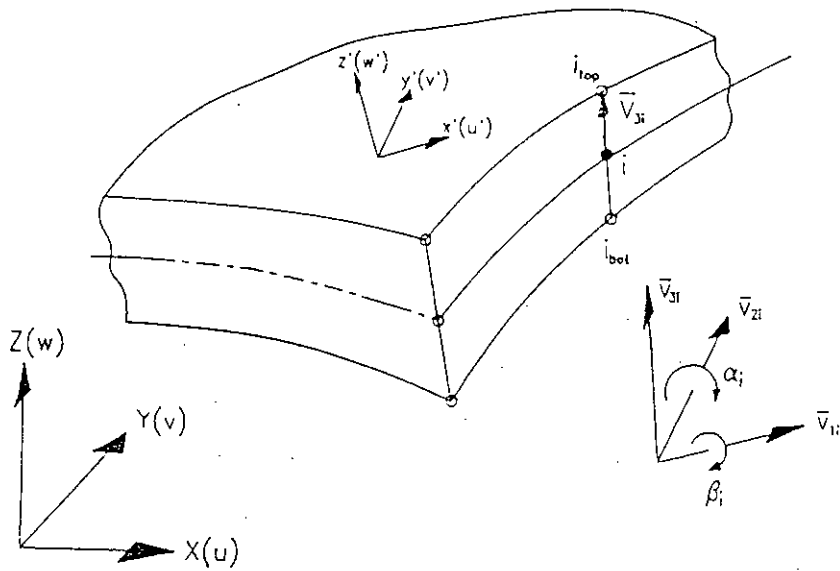
Fig. A.2. Geometry of thick shell element.

Fig. A.3. Local and global coordinate systems and nodal degrees of freedom for thick shell element.

coordinates and two rotations of the nodal vector $\overline{V}_{3i}$ about orthogonal directions normal to it. If two such orthogonal directions are given by vector $\overline{V}_{2i}$ and $\overline{V}_{1i}$ of unit magnitude with corresponding scalar rotations α_i and β_i respectively, the displacement field can be expressed as follows :

$$
\left\{ \begin{array}{c} u \\ v \\ w \end{array} \right\} = \sum N_i \left\{ \begin{array}{c} u_i \\ v_i \\ w_i \end{array} \right\} + \sum N_i \zeta \frac{t_i}{2} [\overline{V}_{1i} - \overline{V}_{2i}] \left\{ \begin{array}{c} \alpha_i \\ \beta_i \end{array} \right\} \qquad (A.4)
$$

A.2 GENERAL FEATURES OF THE PROGRAM

The thick shell program is a FORTRAN code to implement the general thick shell element [Ahmad (1969)]. The geometry of a structure is defined in a global system which is a rectangular Cartesian coordinate system. The loading and boundary conditions must be given in the same unit as the nodal displacements of an element. The stresses are usually calculated at the nodal points in the global system.

The top and bottom coordinates of each node with respect to Cartesian coordinate system are fed into the program. Coordinates for non-corner nodes lying on straight edges are not required to be given. If these coordinates of the nodes are fed into the program, then the shape of the element is automatically defined in the program. Therefore the thickness of the element can vary from node to node and the edges may be curved parabolically and cubically depending on the type of element used. The program as at present can handle isotropic elastic material. The material properties are defined for every element, thus allowing the program to deal with materials varying from element to element. Temperature and pressure can be varied from node to node.

A.2.1 Output from the Program

Displacements are calculated and printed against each node in the ascending order for every loading case. Stresses are first calculated in the local orthogonal system and then transformed into the global Cartesian system. For every node, the top surface stresses are followed by the bottom surface stresses.

Global stresses are also stored separately for top and bottom surfaces against node numbers and in the end, a simple averaging is performed on them. The average stresses are then printed out in the ascending order of the node numbers. The top surface stresses for all the loading cases are followed by the bottom surface stresses.

A.2.2 Division of Structure into Elements

First of all, the structure is divided into suitable elements and the nodes are numbered in any suitable manner as shown in the example of Fig. A.4. The elements are also suitably numbered in some sequence on which they are fed into the computer. Two probable sequences are shown in Fig. A.4 (a) and A.4 (b). Each element is topographically defined by its nodal numbers in a consistent right hand screw system as shown in Fig. A.5 (a) and A.5 (b).

A.2.3 Front Width and Selection of Order of Elimination

The thick shell program uses the frontal solution technique. Here the assembly of an element stiffness and the corresponding right hand side is immediately followed by the process of elimination of the variables corresponding to nodes which occur for the last time. This is indicated to the program by inserting a negative sign before these nodes. This can easily be put in the shell structures once the element sequence has been selected.

To carry out the analysis of a structure using minimum possible computer storage, the elements are selected in such a sequence that the maximum number of variables to be handled at any particular time i.e. the front width, is minimum. For example, the prescribed order of elements in Fig. A.4 (a) will give the smallest front width for the particular structure. This is evident even from inspection for simple structures.

A.3 EVALUATION OF STRESSES AT GAUSS POINTS

Formulation of the element stiffness matrix involves integration of complex polynomial shape functions of the elements and their derivatives. Exact integration of such functions is very troublesome and numerical integration becomes essential. Numerical integration of any function involves evaluation of the function at some representative points within the range of the function for shape functions which is the respective element. The number of representative points required for a certain degree of accuracy depends on the technique of integration employed. It is found that number of sampling points is minimum when Gauss' quadrature is applied. For this reason, virtually all finite element programs use Gauss' quadrature. The Gauss quadrature formula is

$$\int_{-1}^{+1} f(\xi)d\xi = \sum_{i=1}^{n} H_i f(a_i) \qquad (A.5)$$

In the above formula, integration is performed in the range of -1 to +1, a_i is the abscissa of the Gauss points, $f(a_i)$ is the ordinate i.e. the function value at a_i, H_i is the weight coefficient and n is the number of sampling points. Values of a_i and H_i depend on the value of n. Table A.1 lists these values for n ranging upto 3.

In Ahmad's program, 2-point and 3-point Gauss' quadratures are applied for the 8-noded and 12-noded elements respectively. Integration is performed in the local element coordinate system (ξ, η, ζ). Coordinates of the points within the element
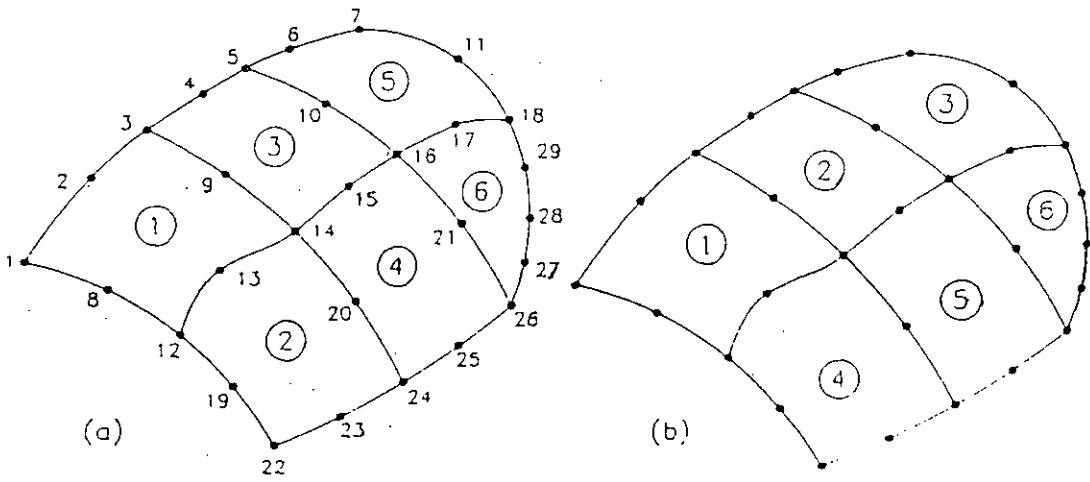
A-5

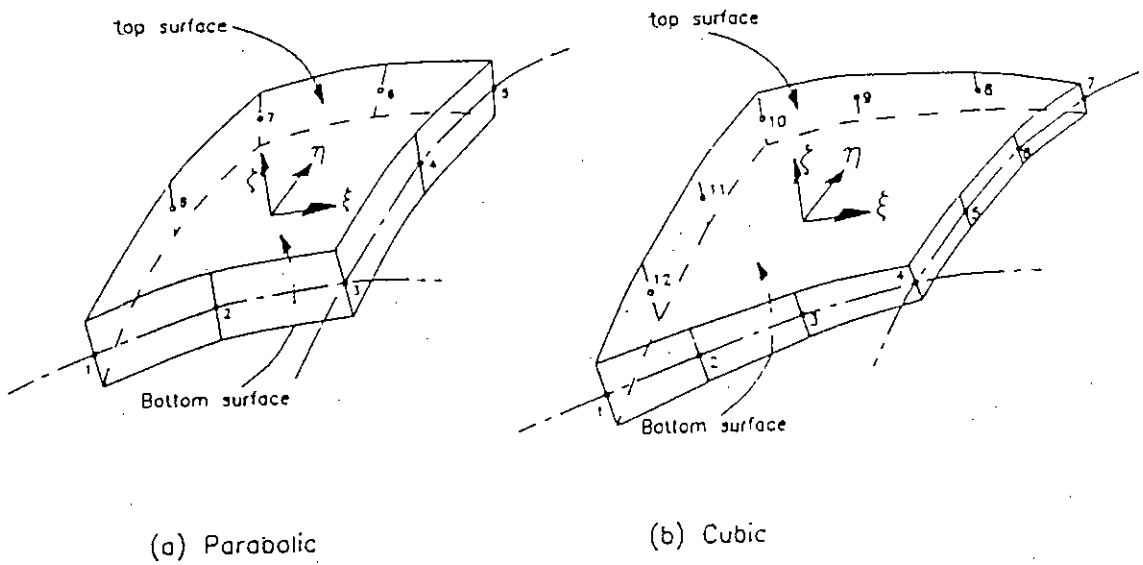Fig. A.4. Division of structure with parabolic elements.

(a) Parabolic

(b) Cubic

Fig. A.5. Definition of element topology.

varies between +1 and -1. If 2-point (n=2) integration is performed on the middle surface, there are four Gauss points since integration is carried out in both ξ and η directions. The coordinates of these four points with respect to (ξ, η) system will be (± 0.577350269, ± 0.577350269). These points are shown in Fig. A.6.

Table A.1.   Values of a_i and H_i for Gauss integration.

n	$\pm$ a	H
1	0.0	2.0
2	0.577350269	1.0
3	0.774596692	0.5555555555
	0.0	0.8888888888

In finite element analysis using displacement methods, the stresses are discontinuous between elements because of the nature of the assumed displacement variation. For this reason, stress at a node is calculated by averaging the stresses obtained at that node from the elements common to that node. Experience has shown that in case of isoparametric elements the Gauss' integration points are the best stress sampling points because shape function derivatives, and hence stresses, evaluated at the interior of the elements are more accurate than those calculated at the element boundary. The element nodes, which are the most useful points for output and interpretation of stresses, appear to be not so good as stress sampling points.

The thick shell element developed by Ahmad (1969) is excellent for analyzing singly or doubly curved shell structures where load is carried by bending as well as inplane forces. In most shell structures, transverse shear is not a very important quantity. It has been found from experience that out of plane shears in such ordinary structures are small in magnitude and they can safely be ignored in design. Consequently, while formulating element characteristics, less importance was given to the evaluation of

transverse shear stresses. However, stresses at Gauss points are predicted with good accuracy in shell or plate structures like mat, where transverse shear is important. For this reason, evaluation of stresses at Gauss points becomes essential with Ahmad's element for such structures.
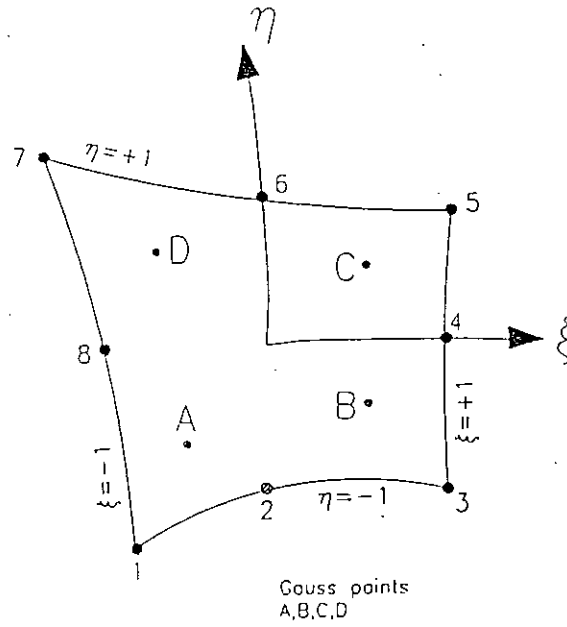

Fig. A.6. Gauss points in an 8-noded element.